

Some pages of this thesis may have been removed for copyright restrictions.

If you have discovered material in AURA which is unlawful e.g. breaches copyright, (either yours or that of a third party) or any other law, including but not limited to those relating to patent, trademark, confidentiality, data protection, obscenity, defamation, libel, then please read our [Takedown Policy](#) and [contact the service](#) immediately

NOISE GENERATED AT THE TYRE/ROAD INTERFACE

by

JOHN CHARLES WALKER

A Thesis Submitted for the Degree of

DOCTOR OF PHILOSOPHY

The University of Aston in Birmingham

Department of Physics

August 1981

This thesis to be confidential for 2 years

To my family

The University of Aston in Birmingham

SUMMARY

NOISE GENERATED AT THE TYRE/ROAD INTERFACE

by

JOHN CHARLES WALKER

A Thesis submitted for the Degree of

DOCTOR OF PHILOSOPHY

August 1981

The work described in this thesis is directed towards the reduction of tyre/road interface noise and embodies a study of the factors involved in its generation.

These factors comprise:

- (a) materials and construction of tyres and road surfaces
- (b) the spectral distribution of the noise

The importance of this work has become greater with reduction in engine noise.

A review of the literature shows what has been achieved so far, and stresses the importance of maintaining other desirable tyre properties such as adhesion in wet conditions.

The work has involved an analysis of mechanical factors in tyre construction and the behaviour of road surfaces.

Measurements on noise have been carried out under practical conditions and also on replica surfaces in the laboratory, and in addition tests of wet road adhesion have been carried out with a variety of road surfaces.

Consideration has been given to the psychological effects of the spectral distribution of noise. A major part of the work undertaken has been the development of a computer program, the results of which have made it possible to design a tyre tread block pattern to give an optimum spectral distribution. Sample tyres built to this design have been subjected to noise measurements and these have been shown to agree closely with the theoretical prediction and other properties of this tyre have proved to be satisfactory.

Key Words

noise / tyres / computer sequencing / computer simulation

ACKNOWLEDGEMENTS

The research reported in this thesis would not have been possible without the help of Professor S E Hunt, Head of the Department of Physics, the University of Aston in Birmingham and Mr G F Morton, Tyre Research & Laboratories Director, Dunlop Limited.

The author wishes to thank his supervisor Dr J A Archer-Hall, Lecturer in the Department of Physics, the University of Aston in Birmingham for his advice and interest during the period of his research.

Thanks are due to his external supervisor, Dr C W Barson, Manager Tyre Research Department, Fort Dunlop, for his guidance and making available the equipment used in this research.

The author acknowledges with gratitude to his colleagues employed by Dunlop Limited the help in computer programming and many of the noise testing and braking results. Over the period involved the author had assistance in the department of one person at a time in three areas of his work; R D Oakes, J Clarke, D J Major and R P Brueton were involved in assisting with noise measurements; R D Oakes and R H Edwards in programming; and A O Davis and F G Court in obtaining and fitting tyres and taking some routine noise measurements. Each of the above received instruction under the author's supervision. The work was approximately 85% initiated and 100% supervised by the author.

With regard to computer programming, the author personally carried out the program modifications and terminal operation for the sequencing work in Chapter 7 and the noise simulation in Chapter 8.

Finally the author thanks Miss A Woolman for typing the thesis and for helping in the presentation of the work.

The opinions, findings and conclusions given in this thesis are those of the author and not necessarily of Dunlop Limited.

CONTENTS

	<u>Page</u>
Summary	i
Acknowledgements	ii
Contents	iii
List of Figures	ix
List of Tables	xvi
<u>CHAPTER 1</u>	
INTRODUCTION	1
1.1.	1
Appreciation of the Problem	
1.2.	2
Scope of the Present Study	
1.2.1.	2
The Measurement and Analysis of Vehicle Coasting Noise on the Road	
1.2.2.	2
The Measurement and Analysis of Tyre/Surface Noise on a Drum in the Laboratory	
1.2.3.	3
The Construction of a Mathematical Model in the Computer in Order to Predict Results and to Automatically Minimise Dominant Tones	
1.2.4.	3
The Achieving of the Best Possible a Correspondence Between the Different Parts of the Work and the Application of the Knowledge Gained to Produce Quieter Tyre/ Road Interfaces, with Other Tyre/ Road Properties Being Borne in Mind	
<u>CHAPTER 2</u>	
REVIEW OF LITERATURE, PAST WORK, AND FACTORS INFLUENCING THE PROBLEM	4
2.1.1.	10
Tyre Design Features	
2.1.1.1.1.	10
Tread Pattern on Various Surfaces	
2.1.1.1.2.	11
Tyre Size	

		<u>Page</u>
2.1.1.1.2.1.	Rim Diameter	11
2.1.1.1.2.2.	Sectional Width	14
2.1.1.1.2.3.	Aspect Ratio	14
2.1.1.1.3.	Tread Profile - Cross Ply Cross Bar Truck Tyres	14
2.1.1.1.4.1.	Shape of Contact Patch	15
2.1.1.1.4.2.	Pressure Distribution	15
2.1.1.2.1.	Tread Compound	15
2.1.1.2.2.	Casing Reinforcement	17
2.1.1.3.1.	Tyre Construction	17
2.1.2.	Operating Conditions	17
2.1.2.1.	Speed	17
2.1.2.1.1.	Direction of Rotation	18
2.1.2.2.	Load and Inflation Pressure	18
2.1.2.3.	Cornering, Traction and Braking	18
2.1.2.4.	Tread Wear	18
2.1.2.5.	Tread Surface Conditions	19
2.1.2.6.	Temperature	19
2.1.2.7.	Time - Ageing	19
2.1.2.9.	Wheels	19
2.1.2.10.	Tyre Screens	20
2.1.2.11.	Tyres per Vehicle	20
2.1.2.12.	Traffic Density and Mix	20
2.1.3.	Noise Generation Mechanisms	22
2.1.3.1.1.	Impacting	22
2.1.3.1.2.	Stroking	23
2.1.3.1.3.	Air Pumping	23
2.1.3.3.	Tyre Vibration	23

	<u>Page</u>	
2.1.4.	Models of Tyre Noise	28
2.2.	Surface Variables and Environment	30
2.2.1.	Road Texture	30
2.2.2.2.	Wet Conditions	30
2.2.2.5.	Obstacle Proximity	30
2.2.2.7.	Wind Velocity	32
2.3.	Types of Noise Measurement	32
2.3.1.1.	Standard Pass-by Tests	32
2.3.1.2.	Distance of Stationary Microphone	33
2.3.1.5.	Directional Characteristics of Noise	36
2.4.	Criteria for Subjective Judgement of Noise	36
<u>CHAPTER 3</u>	<u>COASTING VEHICLE PASS-BY NOISE IN THE DRY AND WET GRIP</u>	40
3.1.	Introduction	40
3.2.	Relevance of decibel to Common Traffic Situation Variables	40
3.3.	Test Conditions	40
3.4.	Transport and Road Research Laboratory Tests	42
3.5.	Truck Coasting Noise - Six Road Surfaces, Two Tread Patterns	44
3.6.	Tyre/Road Noise due to Road Surface Texture	46
3.7.	Delugrip Road Surfacing Materials	48
3.8.	Automobile Tyre/Road Noise and Wet Grip versus Vehicle Speed	52
3.9.	Automobile and Truck Tyre/Road Coasting Noise and Wet Grip	52
3.10.	Wet Tyre/Road Noise	54
3.11.	Coasting Vehicle Pass-by Noise with Studded and Unstudded Tyres	55

		<u>Page</u>
<u>CHAPTER 4</u>	TOTAL TRAFFIC NOISE - THE RESURFACING OF THE HAMMERSMITH FLYOVER	59
4.1.	Introduction	59
4.2.	Road Surfacing Texture	59
4.3.	Histogram of Total Traffic Noise	61
4.4.	Total Traffic Noise - Frequency Spectrum and Probability	65
4.5.	Full probability Spectrum Level v $\frac{1}{2}$ octave band plots	65
<u>CHAPTER 5</u>	THE EFFECT OF DRUM SURFACE TEXTURE ON INDOOR TYRE NOISE TESTING VERSUS COASTING VEHICLE PASS-BY NOISE	72
5.1.	Introduction	72
5.2.	Experimental Procedure	72
5.3.	Discussion of Results	75
5.4.	Comparison with Vehicle Pass-by Noise	77
5.5.	Replica Road Surfaces	77
5.6.	Indoor Testing of Automobile Tyres on Replica Surfaces	81
5.6.1.	Effect of Tyre Size	84
5.6.2.	Frequency Spectra	84
5.6.3.	Separation on the Two Component Parts of Tyre/Road Noise	84
5.6.4.	Correlation - External Automobile Coasting Noise v Indoor Testing on Replica Surfaces	92
5.6.4.1.	Factors Influencing Correlation	94
<u>CHAPTER 6</u>	THE EFFECT OF SINUSOIDAL MODULATION OF TREAD SEGMENT LENGTH ON DOMINANT TONES (CONSTANT MODULATING FREQUENCY, f_g)	97
6.1.	Mechanical Frequency Modulation	97
6.2.	Mathematical Basis of Frequency Modulation Tones	98

	<u>Page</u>	
6.2.1.	Phase Modulation Amplitude	99
6.2.2.	Modulation Index	104
6.3.	Constraints in actual Tyre Design Modulation	109
<u>CHAPTER 7</u>	<u>THE EFFECT OF NON-SINUSOIDAL MODULATION OF TREAD SEGMENT LENGTH AND VARIABLE MODULATING FREQUENCY ON DOMINANT TONES</u>	<u>110</u>
7.1.	The Approach to the Investigation	110
7.1.1.	Introduction to a Digital Computer Method of Tyre Noise Simulation	110
7.1.2.	The Waveform used to Represent the Effect of a Tread Segment	112
7.2.1.	Introduction - The Program	113
7.2.2.	Correlation between Frequencies predicted by the Program and Tyre Drum Test Results	114
7.3.	The Effect of Segment Length Ratio on Dominant Tones	117
7.4.	The Best Sequence	119
7.5.	The Effect of the Maximum Number of Identical Length Adjacent Segments (Long and Short)	119
7.6.	The Combined Effect of Segment Length, Number of Identical Length Adjacent Segments, and Permutation of the Order of Blocks of Segments, on the Dominant Harmonic of Two Pitch Sequences	122
7.7.	Ratio of Segment Lengths (2 Pitch)	122
7.8.	Three Pitch Sequence with Fewer Identical Length Adjacent Segments versus Two Pitch Sequence with more Identical Length Adjacent Segments	125
7.9.	Test of the Effect of Phase of the Saw- tooth Wave within the Segment	125
<u>CHAPTER 8</u>	<u>THE MODELLING OF THE EFFECT OF TREAD PATTERN ON DOMINANT TONES</u>	<u>126</u>
8.1.	Analytical Modelling	126
8.1.1.	Cross Bar Pattern	126

	<u>Page</u>	
8.1.2.	Ribbed Pattern	127
8.2.	Finite Element Modelling	128
8.3.	Simple Digital Simulation	128
8.3.1.	Simple Analogue Model	128
8.3.2.	Digital Equivalent of Simple Analogue Model	129
<u>CHAPTER 9</u>	<u>THE EXTENSION OF THE MODEL TO INCLUDE THE EFFECTS OF MICROPHONE POSITION, TYRE SPEED AND CONTACT PATCH SHAPE</u>	<u>133</u>
9.1.	Introduction	133
9.2.	Tread Pattern Input	133
9.3.	Program Scheme	133
9.3.1.	Program Details	136
9.3.1.1.	To Generate a Simulated Tread Pattern Noise Waveform Suitable to Fast Fourier Transform	136
9.3.1.1.1.	Generation of the Waveform due to a Single Circumferential Strip around the Tyre Circumference at 1024 points	136
9.3.1.1.2.	Accounting for the Contact Patch Geometry and the Microphone Angle Position	137
9.3.2.	Obtaining the Frequency Spectra	139
9.3.3.	To Determine the Optimum Sequence of Groups of Tread Segments	139
9.4.	Tread Pattern Noise Tests - Experimental	139
9.4.1.	Tread Pattern Noise Tests - Simulated	140
9.4.2.	Comparison between Simulated and Experimental Noise Spectra - Tread Patterns, Basic Constant Pitch and Well Sequenced Variable Pitch	140
9.5.	Constant Pitch Tread Pattern Experimental Noise Waveforms	156
9.5.1.	Phase of Constant Pitch Tread Pattern Experimental Noise Waveforms	156
9.6.	Transient Wave from "Space Block Space" Tread Segment in a Plain Ribbed Tyre	159

	<u>Page</u>
9.7. Conclusions	162
<u>CHAPTER 10</u> CONCLUSIONS AND FUTURE INVESTIGATIONS	165
10.1. Conclusions	165
10.2. Future Investigations	168
APPENDIX	169
1.1. The Mechanical Frequency Modulation Program	169
1.2. The Program - Schematic Description of Input	169
2.1. The Tread Pattern Noise Simulation Program Assuming a Side Listening Position	171
3.1. Aspects of the Use of the Fast Fourier Transform	177
3.2. Aliasing	177
3.3. Leakage and Weighting Function	178
4.1. Swept Sine Wave Testing of Acoustic Measuring Conditions	178
4.2. Comments on Results	180
5. Ambient Noise in Tyre Testing Conditions	180
List of References	182
Glossary of Terms	190
LIST OF FIGURES	
2.1. Cross Groove Patterned Tyres - Percentage Void v Noise Level	12
2.2. Diagonal Block Patterned Tyres - Number and Angle of Blocks v Noise Level	13
2.3. Relative Harmonic Noise Amplitude v Phase Angle of Rows of Tread Blocks	16
2.4. Coasting Noise and Total Noise for Light and Heavy Vehicles	21
2.5. Transfer of Input Acceleration Levels to Remote Parts of Tyre	25

	<u>Page</u>	
2.6.	Shoulder View of Third Mode Radial Vibration Resonance at 96 Hz for an HR78-15 Radial Tyre	26
2.7.	Sidewall Flexural Waves	27
2.8.	Collective Estimate of the Acceleration - Coherent Sound and Associated 95% Confidence Interval for Tyre Segments One through Six as Compared to the Total Sound Spectrum	29
2.9.	Effect of Vehicle Speed on Wavelength	31
2.10.	Normalised Plot of the Correlation Coefficient C (τ) Max.	34
2.11.	Directivity Pattern for a Fully Worn Pocket Retread Tyre at 73 km/h (45 mph) on Rough Asphalt	35
2.12.	Sound Levels and Noisiness Ratings for all Test Runs	37
2.13.	Sound Levels and Noisiness Ratings - Averages of Five or More Test Results	38
3.1.	Truck Coasting Noise for Various Tyre/ Road Combinations-4 Tyres 3 Surfaces	41
3.2.	Automobile Coasting Noise for Various Tyre Road Combinations - 4 Tyres 4 Surfaces	43
3.3.	Truck Coasting Noise for various Tyre Road Combinations - 2 Tyres 6 Surfaces	45
3.4.	Relationship between Tyre/Road Noise and Frequency Generation due to Vehicle Speed, Tyre Tread Pitch and Road Aggregate Spacing	47
3.5.	Wet Friction A4 (London) Experiment	49
3.6.	External Car Coasting Noise on Dissimilar Surfaces - Dry with Blank and Patterned Tyres and Peak Braking Force Coefficients - Wet	51
3.7.	Vehicle Coasting Noise Related to Wet Grip for Various Tyre/Road Combinations	53
3.8.	Vehicle Coasting Noise with and without Studs	56
3.9.	Calculated Passing Noise Effect of Studs	57

	<u>Page</u>	
3.10.	Relationship between Maximum Passing Noise and a Defined Studded Tyre Parameter	58
4.1.	Road Section Profile	60
4.2.	Histograms of Noise on Hammersmith Fly-over, before and after Re-Surfacing	62
4.3.	Distribution of dB(A) Levels	63
4.4.	Average Frequency Spectrum over Two Half Hour Periods for 50% of the Time	64
4.5.	Percentage of time above indicated dB Levels in $\frac{1}{3}$ octave bands Hot Rolled Asphalt BS 594.	67
4.6.	Percentage of time above indicated dB Levels in $\frac{1}{3}$ octave bands Delugrip Road Surfacing Material	68
4.7.	Benefit of Delugrip (in dB) Superimposed on Delugrip Road Surfacing Material curves	69
4.8.	Causes of the Probability Distribution of Noise with Frequency	70
4.9.	Contours of Improvement in $\frac{1}{3}$ octave band Levels Obtained when using Delugrip Compared with Hot Rolled Asphalt BS 594, Superimposed on Delugrip Noise Spectra Exceeded for a given Percentage of Time	71
5.1.	Car Coasting Noise for Various Tyre Road Combinations	73
5.2.	Interaction. Tyre Tread Pattern - Drum Surface Texture-4 Tread Patterns - 2 Surfaces - 2 Speeds	74
5.3.	A Comparison of Car Coasting Noise with Drum Tests	76
5.4.	Photomicrographs of Aggregate and Replica	78
5.5.	Replica Road Surfaces	79
5.6.	Plain Tread Tyre Contact Prints on Replica Road Surfaces	80
5.7.	Indoor Testing Tyre/Road Noise on Simulated Road Surfaces for various Tyre-Surface Combinations-4 Tyres 7 Surfaces	82

	<u>Page</u>	
5.8.	Indoor Testing Tyre/Road Noise on Simulated Road Surfaces for a Range of Tyre Sizes-6 Sizes 3 Surfaces	85
5.9.	Frequency Spectra of Noise from Blank Tread Tyre on Replica Surfaces	86
5.10.	Separation of the Total Tyre/Road Noise into Tyre Periodic Noise with a Plain Tread Tyre and the Delugrip Replica Surface	88
5.11.	The Stages of Averaging, Showing the Progressive Isolation of the Synchronous Noise Waves Excited by the Delugrip Surface and the Blank Tread	89
5.12.	Progressive Isolation, until the Value Stabilises of the Synchronous Noise Level Excited by the Delugrip Surface and the Blank Tread	90
5.13.	Winter Pattern Tyre Synchronous Noise on the Hot Rolled Asphalt and Delugrip Replica Surfaces Speed 64 km/h	91
5.14.	Automobile Coasting Noise Generation on Dissimilar Surfaces Correlated with Indoor Tests Using Replicas of the Surfaces	93
5.15.	Effect of Contact Patch Length on Noise Level from Tyres on a Smooth Drum, Constant Pitch v Variable Pitch	96
6.1.	Tread Segment Positions	101
6.2.	Bessel Coefficients versus Maximum Phase Deviation ($\Delta\phi$) and Frequency Spectrum for $\Delta\phi = 3.85$	103
6.3.	The Effect on Frequency Spectra for Increasing Modulation Index	105
6.4.	To obtain Modulation Index from N,m, $\frac{\Delta a}{a_o}$	106
6.5.	To obtain Modulation Index from N/m, $\frac{\Delta a}{a_o}$	108
7.1.	Dominant Harmonics - Drum Tests - Constant Pitch - Block Pattern	111

	<u>Page</u>	
7.2.	Dominant Harmonics Predicted by Computer for Sequence v. Drum Tests	115
7.3.	View of Tyre D1 Tread Pattern	116
7.4.	Effect of Segment Length Ratio on Dominant Harmonics of Sequence	118
7.5.	Distribution of Dominant Tone Intensity after many Permutations	120
7.6.	Number of Adjacent Long Segments required at Different Ratios to get L out of Phase with M and Minimise this Dominant Harmonic	121
7.7.	The Effect on the Dominant Harmonic of 2 Pitch Sequences	123
	1. Permuting Order of Blocks of Segments	
	2. % Ratio Long to Short Segment Length	
	3. Maximum Number of Identical Length Adjacent Segments	
7.8.	The Effect on the Dominant Harmonic of the Segment Length Ratio, 2 Pitch	124
8.1.	Variation along Tread Segment Length of Total Width of Grooves across Tread 185/70-13 - 3 Tread Patterns	130
8.2.	Computer Prediction v Drum Tests Dominant Harmonic 3 Tread Patterns - 2 Drum Speeds	131
8.3.	Tyre Noise on Smooth Drum v Computer Simulated Tread Pattern Noise Harmonic Spectra - 185/70HR13 D1	132
9.1.	Typical Input for Simulation Program from the Tyre Contact Patch and One Tread Segment	134
9.2.	The Elemental Simulated Noise Wave - Generated at Rubber/Air and Air/Rubber Changes along a Thin Strip Down the Length of a Segment	135
9.3.	Simulation of Noise for Different Angles of Microphone Position - Schematic Diagram Showing Compensation for Acoustic Lags on Edge of Patch Furthest from Microphone, at Speed (v)	138

	<u>Page</u>	
9.4.	Contact Patch - In Phase Blocks Tread Pattern	143
9.5.	Contact Patch - Out of Phase Blocks Tread Pattern	144
9.6.	Contact Patch - In Phase Cross Grooves Tread Pattern	145
9.7.	Experimental Results - Out of Phase Blocks Tread Pattern Side v Front Microphone Position	146
9.8.	Simulated Results - Out of Phase Blocks Tread Pattern Side v Front Microphone Position.	147
9.9.	Experimental Results - Side Microphone Position In Phase Blocks v In Phase Cross Grooves Tread Pattern	148
9.10.	Simulated Results - Side Microphone Position In Phase Blocks v In Phase Cross Grooves Tread Pattern	149
9.11.	Experimental Results - Stacked Spectral Plots at 5 km/h Intervals Over the Speed Range 50 - 80 km/h In Phase Cross Grooves Tread Pattern - Side Microphone Position	150
9.12.	Experimental Results - Stacked Spectral Plots Over Speed Range 30 - 125 km/h In Phase Blocks Tread Pattern - Side Microphone Position	151
9.13.	Contact Patch - Sequenced Diagonal Blocks Tread Pattern	152
9.14.	Experimental Spectra for Well Sequenced Diagonal Block Pattern - Side Microphone Position	153
9.15.	Simulated Spectra for Well Sequenced Diagonal Block Pattern - Side Microphone Position	154
9.16.	Experimental Results - Stacked Spectral Plots over Speed Range 35 - 125 km/h Well Sequenced Diagonal Block Pattern - Side Microphone Position	155
9.17.	Time History (0.2 Seconds) of Sound Wave from a Constant Pitch in Phase Block Pattern Tyre over a range of Speeds, Triggered from a Fixed Point on the Tyre Circumference - Side Microphone Position	157

	<u>Page</u>	
9.18.	Time History (0.04 sec) of Sound Wave from a Constant Pitch in Phase Block Pattern Tyre over a range of Speeds, Triggered from a Fixed Point on the Tyre Circumference - Side Microphone Position	158
9.19.	Cross Correlation Function between two Microphone Recorder Channels	160
9.20.	Time History (0.02 sec) of Sound Wave from a Constant Pitch in Phase Block Pattern Tyre over a range of Speeds, Triggered from a Fixed Point on the Circumference - Front Microphone Position, together with a Photo Pick up Wave from each Tread Block	161
9.21.	Transient Wave from "Space Block Space" Single Tread Segment - Front Microphone Position - over a Speed Range 85 - 125 km/h	163
9.22.	Transient Wave from "Space Block Space" Single Tread Segment - Front Microphone Position - over a Speed Range 40 - 80 km/h	164
A.4.	Swept Sine Wave Testing of Acoustic Measuring Conditions	179
A.5.	Ambient Noise Versus Blank Tread Tyre Noise on Smooth Steel Drum	181

		<u>Page</u>
	LIST OF TABLES	
2.1.	Tyre Variables and Test Conditions	5 - 7
2.2.	Surface Variables and Environment	8
2.3.	Types of Noise Measurement - dB Levels and Frequency Spectra	9
2.4.	Differences in Noise Level Due to Changes in Tread Pattern	10
2.5.	Reduction in L_{10} due to Reduction in Noise of Individual Vehicles	22
2.6.	Radial Mode Resonant Frequencies versus Tyre Construction	24
2.7.	Change in Pass-by Level versus Ground Speed and Air Speed	32
2.8.	Difference in Pass-by Level for Different Vehicles due to Doubling Microphone Distance	33
7.1.	Relative Power Ratios of Harmonic Orders Experimental versus Sawtooth Wave	113
9.1.	Comparison Between Experimental and Simulated Noise	141
A.5.	Ambient Noise versus Blank Tread Tyre Noise on Smooth Steel Drum	180

CHAPTER ONE: INTRODUCTION

1.1. Appreciation of the Problem

Whatever changes in tread pattern design are made to reduce noise, the necessity to retain grip under poor ground surface conditions, such as in rain, mud and snow must be borne in mind. As long as 35 - 40 years ago tyre treads were designed with variable pitch tread segments to produce a spread of the tones in the frequency spectrum and to reduce their amplitude. Once some improvement had been obtained by the application of the techniques available at that time, noise work was mainly concerned with internal vehicle noise (Tompkins 1965). The report in 1963 by Wilson expressed the desirability of research to reduce the external noise of vehicles. Since then increasing attention has been paid to vehicle external noise (Henson 1968).

The problem of traffic noise is becoming of increasing importance to local authorities as a result of the introduction of urban motorways and similar high speed flow roads. To some extent this problem can be dealt with by the use of noise barriers at the road side, and noise insulation for houses. Thus quite large sums of money are being spent mainly to comply with the Land Compensation Act (HMSO 1973), along the lines of Development and Compensation - Putting People First. (HMSO 1972).

Underwood (1973) reported on the Transport and Road Research Laboratories work (T.R.R.L.), Department of the Environment, on the effects of tyres and surfaces on rolling noise. Rolling noise includes that from aerodynamic sources, from the transmission beyond the lay shaft, body rattles, and tyre/road interface noise emanating from tyre, road and vehicle. He stated that tyre/road interface noise could become one of the salient features of truck noise, if the target of 10 dB(A) reduction in power train noise is achieved. Power train noise includes the noise from the engine, inlet, exhaust, cooling systems and transmission as far as the lay shaft.

A reduction of lorry power train noise by 10 dB(A) is thought to be within reach of our existing technology, according to Harland (1974), but the benefits of such changes will not be fully realised unless at the same time rolling noise can be brought down by about 5 dB(A).

The progress of the quiet heavy lorry project is encouraging, as reported by Watkins (1974) and demonstrated at TRRL (1978). He also develops the case for reducing automobile noise, which is often dominated by tyre/road noise with current tread patterns and road textures at steady speeds above 50 km/h (32 mph). This emphasizes the importance of gaining a deeper understanding of tyre/road noise with a view to its reduction.

Other tyre construction factors to be optimised are wet grip, irregular treadwear, endurance, stone trapping, chunking of the tread and vehicle stability. These are fairly easily overcome on car tyres but more skill and research is needed to obtain optimisation on truck tyres.

1.2. Scope of Present Study

The approach to investigate the nature of tyre/road noise is in four main parts in addition to the literature reviews:-

1.2.1. The Measurement and Analysis of Vehicle Coasting Noise on the Road

This covered tests for a wide range of tread patterns on a range of road surfaces for both a truck and an automobile. Wet grip measurements were also taken. These results are discussed in Chapter 3. In Chapter 4 total traffic noise measurements are given showing the effect of improving the road surface.

1.2.2. The Measurement and Analysis of Tyre/Surface Noise on a Drum in the Laboratory

Further tests on automobile tyres with a wide range of tread patterns

have been carried out on a range of simulated road surfaces, and are discussed in Chapter 5. Also basic tread patterns have been cut from blank treads and then tested. The tests have included measurements at different microphone positions.

1.2.3. The Construction of a Mathematical Model in the Computer in Order to Predict Results and to Automatically Minimise Dominant Tones

This has been carried out in four main stages:

- (1) Using a sawtooth wave to represent a tread segment, the intensity of dominant tones can be predicted in patterned tyres as shown in Chapter 7.
- (2) By permuting the order of blocks of tread segments, the intensity of the dominant tones can be minimised.
- (3) The influence of different tread patterns and tread widths were included by replacing the sawtooth wave with the variation along the segment of "the total groove width across the tread" as detailed in Chapter 8.
- (4) The effects of contact patch shape, microphone position, tyre speed and waveform shaping to extend the range of tread patterns modelled was carried out using a two dimensional pattern input to the program and including the edge flipping effect of tread blocks as discussed in Chapter 9.

1.2.4. The Achieving of the Best Possible a Correspondence Between the Different Parts of the Work and the Application of the Knowledge Gained to Produce Quieter Tyre/Road Interfaces, with other Tyre/Road Properties being borne in mind

Correlation of results between testing on road and simulated surfaces on drums is discussed. Also correlation between the computer model results and drum test results are compared.

CHAPTER TWO: REVIEW OF LITERATURE, PAST WORK, AND FACTORS
INFLUENCING THE PROBLEM

Much work has been carried out on tyre/road noise. It is mainly concerned with mechanical factors which can give a useful but limited reduction of the intensity of the total noise. Nine extensive review papers are as follows. Millard (1970) reviewed road traffic noise and suggested targets for noise reduction. Flanagan (1972) compiled a review from reports by the National Bureau of Standards, Rubber Manufacturers Association and Society of Automotive Engineers Truck Tyre Noise Sub-Committee. This covered a range of truck tyre patterns.

Mukai et al (1974) gave a very comprehensive review of the state of the art at that time including a discussion on analogue simulation of tyre noise. Waters (1974) reviewed tyre/road noise in relation to truck engine noise. Leasure and Bender (1975) discussed the important parameters influencing tyre noise, and areas for future research were identified based on gaps in the existing physical data base and a rather primitive understanding of noise generation mechanisms.

The SAE Highway Tyre Noise Symposium (1976) comprehensively covered the state of the art at that time, as did also the International Tyre Noise Conference (1979). The document entitled "Foreign Research in Tyre Noise" prepared for the U.S. Environmental Protection Agency (1980) surveys the research outside the U.S.A. and extensively quotes the work of J C Walker, the author of this thesis.

A review given by J C Walker and Major (1975) provided a basis for the Tables 2.1., 2.2. and 2.3. which include forty eight factors influencing noise level. Some of the factors may be divided into many more influences and these will be discussed in the order in which they occur in these tables.

TABLE 2.1. TYRE VARIABLES AND TEST CONDITIONS

		FACTOR	ASPECT	EXAMPLE
2.1.1. 2.1.1.1. 2.1.1.1.1.	Tyre Design Features Geometrical Factors	Tread Pattern	Variable Pitch Segment Geometry	Blank & Plain Rib Commercial Rib Rib & Shoulder Lugs Traction Microslots
2.1.1.1.2. 2.1.1.1.2.1. 2.1.1.1.2.2. 2.1.1.1.2.3. 2.1.1.1.3. 2.1.1.1.4.1.		Tyre Size Tread Profile Tread Contact Patch	Rim Diameter Sectional Width Aspect Ratio Tread Radius Shape & Length	Automobile & Truck Phase Between Tread Blocks at Front and Rear of Patch
2.1.1.1.4.2.			Pressure Distribution	
2.1.1.2. 2.1.1.2.1. 2.1.1.2.2.	Material Factors	Tread Compound Casing Reinforcement	Hardness & Resilience	Nylon, Polyester, Rayon & Steel
2.1.1.3. 2.1.1.3.1.	Other Factors	Tyre Construction		Radial Ply & Cross Ply

TABLE 2.1. TYRE VARIABLES AND TEST CONDITIONS (Continued)

		FACTOR	ASPECT	EXAMPLE
2.1.2.	Operating Conditions	Speed Direction of Rotation Load & Inflation Pressure Cornering, Traction & Braking Tread Wear Tread Surface Condition Temperature Time Vehicle Wheels Tyre Screens Tyres Per Vehicle Traffic Density & Mix	Tread Depth & Irregular Wear	Alloy & Steel
2.1.2.1.				
2.1.2.1.1.				
2.1.2.2.				
2.1.2.3.				
2.1.2.4.				
2.1.2.5.				
2.1.2.6.				
2.1.2.7.				
2.1.2.8.				
2.1.2.9.				
2.1.2.10.				
2.1.2.11.				
2.1.2.12.				
2.1.3.	Noise Mechanisms	Generation Resonances Vibration	Automobile & Truck Impacting Stroking Air Pumping Contained Air Tread Casing	
2.1.3.1.1.				
2.1.3.1.2.				
2.1.3.1.3.				
2.1.3.2.1.				
2.1.3.2.2.				
2.1.3.2.3.				
2.1.3.3.				

TABLE 2.1. TYRE VARIABLES AND TEST CONDITIONS (Continued)

		FACTORS	ASPECT	EXAMPLE
2.1.4.	Models of Tyre Noise			
2.1.5. 2.1.5.1.	Other Properties	Optimise Wet Grip		

TABLE 2.2. SURFACE VARIABLES AND ENVIRONMENT

			FACTOR	ASPECT	EXAMPLE
2.2.1.	Road Texture		Macrotexture Profile		Polished Smooth Concrete Delugrip R.S.M. Friction Course Motorway H.R.A. Brushed Concrete Grooved Concrete
2.2.2.	Operating Conditions		Dry Wet Road Wear Absorption Obstacle Proximity Ambient Noise Wind Velocity		Grass Buildings & Fences Vehicle & Microphone
2.2.3.	Drum Texture			Aerodynamic Noise	Smooth Steel Safety Walk Replica Surfaces
2.2.4. 2.2.4.1.	Operating Conditions		Acoustical Environment	Ambient Noise Absorption by Room	

TABLE 2.3. TYPES OF NOISE MEASUREMENT - dB LEVELS AND FREQUENCY SPECTRA

		FACTOR	ASPECT	EXAMPLE
2.3.1. 2.3.1.1. 2.3.1.2. 2.3.1.3. 2.3.1.4. 2.3.1.5.	Road	Isolated Vehicle Noise Standard Pass-by Tests Distance of Stationary Microphone Time Response of Sound Level Meter Time History During Pass- by Travelling Boom Microphone with Wind Shield	Frequency Spectra Harmonic Spectra Synchronous Spectra relative to Tyre Rotation, Coherence	
2.3.1.6.	Total Traffic Noise		Distribution of Noise Levels and Spectrum Levels	
2.3.2.1.	Drum	Directional Characteris- tics of Noise	Frequency Spectra Harmonic Spectra Synchronous Spectra & Noise Waves relative to: (1) Tyre Rotation (2) Wheel Rotation	
2.3.3.	Accuracy of Measurement			

2.1.1. Tyre Design Features

2.1.1.1.1. Tread Pattern on Various Surfaces

In investigations by Robertson and Cox (1957) (1958) of truck tyre noise, various tyres were fitted to a truck and the rear wheels supported on a chassis dynamometer. The tyres were allowed to coast from 95 km/h (60 mph) to a stop. Tape recordings were made and these were analysed subjectively by replaying them to an audience, and objectively with a measuring instrument in terms of phons. Both analyses showed that the smooth tyres were quietest, followed in order of increasing noisiness by tyres with a tread pattern of widely spaced transverse grooves, tyres with a pattern of blocks, and tyres with a pattern of uniform pockets.

The National Bureau of Standards with Leasure et al (1970) (1972) showed dB(A) differences in noise levels between the following cross ply truck tyres. The noisiest pattern in each pair is referred to first.

TABLE 2.4. DIFFERENCES IN NOISE LEVEL DUE TO CHANGES IN TREAD PATTERN

Pattern Differences	Concrete	Asphalt
Pocket Retread versus Noisiest Cross bar	4-11	2-6
Quietest Cross bar versus Noisiest Rib	4-8	4-5
Circumferential Rib versus Blank Tread	1-2	1-2

Using a microphone attached to the vehicle 152 mm (6 in) behind the tyre and 202 mm (8 in) above the road, Reiter et al (1974) showed that dominant frequencies showed up with lug pattern tyres on smooth road surfaces.

The effect on automobile tyre noise of varying the percentage

void or groove volume in the tread pattern, over an extreme range for simple experimental cross grooved patterns was tested by Landers (1976). He used a travelling boom microphone behind the tyre on an asphalt surface. The tread patterns and the results are shown in Figure 2.1. A decrease of 15 dB(A) occurred as the percentage void was decreased from 60% to 10%.

The influence, on automobile tyre noise, of the number of tread blocks and the angle of the diagonal blocks (0° implies circumferential) was investigated by Dorsch (1976) using indoor testing. The type of tread pattern is shown in Figure 2.2. together with the results. The maximum noise level occurred with 60 blocks cut at 90° and 50 blocks cut at 20° and the latter were 1.2 dB(A) quieter. Both the extremes of the range, either a very high or a very low number of blocks, will reduce the noise by 5dB(A) but are unsuitable due to diminished tyre to surface grip in wet conditions.

Tread geometry is discussed in Chapter 2.1.1.1.4.1.

The Transport and Road Research Laboratories work, Underwood (1973) is considered in more detail in Chapter 3.

The review on the effects of tread segment pitch on dominant tones of the tyre noise is given in Chapter 6.1.

2.1.1.1.2. Tyre Size

2.1.1.1.2.1. Rim Diameter

In smooth drum tests J C Walker and Major (1975) found that with block pattern radial ply automobile tyres, of the same section and tread width, 254 mm (10 in) rim diameter tyres were 1.2 dB(A) noisier than 330 mm (13 in).



Figure 2.1.

CROSS GROOVED PATTERNED TYRES - PERCENTAGE VOID v NOISE LEVEL

(Landers, 1976)



Figure 2.2.

DIAGONAL BLOCK PATTERNED TYRES – NUMBER AND ANGLE OF BLOCKS v NOISE LEVEL

(Dorsch, 1976)

2.1.1.1.2.2. Sectional Width

J C Walker and Major (1975) showed the effect of section width at constant load on 330 mm (13 in) radial ply tyres with a serrated rib and siped tread pattern. The 145 mm section was 2.5 dB(A) quieter than a 185 section tyre on both hot rolled asphalt B.S. 594 and smooth asphalt. As sectional width decreases the tread diameter also decreases for the same aspect ratio. In this case the diameter effect opposes the tread width effect.

An 8.25-20 cross ply tyre was 1.3 dB(A) quieter than a 10.00-20 tyre at the same load as shown by the Rubber Manufacturers Association (1971).

2.1.1.1.2.3. Aspect Ratio

J C Walker and Major (1975) demonstrated that a low aspect ratio (low percentage height divided by sectional width) 60 series tyre is 0.7 dB(A) noisier than an 80 series tyre on smooth asphalt and 1.2 dB(A) noisier on B.S. 594 hot rolled asphalt. This compares with the findings of Hillquist and Carpenter (1974), that 60 series belted bias tyres are 2 dB(A) noisier than 78 series. With these tyres of constant sectional width, as aspect ratio decreases, tread diameter decreases and tread width remains constant. Thus part of the dB(A) difference is due to the diameter effect.

2.1.1.1.3. Tread Profile - Cross Bar Truck Tyres

Tetlow (1971) demonstrated that tyres wore to a greater tread radius than in the new state. This gave a 6dB(A) increase with half worn cross-bar tyres. Grinding the tyre to the original smaller tread radius reduced the noise level to the original value for the new tyres, this reduced the load on the tread blocks in the edge of the tread and increased load on the centre rib.

The tread contour or radius is defined as the unloaded cross

sectional shape of the tread, neglecting the tread pattern depressions, usually given as a radius or radii.

The author notes that on the front wheel steering position the wear is greatest on the shoulders, thus giving a smaller tread radius. Conversely on rear wheel drive positions, the wear is greatest on the centre of the tread, leading to a greater tread radius.

Tread Contact Patch

2.1.1.1.4.1. Shape of Contact Patch

With regard to the geometry of the tread pattern, Richards (1974) shows that if the contact patch has a fairly flat leading edge, staggering the rows of blocks across the tread has a considerable effect as shown in Figure 2.3. The aim is to get the blocks out of phase at the leading and trailing edge of the contact patch.

2.1.1.1.4.2. Pressure Distribution

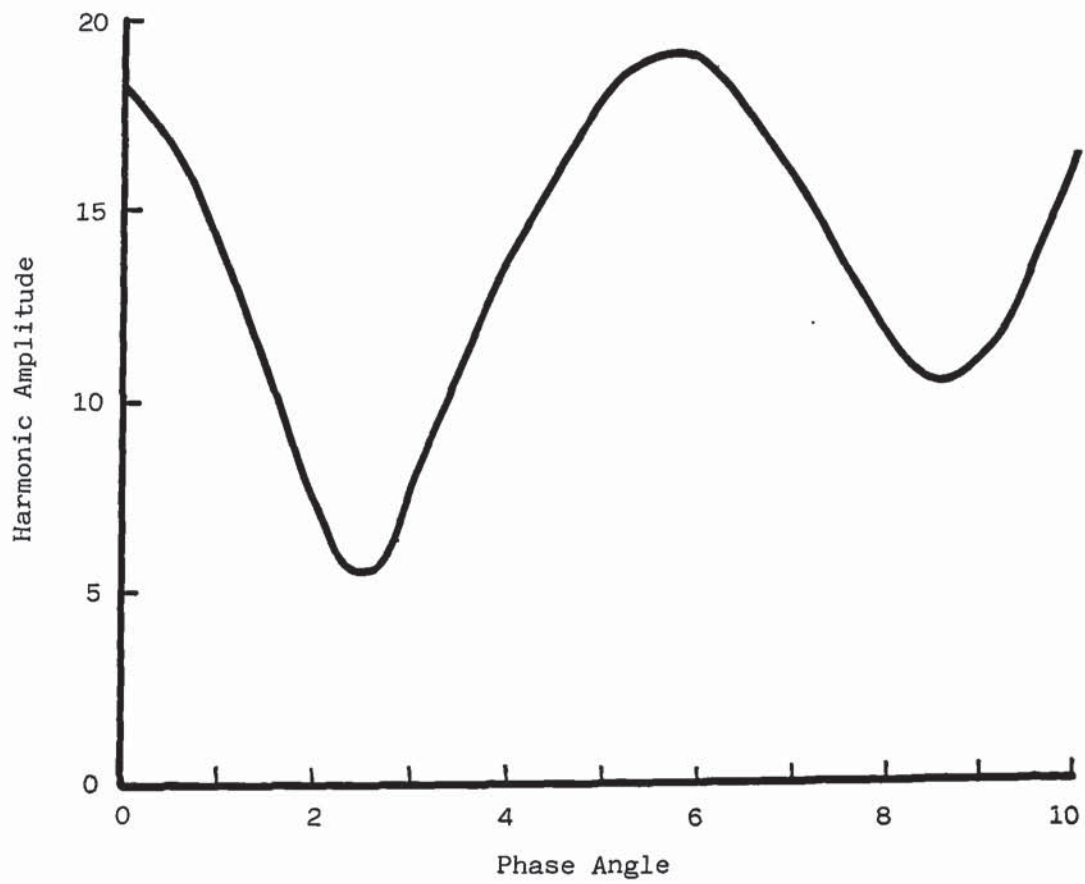
The normal pressure distribution has an effect on the shape of the contact patch and the tread profile has an effect on the contact pressure.

Material Factors

2.1.1.2.1. Tread Compound

Underwood (1973) found that the average differences between high hysteresis (HH) tread compound and natural rubber compound were less than 1.0 to 1.5 dB(A). In dry conditions the H.H. blank tyre is 1 dB(A) noisier and the H.H. traction tyre is 1 dB(A) quieter.

H.H. serrated rib radial ply car tyres were 0.9 dB(A) quieter on



RELATIVE HARMONIC NOISE AMPLITUDE v TREAD ROW PHASE ANGLE

(Richards, 1974)

Figure 2.3.

smooth asphalt and 1.7 dB(A) quieter on hot rolled asphalt (BS 594) as demonstrated by J C Walker and Major (1975).

2.1.1.2.2. Casing Reinforcement

The effects of different synthetic fibre casings were tested by Wiener (1960). He showed, with a microphone attached to an automobile, at a speed of 80 km/h (50 mph), a significant difference in the spectrum level around 500 Hz on both a smooth and a rough road.

Other Factors

2.1.1.3.1. Tyre Construction

J C Walker and Major (1975) tested block pattern automobile tyres with the same tread width and found the radial ply tyre to be 0.7 dB(A) quieter than the cross ply tyre. It is known that in the case of the radial ply tyres there is less tread shuffle or micro-movement on the road.

2.1.2. Operating Conditions

2.1.2.1. Speed

Leasure (1975), in his review, says truck tyres are characterised by an increase of 6 - 12 dB(A) for a doubling of vehicle speed in the range 48 - 96 km/h (30 - 60 mph).

10 dB(A) with doubling of speed corresponds to 33 dB(A) per decade and 3 dB(A) per 25% increase in speed. With regard to the accuracy of pass-by testing a 2% change in speed causes approximately 0.3 dB(A) change in level.

Increases from 6 - 15 dB(A) per doubling of speed on dry surfaces for cross ply truck tyres were found by Harland (1974).

2.1.2.1.1. Direction of Rotation

A chevron type tyre pattern is quieter with the tip of the V facing backwards in the contact patch, Wilken et al (1976).

2.1.2.2. Load and Inflation Pressure - Cross Ply Truck Tyres

Flanagan (1972) reported that if the load is kept in the 75% to 100% range of the maximum rated load, and the scheduled pressure used, the sound level does not change appreciably. Leasure (1970) showed that increasing the load per tyre from 690 to 2010 kg (1530 - 4430lb) on cross bar tyres gave a greater sound level increase, 6 - 8 dB(A), than on rib tyres, 1 - 3 dB(A).

2.1.2.3. Cornering, Traction and Braking

Tyre squeal is the characteristic tonal noise made by certain tyres when cornering, accelerating or braking fiercely enough almost to induce skidding. It is more likely to occur in hot weather. The tendency has been considerably reduced by the use of high hysteresis compounds.

The calculation of tyre squeal from material properties was given by Trivisonno et al (1967). The squeal frequency decreases with slip angle and decreases as tread depth increases, as discussed by J C Walker and Major (1975).

Normal braking or driving torque does not appear to affect truck tyre noise according to Tetlow (1971).

2.1.2.4. Tread Wear - Cross Ply Truck Tyres

Seldom does a tyre grow quieter at any speed as it wears out. The increase in noise level from new to half worn treads is typically 2.5 dB(A) for ribbed patterns and 4.2 dB(A) for cross bar patterns. The noise level then decreases as the fully worn

state is approached, unless the tread pattern is such that pockets of air can be trapped, as discussed by Flanagan (1972). Irregular wear tends to occur occasionally on truck tyres, especially when the wear due to lightly laden motorway running predominates in the duty cycle. This is fairly rare in the U.K. because of the limited unbroken motorway mileages. Some examples of this type of wear can increase noise.

2.1.2.5. Tread Surface Condition

When tyres are run on a smooth drum, the polishing of the tread is considerable, and wear is negligible. This can give a sticky surface to the tread which is not representative of the surface of the tyre when running on the road.

2.1.2.6. Temperature

The effect of temperature on tyre squeal has been discussed in section 2.1.2.3. In straight ahead rolling, temperature causes no significant change in noise level when drum testing both rib and cross ply truck tyres between 25^o and 125^oF according to Tetlow (1971). However, in the case of nylon car tyres which have flatted, that is parked overnight in the cold immediately after a high speed run, the flats should be run out before testing commences (J C Walker and Major 1975).

2.1.2.7. Time - Ageing

Over a period of two years rubber will slightly harden and the noise can increase by 1 - 2 dB(A) according to Favre and Pachiaudi (1974).

2.1.2.9. Wheels

In drum tests with block pattern tyres J C Walker and Major (1975) showed that a 254 mm (10 in) light alloy wheel was 1.5 dB(A)

quieter than a steel wheel.

2.1.2.10. Tyre Screens

With local enclosures over each wheel and a gap of 5 - 100 mm between the screen and the road, a $5_{\pm 2}$ dB(A) reduction occurred on dry roads, and $7_{\pm 3}$ dB(A) when the inside of the screens was lined with sound absorbent. There was a 10°C rise in tyre temperature, Gedefelt and Voight (1976).

2.1.2.11. Tyres per Vehicle

Doubling the load and number of wheels raises the sound level by approximately 2 dB(A) as shown by Tetlow (1971). Doubling the sound power would give an increase of 3 dB but in practice some degree of shielding occurs of the noise from the far side wheels.

2.1.2.12. Traffic Density and Mix

The effect on noise level of the percentage of heavy goods vehicles is discussed by Millard (1970) and Nelson and Piner (1977). The relative speed limits in force for cars and trucks has a large effect on the traffic noise.

The relative levels of trucks and automobiles under load and coasting conditions are shown in Figure 2.4., Harland (1974). The results were obtained with two automobiles and two trucks on hot rolled asphalt surfaces.

The following table by Watkins (1974) "shows the values by which L_{10} is reduced (L_{10} is the noise level exceeded for 10 per cent of the time and is commonly accepted in the United Kingdom as having reasonable correlation with annoyance). The reductions are given for four different values of traffic flow, and for four different proportions of lorries to automobiles. In each space in the table there are two values, the first gives the reductions if all lorry noise levels were reduced by 10 dB(A), and the second (in brackets) gives the corresponding value if in addition to this reduction in lorry noise, all car noise levels

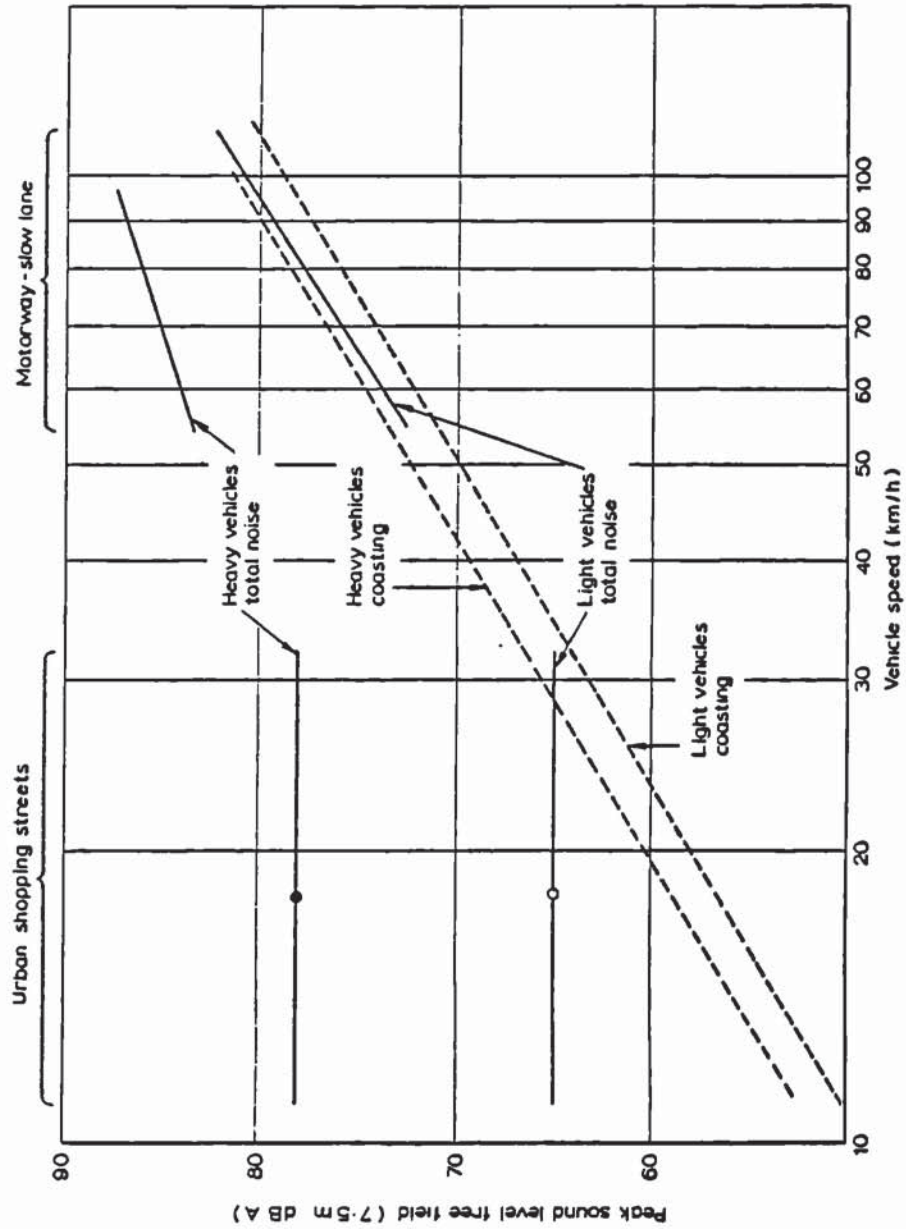


Figure 2.4.

COASTING NOISE AND TOTAL NOISE FOR LIGHT AND HEAVY VEHICLES

(Harland, 1974)

were reduced by 5 dB(A).

The table establishes a strong case for not resting content with producing quieter lorries, but for also proceeding to reduce the noise levels of cars."

TABLE 2.5. REDUCTIONS IN L₁₀ DUE TO REDUCTION IN NOISE OF INDIVIDUAL VEHICLES

Flow (vehicles/hour)	Reduction in L ₁₀ (dB(A))			
	10% lorries	20% lorries	40% lorries	80% lorries
200	1.4 (5.6)	2.5 (6.3)	4.5 (7.3)	8.4 (9.3)
400	1.4 (5.6)	2.5 (6.4)	5.1 (7.9)	8.8 (9.6)
800	1.5 (5.9)	3.1 (7.0)	5.9 (8.8)	9.0 (9.8)
1500	2.0 (6.4)	4.2 (7.8)	6.3 (9.1)	9.0 (9.8)

2.1.3. Noise Generation Mechanisms

Introduction

Three mechanisms for tyre/road noise generation are:

- (a) impacting between the tread and the road
- (b) micro-movements of rubber on the road
- (c) air pumping by the tread pattern

Three possible resonances are those of:

- (a) the tyre
- (b) the air in the tyre
- (c) the tread elements

2.1.3.1.1. Impacting

The impacting mechanism has been studied by Richards (1974).

Accelerometers inserted inside the tyre showed over 600g change in acceleration as the tread entered and left the contact patch at a speed of 113 km/h (70 mph). Carpeting the surface to soften the impact reduced the noise level of a block pattern tyre by 8 dB(A) at 48 km/h (30 mph) and 3.5 dB(A) at 113 km/h (70 mph).

2.1.3.1.2. Stroking

With micro-movements of the tread, J C Walker and Major (1975), showed with glass plate studies of a blank tread steel radial ply tyre, that up to 2.5 mm total movement of a point on the tread relative to a point on the ground occurs as it passes through the contact patch. It has been suggested that this is the main cause of the noise of a smooth tyre on a smooth surface, Richards (1974).

2.1.3.1.3. Air Pumping

The third mechanism of air pumping was discussed by Hayden (1971) and the theory was further developed to predict directivity patterns by Samuels and Alfredson (1974). Air is ejected between tyre and road during contact and injected just after contact. Air pumping is a dominant mechanism in the case of treads which can trap pockets of air on smooth road surfaces. However Richards (1974) concluded that the impacting mechanism was dominant as regards noise from cavity pockets in the road.

2.1.3.3. Tyre Vibrations

Tyre vibrations have been discussed by Leasure and Bender (1975). The vibrational characteristics and mechanisms of sound radiation may be evaluated together in three frequency regimes as illustrated in Figure 2.5., by the acceleration response of different points on the tyre to a point excitation as shown by Hayden (1971).

At low frequencies 30 - 100 Hz, the tyre would respond in the vicinity of the tyre contact area. The radiation is likely to be monopole in nature. This mechanism is unimportant as the ear is less sensitive in this frequency region.

At higher frequencies 80 - 150 Hz, the carcass responds in a modal manner. Modes were investigated for 10 - 22 cross ply truck tyres by Reiter (1974) and H78-15 car tyres by Potts (1973).

TABLE 2.6. RADIAL MODE RESONANT FREQUENCIES VERSUS TYRE CONSTRUCTION

Radial Mode Number	Radial Mode Resonant Frequencies (Hz)					
	1	2	3	4	5	6
Automobile Tyre - Radial Ply	59	80	96	112	130	151
Automobile Tyre - Cross Ply	140	168				
Truck Tyre - Cross Ply		103	116	159	196	

An example of the third radial mode is given in Figure 2.6. by Potts (1975). However this mechanism is also unimportant since the tyre carcass is an inefficient radiator, while responding in a modal manner, because the ratio of the distance between the contracting and expanding parts of the tyre to the wavelength of sound in air, is small.

At still higher frequencies, flexural waves in the carcass will be generated at the tyre/road interface as sketched in Figure 2.7. by Leasure (1975). "These waves are expected to attenuate rapidly with distance from the contact area. The sound radiated by these waves depends on a number of factors, the most important of which is the phase velocity in the tyre. The propagation speed of a complex wave is frequency dependent, with the high frequency components travelling faster than the low frequency components, thereby altering the shape of the wave. Each frequency component of the complex wave progresses at its own velocity, the so-called phase velocity of the component. If this velocity is above critical (i.e. above the speed of sound in air) the waves will radiate very efficiently. However, even sub-critical waves may radiate significant sound levels owing to low wave number components associated with damping, edge effects, and the structural near field associated with the excitation point."



Illustration removed for copyright restrictions

TRANSFER OF INPUT ACCELERATION TO REMOTE PARTS OF TYRE

Figure 2.5.

(Hayden, 1971)



Illustration removed for copyright restrictions

SHOULDER VIEW OF THIRD MODE RADIAL VIBRATION RESONANCE AT 96 Hz
FOR A HR 78-15 RADIAL TYRE

Figure 2.6.

(Potts, 1975)



Illustration removed for copyright restrictions

SIDEWALL FLEXURAL WAVES

(LEASURE 1975)

Figure 2.7.

Preliminary accelerometer data indicates that waves are also propagated out from the contact patch along the tread circumference, Eberhardt (1975).

Eberhardt recorded in service truck tyre sidewall vibrations and periodically repeated segments were chosen for analysis based on consideration of data periodicity, stationarity and normality. The segmented data is then subjected to analysis by digital processing methods, and results are presented in detail for sound power spectra and coherence between vibration and sound as shown in Figure 2.8. The high values of coherence support carcass vibration as a major source of noise for the cross bar truck tyre.

Coherent peaks in the spectrum tend to follow harmonics of the 400 Hz lug passage fundamental frequency.

Eberhardt (1979) extended his work and showed that vibrations of the tread band rather than those of the sidewall are the dominant noise source. Application of the Rayleigh integral to the experimentally measured tyre vibration field resulted in sound pressure levels that agree closely with those measured by experiment.

2.1.4. Models of Tyre Noise

Reiter (1973) modelled two simple tread patterns, a typical rib tyre and a simple cross bar tyre.

The cross bar pattern is considered as a series of damped parallel-pipedes resting on a rigid foundation. It predicts a 3 dB(A) increase in sound pressure as tread depth is reduced by 50%. A doubling of the tyre load increases the sound pressure level by 6dB.

The rib pattern is considered as a flexible string embedded in an elastic foundation. Figure 2.9. shows how the Doppler effect due



Illustration removed for copyright restrictions

COLLECTIVE ESTIMATE OF THE ACCELERATION-COHERENT SOUND AND ASSOCIATED 95% CONFIDENCE INTERVAL FOR TYRE SEGMENTS
ONE THROUGH SIX AS COMPARED TO THE TOTAL SOUND SPECTRUM
(Eberhardt, 1975)

to tyre motion shortens the wavelength at the front of the tyre and lengthens it at the rear. This causes the rear to be a more efficient radiator than the front.

Samuels (1974) modelled the directivity patterns of simple constant pitch, in phase block pattern tyres, assuming the air pumping noise generating mechanism to be dominant.

2.2. Surface Variables and Environment

2.2.1. Road Texture

Fuller (1976) obtained a correlation between the dB(A) level of a vehicle coasting with circumferentially grooved tyres and pavement roughness. A nominal level of surface macrotexture is desirable to achieve minimum tyre/road noise generation. The correlation held for three parameters expressing pavement roughness including texture height. Tests were carried out on seven surfaces.

The work by Underwood (1973) on road texture effect on noise is discussed in detail in Chapter 3.

2.2.2.2. Wet Conditions

If bulk water does lie on the surface then the noise can be 7 - 11 dB(A) higher than in the dry with truck tyres according to Underwood (1973). However, the author notes that if the road surface has enough drainage including adequate camber, to drain away the surface water, such as the porous surface of friction course or the Delugrip type of surface, then noise in the wet is hardly any higher than noise in the dry.

2.2.2.5. Obstacle Proximity

A guard rail and curb on the side of the lane opposite the



Figure 2.9.

EFFECT OF VEHICLE SPEED ON WAVELENGTH

(Reiter, 1973)

microphone gave approximately a 0.6 dB(A) increase in noise level at 15.2 m (50 ft) as shown by Miller and Thrasher (1976).

2.2.2.7. Wind Velocity

The effect of wind in the direction of travel of the vehicle was investigated by Oswald and Hickling (1976). The airspeed of the truck was measured by a pitot tube. The road surface was smooth asphalt. The tyre/road noise levels were corrected for vehicle aerodynamic noise assuming a 6th power law.

TABLE 2.7. CHANGE IN PASS-BY LEVEL VERSUS GROUND SPEED AND AIR SPEED

	Change in Level dB(A)	Level at 15 m dB(A)	Change in Level dB(A)	Corrected Tyre/Road Noise Level dB(A)
Tyre Tread Pattern				
Ribbed	+2.5	67.0	-1.3	65.3
Blank	+5.0	62.5	-3.6	57.3
Air Speed (km/h)	100	80	60	0
Ground Speed (km/h)	80	80	80	80

2.3. Types of Noise Measurement

2.3.1.1. Standard Pass-by Tests

The conditions for coasting pass-by tests are according to BS 3425 in the U.K. and SAE J57 in the U.S.A. However even low wind speeds can effect the noise level of the quieter tyres due to aerodynamic vehicle noise.

2.3.1.2. Distance of Stationary Microphone

In a free field, doubling the distance from a point source drops the noise level by 6 dB(A), whereas doubling the distance from a line source gives a 3 dB(A) drop.

On the road, the wheelbase of the vehicle determines the degree of departure from the point source condition. The figures given below show the difference in level between 7.6 m (25 ft) and 15.2 m (50 ft) during coasting pass-by tests. The figures are the average with concrete and asphalt surfaces. The author averaged Leasure's raw data, to obtain the differences for truck tyres.

TABLE 2.8. DIFFERENCE IN PASS-BY LEVEL FOR DIFFERENT VEHICLES DUE TO DOUBLING MICROPHONE DISTANCE

Vehicle	Difference	Reference
Automobile	5.8 dB(A)	Veres (1976)
Truck-single chassis 20 ft body-ribbed tyres	5.1 dB(A)	Leasure et al (1970)
Tractor and (trailer 40 ft long) ribbed tyres	4.5 dB(A)	Leasure et al (1972)

On a painted road surface, with an automobile, Veres (1976) obtained a difference of 6.5 dB(A). This higher value is believed to be due to the generation of higher frequency sound on the painted surface and the rapid attenuation of this sound with distance.

With regard to the accuracy of pass-by testing, a 0.3 m (1 ft) deviation of the vehicle causes an 0.17 dB(A) change at a microphone distance of 15.2 m (50 ft), and an 0.34 dB(A) change at 7.6 m (25 ft).



NORMALIZED PLOT OF THE CORRELATION COEFFICIENT $C(\tau)$ Maximum (Siddon, 1972)

Figure 2.10



DIRECTIVITY PATTERN FOR A FULLY WORN POCKET RETREAD
TYRE AT 73 km/h (45 mph) on ROUGH ASPHALT
(Close, 1974)

Figure 2.11

2.3.1.5. Directional Characteristics of Noise

Siddon (1972) made correlation measurements between sound from positions near to the tyre and sound from the far field 1.83 m (6 ft) from the tyre. As shown in Figure 2.10. the maximum correlation is obtained just behind the tyre.

Close (1974) demonstrated that tyres emit noise more strongly to the rear. Figure 2.11. shows this effect for a fully worn pocket retread tyre at 72 km/h (45 mph) on rough asphalt.

2.4. Criteria for Subjective Judgement of Tyre/Road Noise

Recommendations and legislation for traffic noise are based on dB(A) values and are discussed by Millard (1970).

Maximum L_{10} values are commonly used, that is the level exceeded for 10% of the time.

In order to confirm, supplement or replace the peak A weighted level, the SAE Truck Tyre Subcommittee carried out a program of tests in 1970. The twenty three members of the jury were positioned 22.5 m to 25.6 m (74 to 84 ft), and the microphone 18.3 m (60 ft), from the centre line of the vehicle path. The types of tyres used included twelve crossbar patterns and five rib patterns. The vehicle was either coasting, or under road load power for maintaining the speed. The road surface, of Portland cement, had been recently constructed and lightly used.

The sound levels and mean noise ratings for all test runs (Hillquist 1972) are shown in Figure 2.12. The averaged figures separating tread patterns (rib or cross bar) and vehicle operating conditions (vehicle coasting or engine under load) are shown in Figure 2.13.

The conclusion from these tests as discussed by Lippman (1972) indicates that the A weighted sound level accounts for the bulk



Figure 2.12

SOUND LEVELS AND NOISINESS RATINGS FOR ALL TEST RUNS

(Hillquist, 1972)



SOUND LEVELS AND NOISINESS RATINGS – AVERAGES OF FIVE OR MORE TEST RUNS

Figure 2.13

of the annoyance ratings. Variations equivalent to ± 3 dB(A) in ratings appear to be accountable, partly in terms of the persistence of the noise which is due to the directional properties of the noise emission causing it to be heard for a longer time, and possibly in terms of spectral characteristics.

The effect of spectral characteristics is discussed in Section 6.1.

CHAPTER THREE: COASTING VEHICLE PASS-BY NOISE IN THE DRY AND
WET GRIP

3.1. Introduction

Although much work has been carried out on coasting pass-by noise of various tyres on various road surfaces as referred to by J C Walker and Major (1975), very little work had been done on a combined study with wet grip included. The first important work of this type in the U.K. was the Transport and Road Research Laboratory (T.R.R.L.) work on the quiet heavy lorry project Underwood (1973).

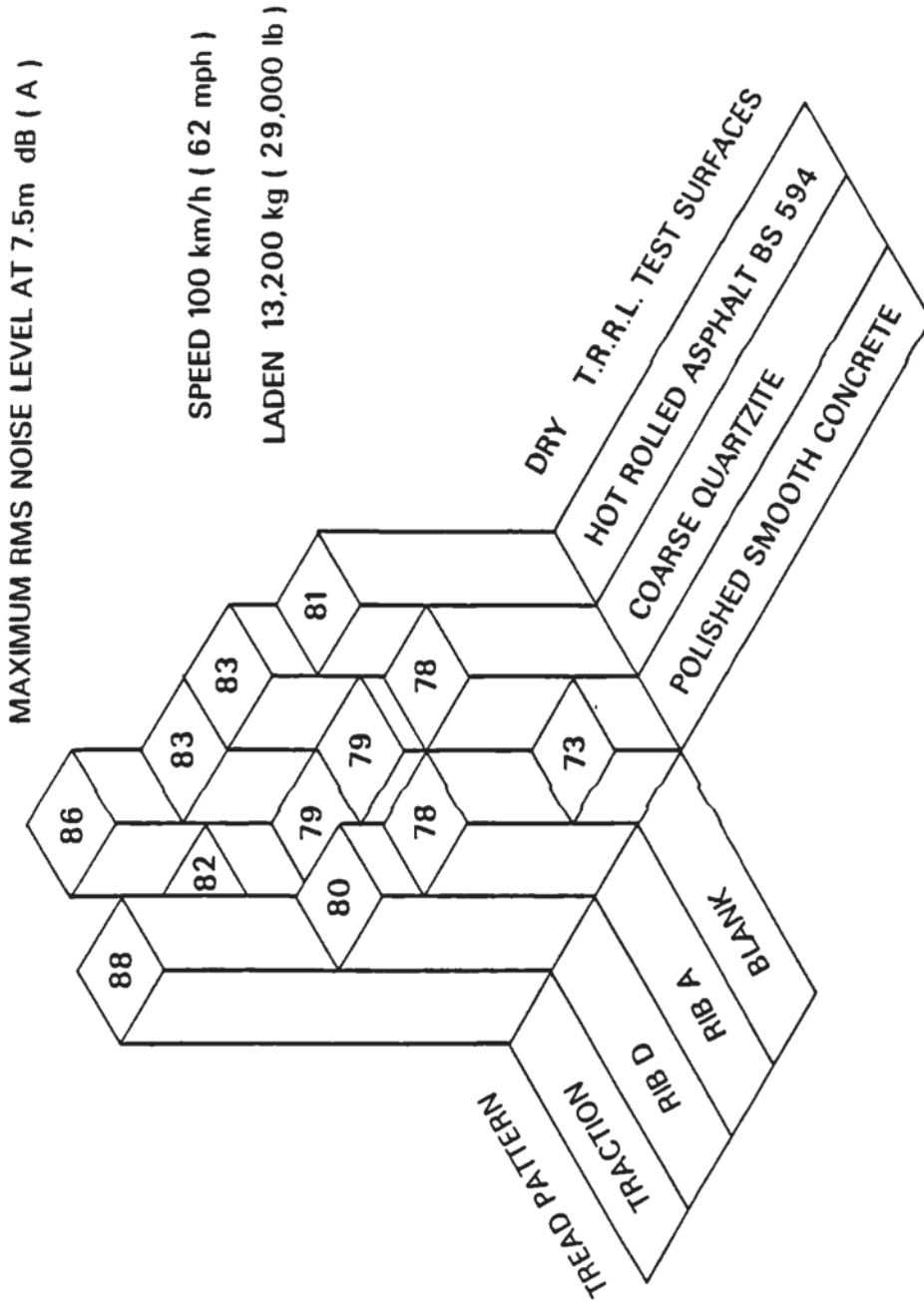
3.2. Relevance of decibel to Common Traffic Situation Variables

It is useful to consider the expected reduction in the measured sound level due to a traffic stream as a consequence of fitting quieter tyres or running on a quieter road surface, and relate this to other variables in this situation.

The traffic can be considered to be a line source when the distance between the highway is greater than half the average headway between the vehicles. A 3 dB(A) reduction which is halving of sound intensity, is equivalent to doubling the distance from the highway or to halving of traffic volume Millard (1970) or to reducing the traffic speed by 25%. Although 1 dB is fairly insignificant from a subjective point of view, it is of great importance to U.K. authorities paying compensation under the British Land Compensation Act when the measured noise is close to the limit.

3.3. Test Conditions

The pass-by tests are to B.S. 3425 conditions, with the vehicle coasting past the microphone at the required speeds. The microphone is 7.5 m from the centre line of the vehicle track and 1.2 m



TRUCK COASTING NOISE FOR VARIOUS TYRE ROAD COMBINATIONS

Figure 3.1.

off the ground. The Impulse Sound Level Meter B & K Type 2209 gives consistent readings and tape recordings are also taken.

3.4. Transport and Road Research Laboratory Tests

Figure 3.1. obtained from the results by Underwood (1973) summarises the main dB(A) results. It shows the coasting noise levels in dB(A) fast sound level meter response, at the standard distance of 7.5 m (25 ft) from the centre line of the vehicle for a laden truck 13,200 Kg (29,000 lb) travelling at 100 km/h (62 mph).

Here, there are three dry surfaces, polished smooth concrete, coarse quartzite and motorway surfaces, and three types of tyre pattern, blank tread, ribbed pattern and tractive pattern, on the 10.00-20 cross ply tyres. A blank tread is one of full tread thickness without a tread pattern.

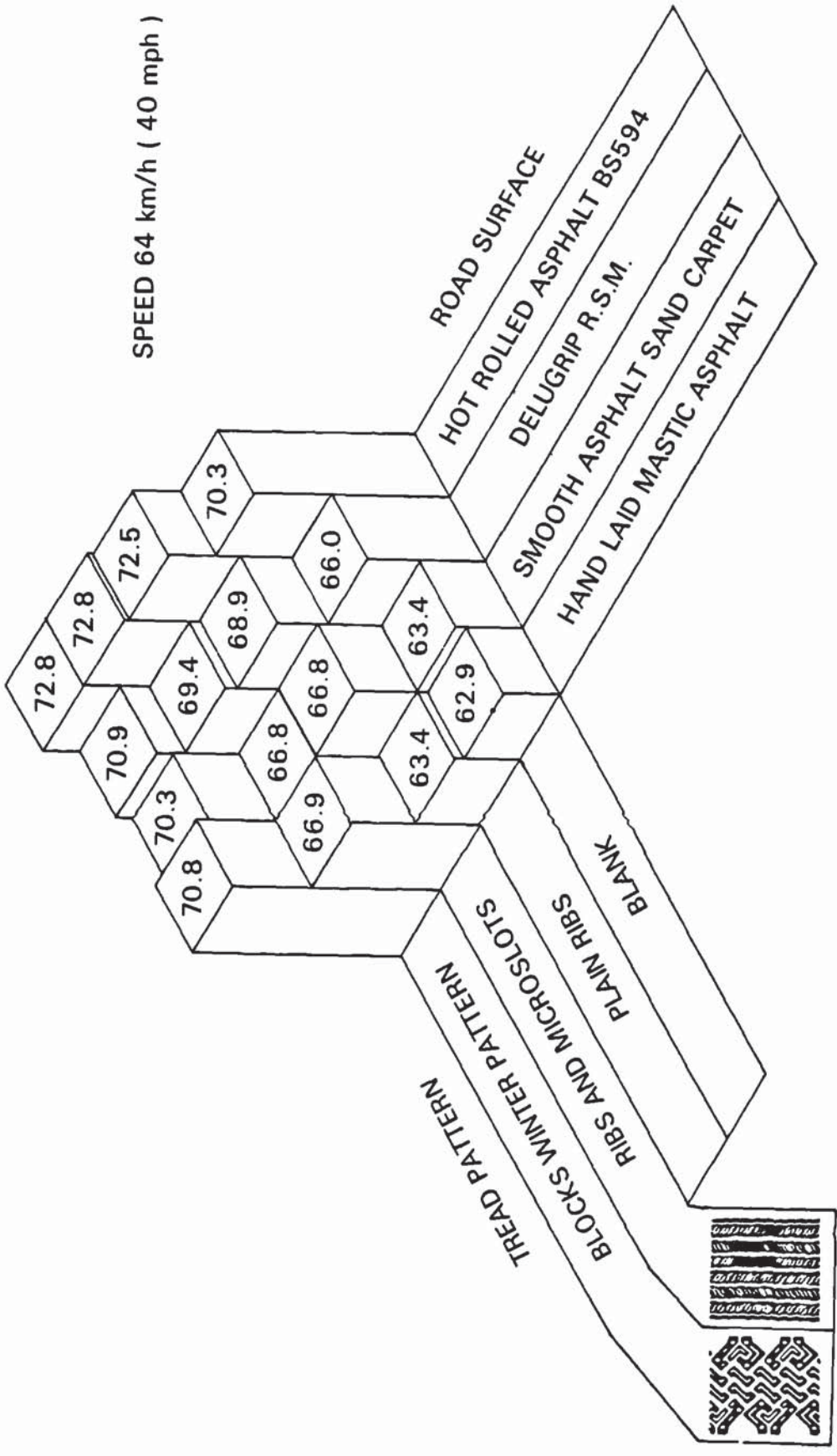
The polished smooth concrete surface shows a much greater contrast in tread pattern/road noise than the surfaces with the greater macrotexture which is the large scale texture of the road surface for water drainage. In the latter cases, ribbed tyres are 1 - 2 dB(A) noisier than smooth tyres and traction tyres are 3 dB(A) noisier than the ribbed tyres. Thus the total effect of any major pattern feature is of the order of 3 dB(A).

The author considers that this figure shows two distinct effects of the road surface on the tyre/road noise.

First is the excitation effect. The greater the macrotexture the more the tyre is excited and the greater the noise emitted, unless the frequency is high enough to be outside the sensitive region for the tyre. This is seen in the blank tyre results which get noisier as the macrotexture increases. There is no tread pattern effect in this case.

MAXIMUM RMS NOISE LEVEL d B (A) 7.5m DISTANCE

SPEED 64 km/h (40 mph)



AUTOMOBILE COASTING NOISE FOR VARIOUS TYRE ROAD COMBINATIONS

Figure 3.2.

Second is the break-up of the tread pattern effect. Up to a point, the greater the macrotexture the less the tread is in contact with the road. As it contacts just the tops of the stones, then the greater is the break-up and the less will be the noise due to the tread pattern. This is shown in the traction pattern results, where because of the transverse lug pattern (no centre rib) the effect of the break-up dominates over the excitation effect and the tyre gets quieter as the macrotexture gets greater.

The coarse quartzite surface is 3 - 4 dB(A) quieter than the motorway surface for all tread patterns.

The figures for the blank tyres on polished smooth concrete are not as low as they would be if corrected for vehicle aerodynamic noise, propeller shaft and rear axle noise.

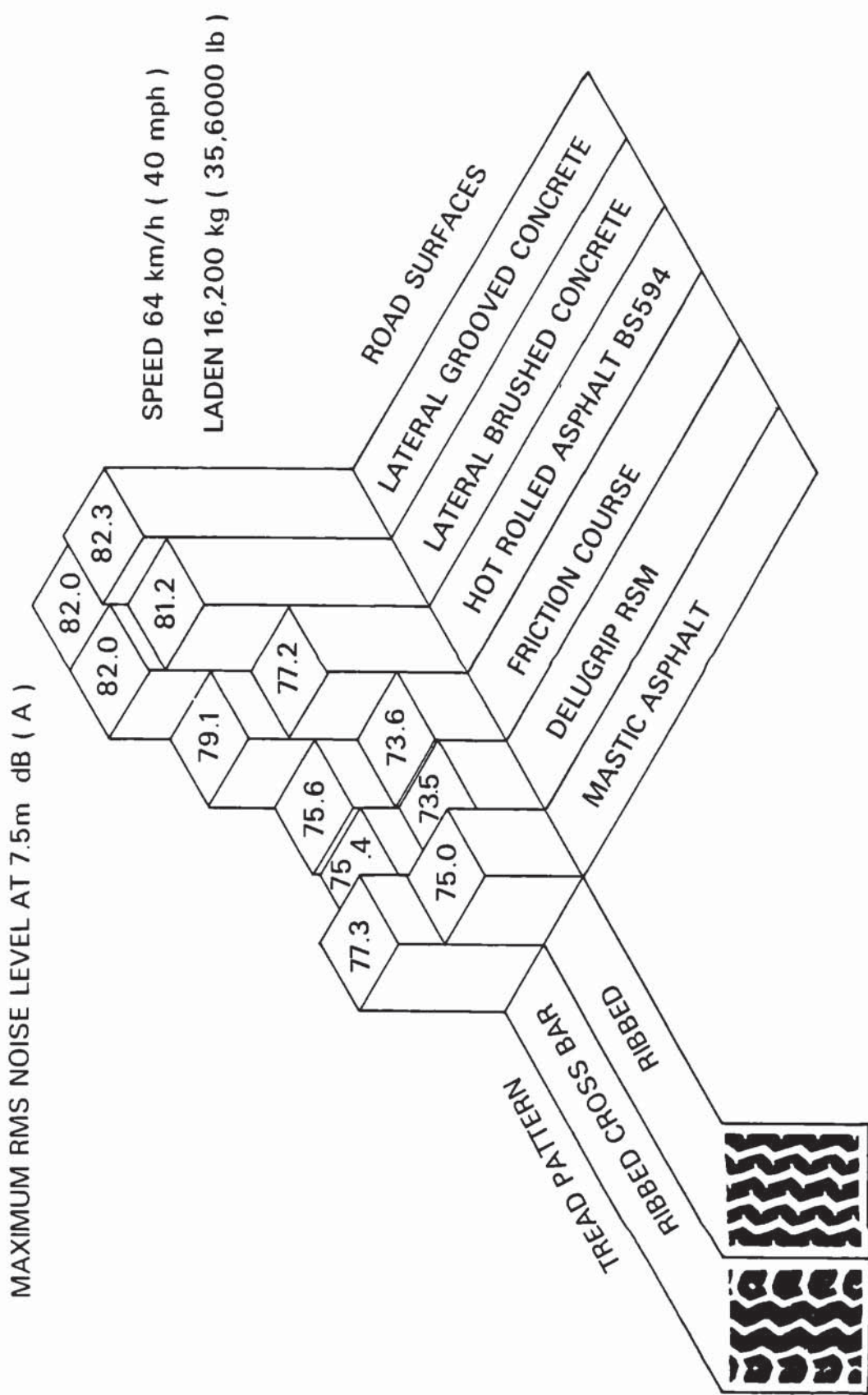
Oswald and Hickling (1976) showed blank tyre noise to be less than aerodynamic noise at this speed.

Turning to automobile pass-by results from J C Walker and Major (1975), Figure 3.2. again shows a similar pattern of results. These will be discussed later in the correlation with indoor tests.

3.5. Truck Coasting Noise - Six Road Surfaces, Two Tread Patterns

Figure 3.3. shows the author's measurements of coasting noise levels in dB(A) at 7.5 m (25 ft) from a laden truck 16,200 kg (35,600 lb) travelling at 64 km/h (40 mph). The figures are the average from eight runs. The noise measurements were taken with a Bruel and Kjaer precision Sound Level Meter Type 2209 using the fast response. The wind velocity was below 8 km/h (5 mph).

DR 22.5 radial ply tyres were used. Ribbed pattern tyres were



TRUCK COASTING NOISE FOR VARIOUS TYRE ROAD COMBINATIONS

Figure 3.3.

fitted to the front truck axle in all tests, and the ribbed pattern or the traction pattern (centre ribs and shoulder lugs) were fitted to all four wheels of the rear drive axle respectively. There are six road surfaces:

1. Mastic asphalt - a skidding test strip, with very low macro and microtexture.
2. *Delugrip Road Surfacing Material (R.S.M.) with a maximum aggregate size of 10 mm.
3. Friction course - pervious macadam.
4. Motorway - hot rolled asphalt BS 594 with 19 mm pre-coated chippings.
5. Lateral brushed concrete - brush marks 1 to 2½ mm deep and 3 to 10 mm apart.
6. Random lateral grooved concrete - grooves 10 mm wide and 30 to 55 mm apart.

The surfaces 2 to 6 are from 1 to 3 years old with medium traffic density up to 500 commercial vehicles a day.

The tyre pattern effects are shown in perspective with the road surface effects. Starting on the left hand side of the Figure, a certain amount of macrotexture decreases the pattern effect and then added macrotexture excites more noise. In the cases of lateral brushing and grooving of the surface, the tyre impacts the lateral ridges at the same time across the width of the tread, which is the worst way of noise generation.

3.6. Tyre/Road Noise due to Road Surface Texture

Figure 3.4. J C Walker and Major (1975) shows the relationship between length of tyre tread pitch or mean aggregate spacing, vehicle speed and the corresponding frequency generated. The

* Delugrip is a registered trade mark of Dunlop Limited.

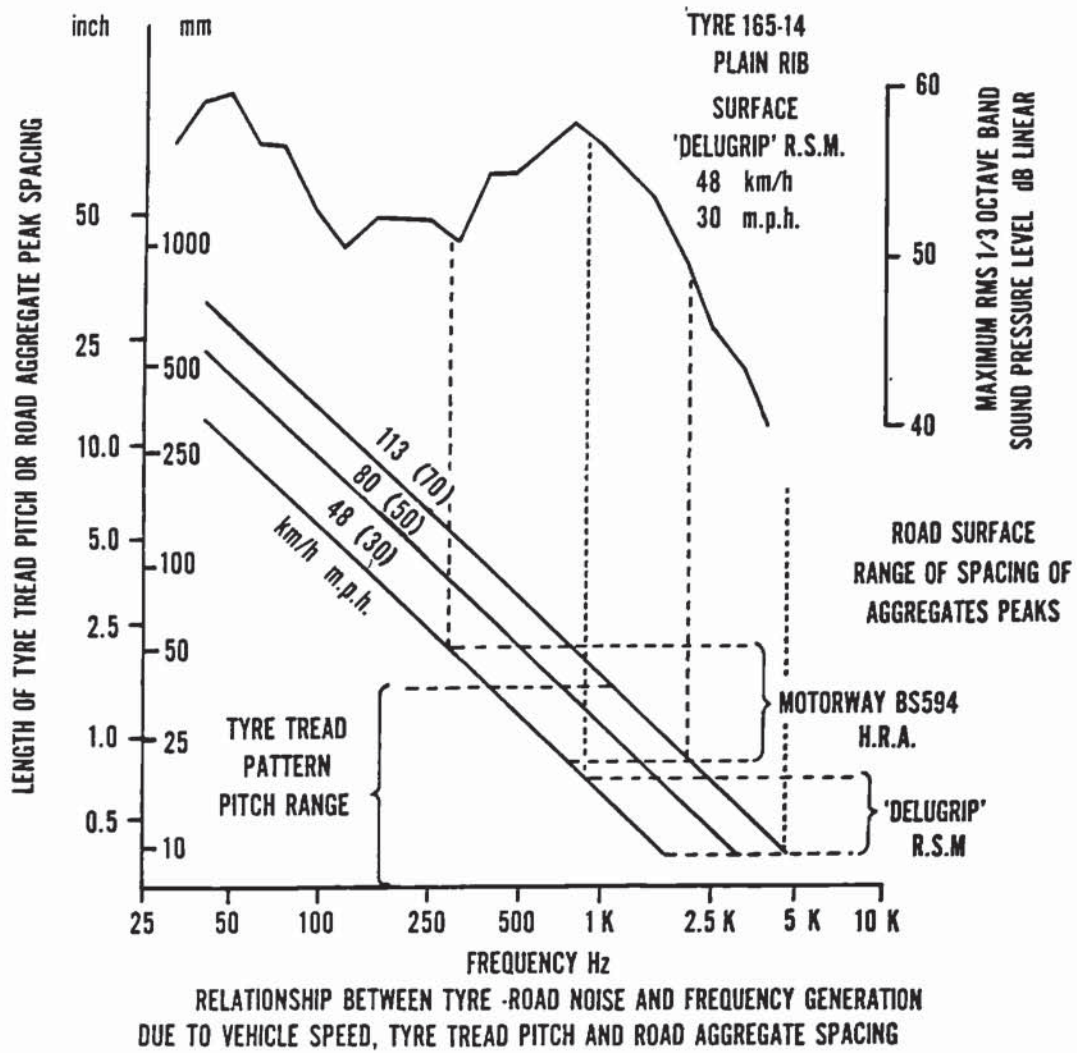


Figure 3.4.

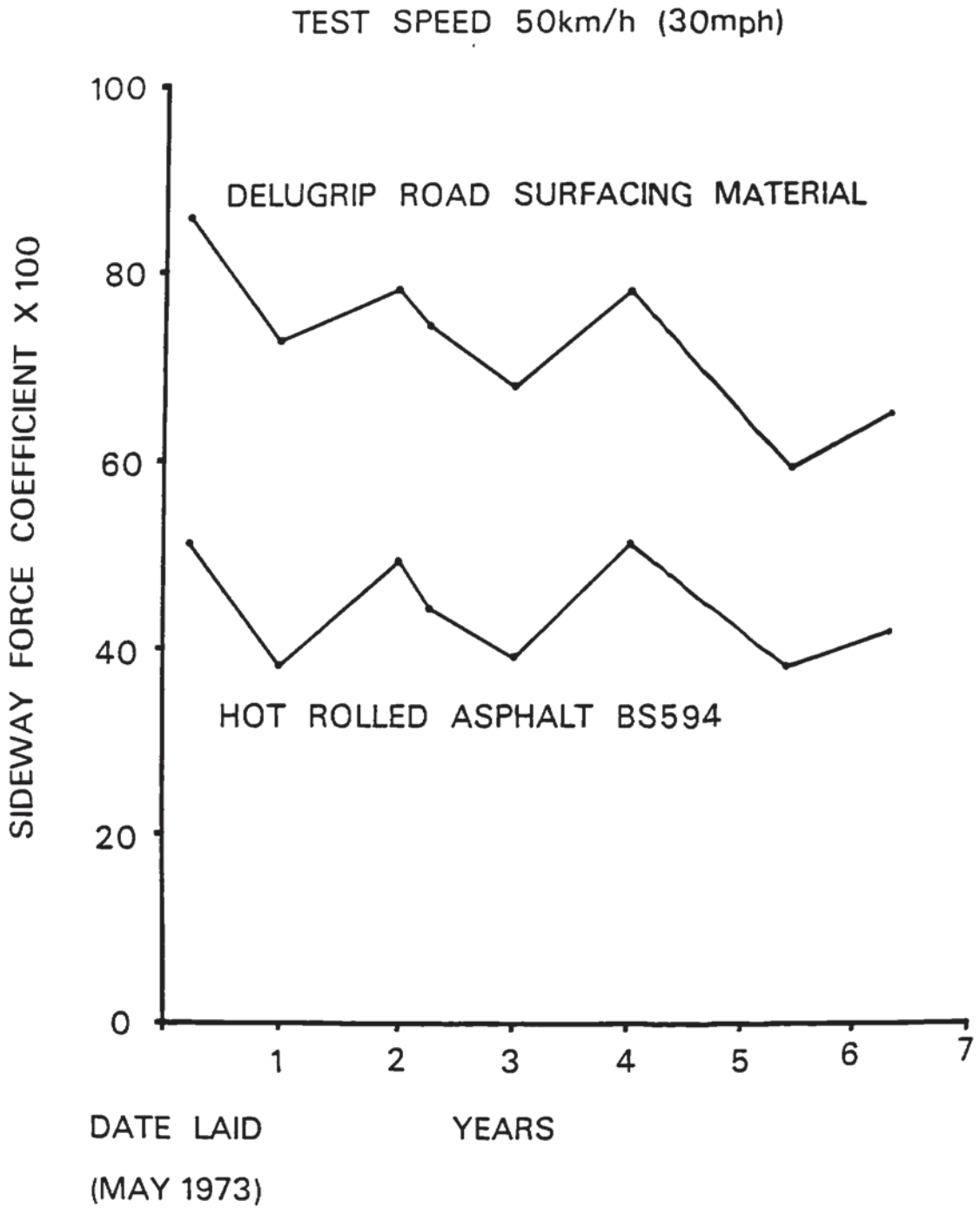
aggregate spacing is shorter on the Delugrip type of surface than hot rolled asphalt, resulting in higher frequencies from Delugrip for a given speed. Figure 3.4. shows in addition the third octave spectrum of a plain rib steel breaker automobile tyre on Delugrip. A broad peak in the order of 1000 Hz which is independent of speed together with a rapid decay rate as frequency rises further is shown in this spectrum. It also occurs with the blank treaded tyre on a smooth asphalt sand carpet surface at lower levels. Blank treaded truck tyres also show a fall in the noise in the high frequency region.

The higher frequencies from the Delugrip type of surface are in the less sensitive region for the tyre/road noise. It is evident that both the road designer and the tyre designer have to be careful in choice of aggregate size and tyre tread element pitch so that excitation is, as far as possible, in the less sensitive high frequency region.

3.7. Delugrip Road Surfacing Materials

In order to optimise wet grip at the tyre/road interface, research was directed initially towards the improvement of the tyre contribution, resulting in a steady improvement in the wet grip of tyres over the years. It was then realised that the greatest room for substantial improvement lay in the second half of the problem, that is, the potential grip of the road surface, and attention was directed towards improving this.

Delugrip Road Surfacing Materials have been developed after eight years of joint research between Dunlop and the University of Birmingham, theses Williams (1971) and Katekhda (1974). These materials have increased wet skid resistance, reduced spray generation and reduced tyre/road noise. These properties are maintained throughout their life.



WET FRICTION A4 (LONDON) EXPERIMENT

Figure 3.5.

The large scale texture of the surface, the macrotexture, is optimised for the drainage of bulk water across the surface and to aid water drainage from under the contact patch, as shown by Bond et al (1973).

The microtexture for adequate skidding resistance at any speed by rupture of the thin remaining water film should be within the range 0.01 to 0.1 mm as shown by Williams and Lees (1970) and (1973).

The Delugrip type of surface is a wearing course material designed to a rational method of aggregate grading as described by Lees (1970) and complies with the above requirements for macrotexture and microtexture. The macrotexture is achieved through mix design principles to give adequate sub-tyre drainage for the average traffic speed of the site and is maintained by differential wear rates of the aggregates. The microtexture required is achieved and maintained by selection of suitable aggregates having resistance to polishing.

The substantial benefit in wet grip is illustrated by the sideways (lateral) force coefficient figures in Figure 3.5. An advantage of greater than twenty points has been sustained over the years. The figures were taken over a six year period for a trial area of the A4, London, comparing the Delugrip type of surface with hot rolled asphalt. The traffic on this road is very heavy. The values were measured by the Greater London Road Authorities using the Sideway Force Coefficient Routine Investigation Machine S.C.R.I.M. (T.R.R.L.) which has become the standard wet grip testing machine for road authorities in the U.K. In this machine the lateral force coefficient of a blank tread motor cycle tyre at a slip angle of 20° is measured in the wet at a speed of 50 km/h (30 mph).

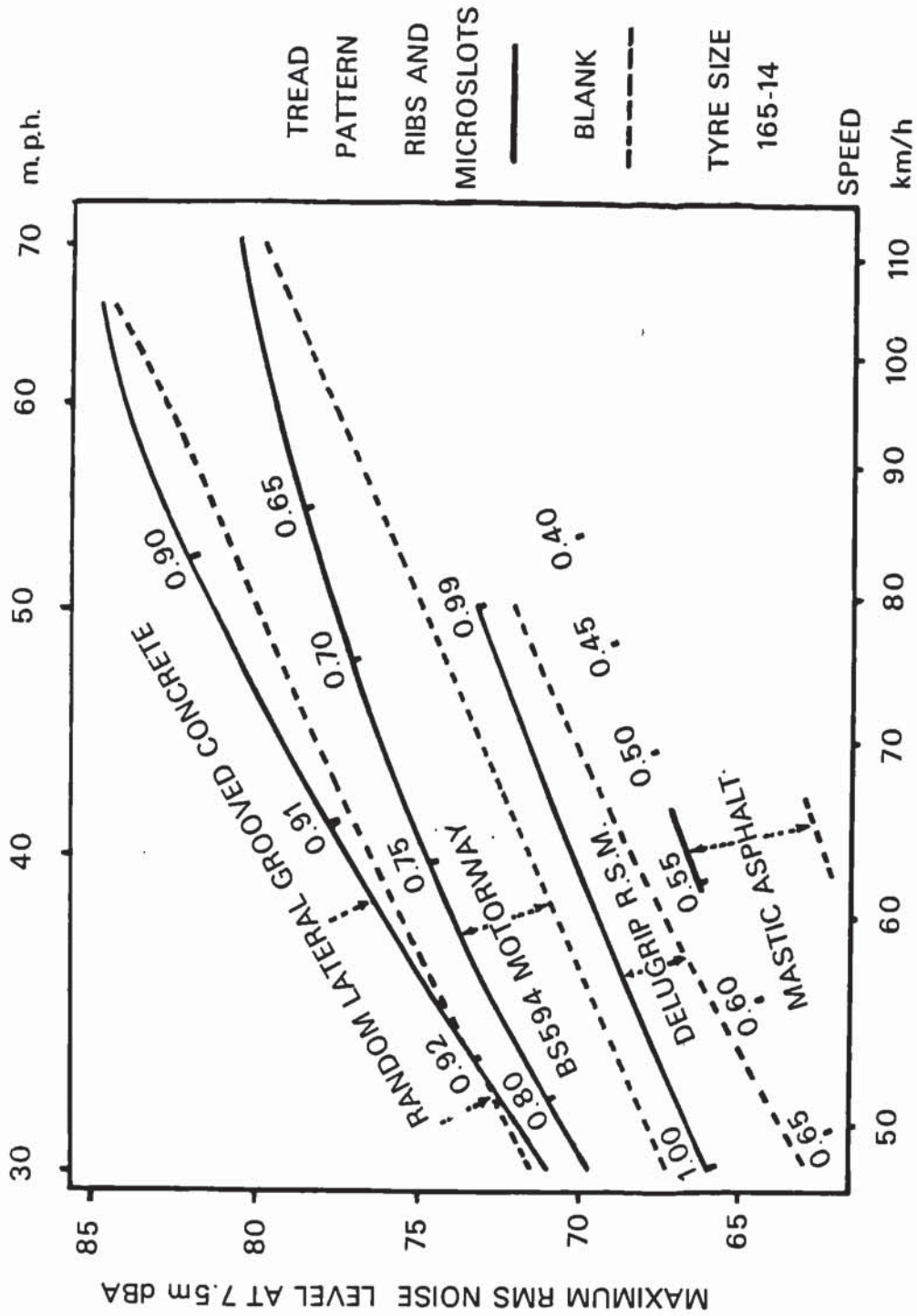


Figure 3.6. EXTERNAL CAR COASTING NOISE GENERATION ON DISSIMILAR SURFACES - DRY WITH BLANK AND PATTERNED TYRES & PEAK BRAKING FORCE COEFFICIENT FIGURES - WET

3.8. Automobile Tyre/Road Noise and Wet Grip versus Vehicle Speed

Figure 3.6. shows the increase in automobile coasting noise levels with speed at 7.5 metres (25 ft) distance with blank tread tyres and ribbed and multislotted tread tyres. The peak braking force coefficient figures in the wet are shown for the latter.

The braking tests are with the front wheels only braked, as described by Allbert and J C Walker (1965), and the deceleration is measured with a decelerometer and U.V. recorder. Load transfer effects are allowed for as shown by Williams T. et al (1973).

With doubling of speed, the increase in noise level with speed, ranges from 9 to 12 dB(A). The truck tyre tests previously discussed show an average of 10 dB(A) increase with doubling of speed. This corresponds to 3 dB(A) per 25% increase in speed.

The surfaces range in coarseness from the random spacing grooved concrete, which has good wet grip but is the noisiest, through British Standard hot rolled asphalt BS 594 which has lower wet grip when worn and is noisy, through Delugrip Road Surfacing Material which has good wet grip when worn and is quieter, to the smooth mastic asphalt skidding test track surface which has poorest wet grip and is the quietest. Thus, Delugrip Road Surfacing Material is an attempt to optimise both wet grip and noise.

3.9. Automobile and Truck Tyre/Road Coasting Noise and Wet Grip

Figure 3.7. shows the form of the relationship between wet grip and noise in the dry for various tyre/road combinations. The truck figures are from Transport and Road Research Laboratories work Harland (1974) and the coasting noise levels are those which

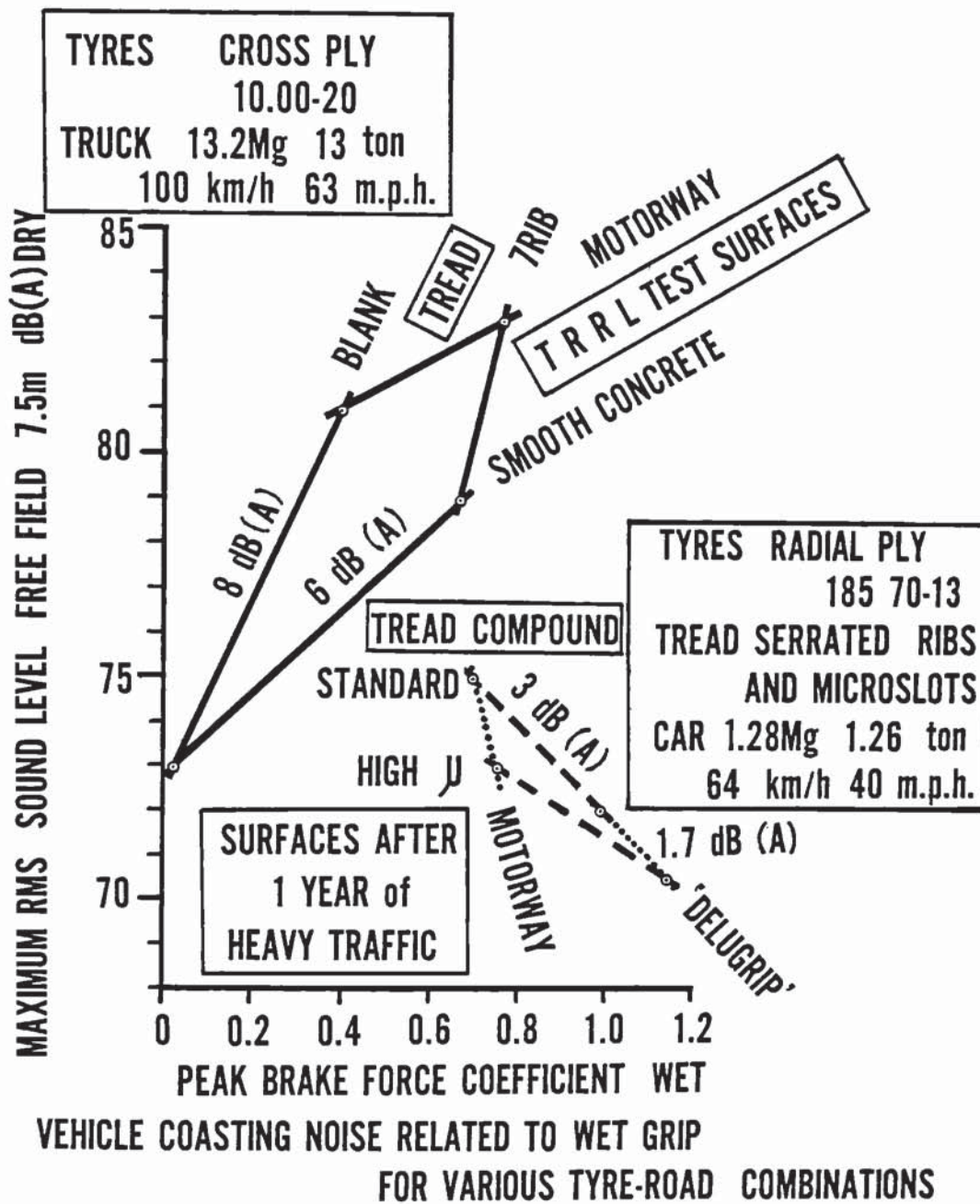


Figure 3.7.

were shown in Figure 3.1.

The 13,200 Kg (29,000 lb) truck at 100 km/h (62 mph) with blank tyres on smooth concrete has a low braking force coefficient of 0.03 and a low noise level of 73 dB(A). The tyre/surface grip may be improved by the following methods:-

- (a) increasing the coarseness of the road texture, which unfortunately gives an 8 dB(A) noise increase.
- (b) by the use of a ribbed pattern on the tyres and running them on the smooth concrete. This measure increases the noise by about 6 dB(A).
- (c) by a contribution of coarse road texture and ribbed tyres, which gives 10 dB(A) greater noise.

However this is not necessarily inevitable since the grip can be increased and the noise reduced. In the case of the author's work with a 1,280 kg (2,800 lb) car travelling at 64 km/h (40 mph) on surfaces after one year of heavy traffic (approximately 1000 commercial vehicles per day); with increasing grip, the noise level drops by 3 dB(A) when changing from BS 594 Motorway to Delugrip Road Surfacing Material, and by a further 1.7 dB(A) when high friction tread compounds are used.

It will be noted that the braking force coefficients are rather higher with the truck on the test track motorway surface, than with the automobile on the actual motorway. This is because on the track the roughening, due to weathering, dominates any traffic polishing whereas on the motorway the reverse is true. In fact, an automobile has a higher grip than a truck on the same surface.

3.10. Wet Tyre/Road Noise

If bulk water does lie on the surface then the noise can be 7 - 11 dB(A) higher than in the dry with truck tyres, Underwood (1973).

However if the road surface has enough drainage and the correct camber to drain away the surface water, such as the porous surface of friction course or the Delugrip type of surface, then noise in the wet is hardly any higher than noise in the dry, and the spray is greatly reduced, Katekhda (1974).

3.11. Coasting Vehicle Pass-By Noise with Studded and Unstudded Tyres

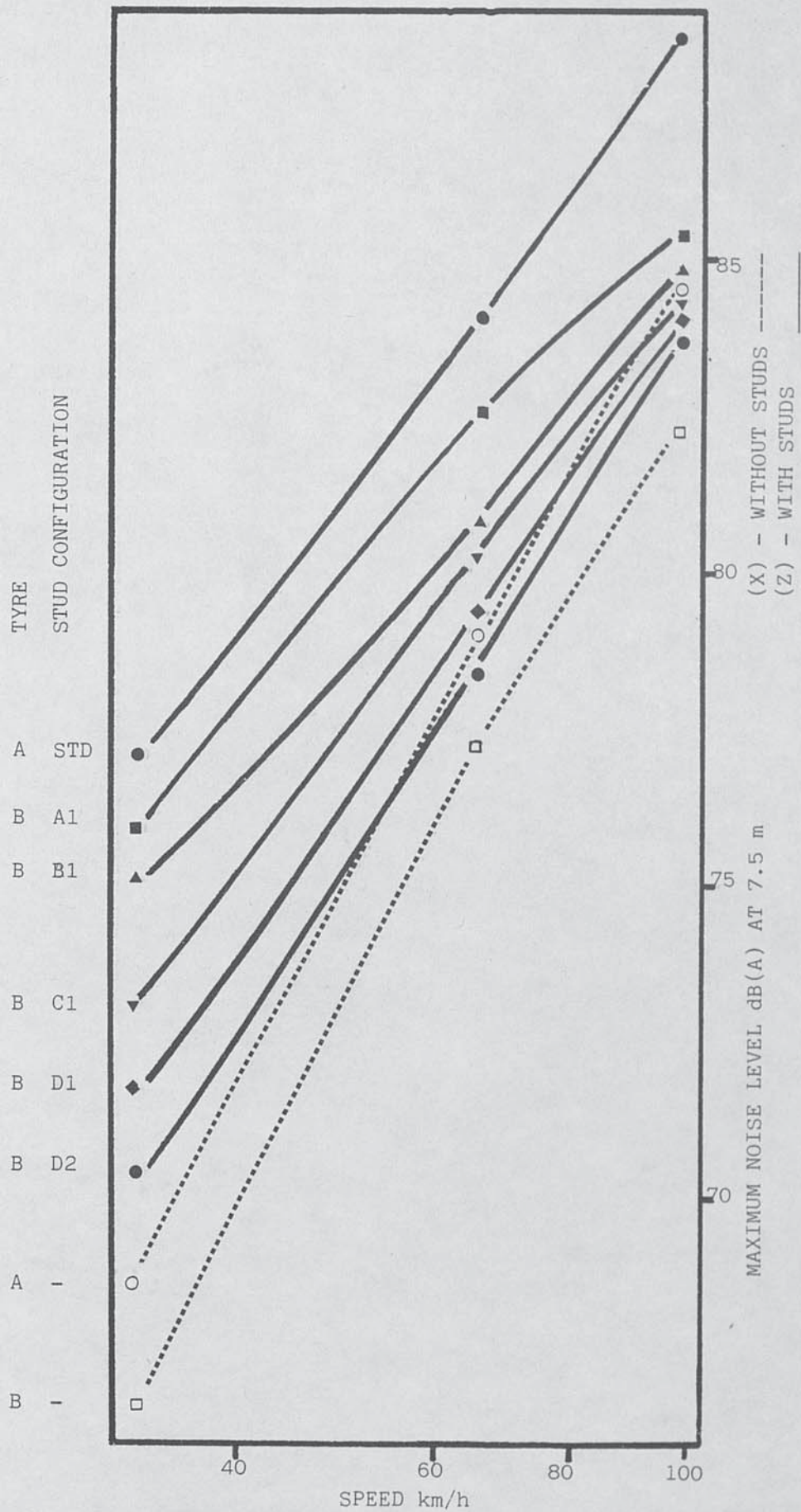
Pass-by noise testing was carried out by the author under BS 3425 conditions on hot rolled asphalt (BS 594) using a Ford Granada fitted with tyres having differing densities and configurations of studs.

The noise levels with and without studs are shown in Figure 3.8. These are of the same order as found by Johansen (1979). The calculated passing noise effect is shown in Figure 3.9. These results are related to a defined studded tyre parameter in Figure 3.10. where:

$$\text{Power} = (\text{Vertical Force Exerted by a Stud}) \times (\text{Speed of Vehicle}) \times (\text{Acceleration due to Gravity})$$

$$\text{Stud Density} = \frac{\text{Number of Studs}}{\text{Tread Width} \times \text{Tread Circumference}}$$

The vertical force exerted by a stud depends on the stiffness of the support of the stud and the force contribution due to the absorption of the kinetic energy of the stud. Since the product of the stud vertical force and the stud density is related to the road surface damage performance of studded tyres, then this performance may be predicted from the noise results, thus saving both time and cost, as discussed by Bond (1977).



PASSING NOISE LEVELS WITH AND WITHOUT STUDS

Figure 3.8.

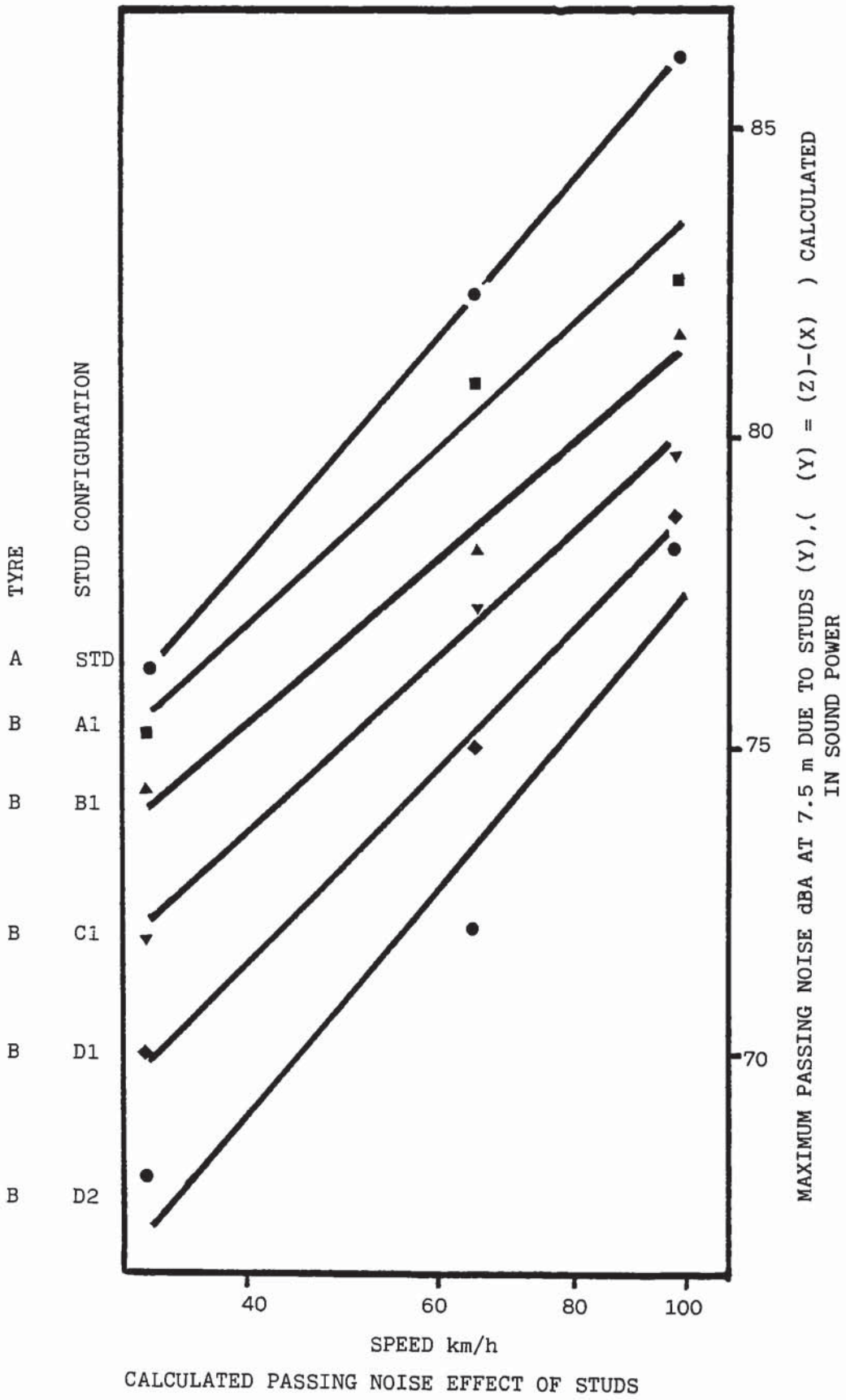


Figure 3.9.



RELATIONSHIP BETWEEN MAXIMUM PASSING NOISE AND A DEFINED
STUDED TYRE PARAMETER

Figure 3.10.

(Bond, 1977)

CHAPTER FOUR: TOTAL TRAFFIC NOISE - THE RESURFACING OF
HAMMERSMITH FLY-OVER, U.K.

4.1. Introduction

In March 1975 the eight year old hot rolled asphalt surface on the Hammersmith fly-over, U.K., was relaid with Delugrip Road Surfacing Material. The opportunity was taken, with the author's involvement, to carry out an exercise to investigate traffic noise before and after re-surfacing, Major (1975). The traffic flow is very high at 69,000 vehicles per day and approximately constant from week to week. Tape recordings were taken of the noise in January over two half hour periods, namely early and late afternoon. Recordings were repeated on the same day of the week in April after re-surfacing. Each day was similar in weather conditions. The average traffic speed was fairly consistent 65 km/h (40 mph) during the test periods.

In addition to measurement of the total traffic noise, advantage was taken of the closed periods of the fly-over to carry out individual noise tests. These involved an automobile coasting past a microphone at 7.5 m (25 ft) distance over a range of speeds.

The microphone position for the traffic noise tests was on the roof of the local Odeon Cinema. This gave a good position some 9.1 m (30 ft) above the carriageway and approximately 18.2 m (60 ft) from the centre of the road.

4.2. Road Surface Texture

The difference in surface texture is shown in Figure 4.1., the scales being compressed horizontally and expanded vertically to show the difference with clarity. These sections were obtained by taking a cast of the road surface in the wheel rut area along the direction of travel. The casts were sectioned, photographed, and the profile trace digitised to produce punched tape. This was fed to the IBM 370 computer and the magnetic tape output was fed to the

ROAD SECTION PROFILE



H.R.A. (B.S.594) WITH 19mm CHIPPINGS

4] SCALES mm

0 40



DELUGRIP

Figure 4.1.

autodraft equipment.

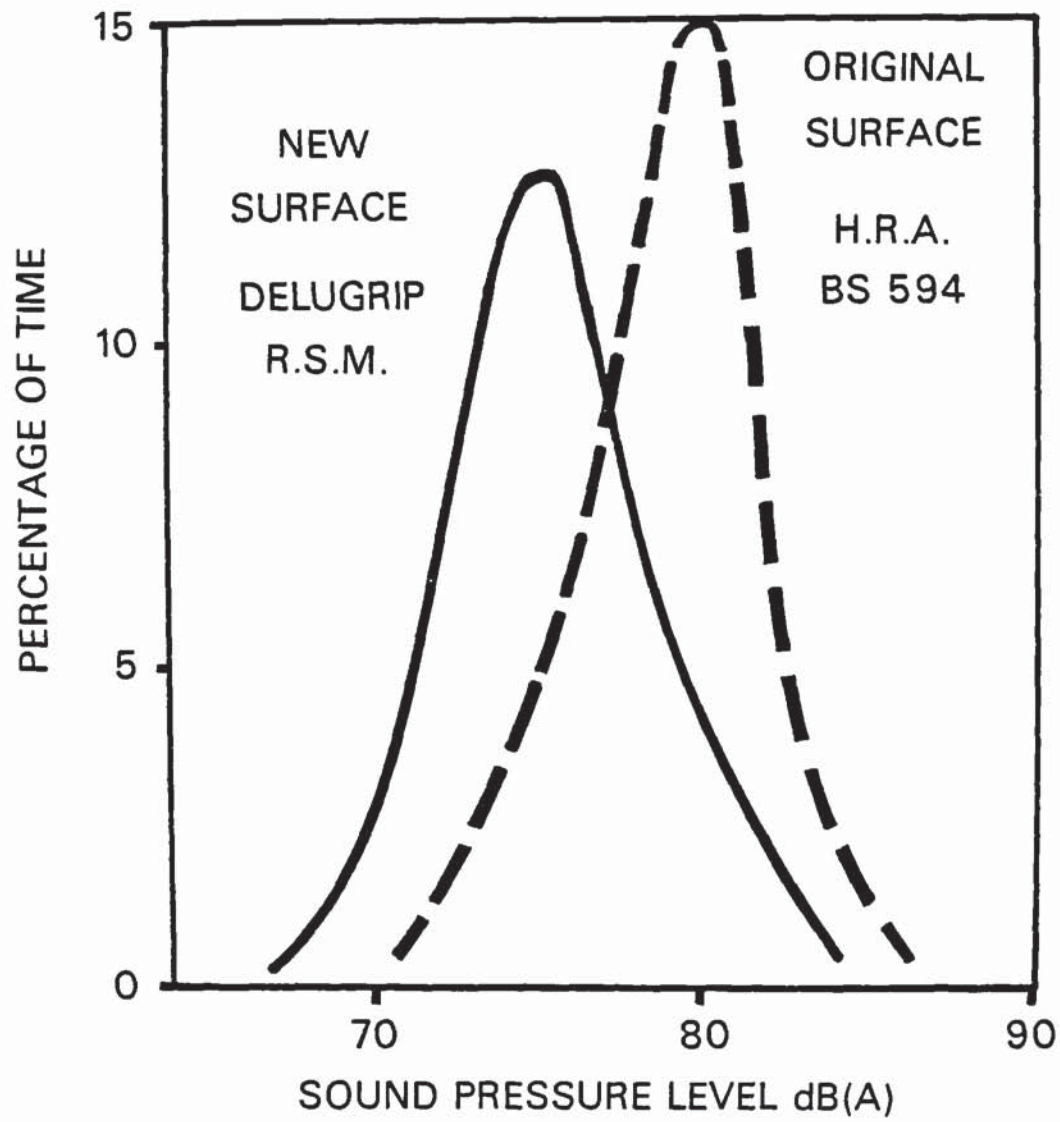
The upper trace shows the hot rolled asphalt with the binder worn away. The tops of the stones were severely polished giving poor wet grip. This surface will excite considerable tyre vibration and hence, considerable tyre/road noise.

The lower trace shows the Delugrip type of surface which has a much finer macrotexture. This causes much less tyre vibration and this is at higher frequencies in the less sensitive region of the spectrum and thus gives quieter tyre road noise. The valleys in this profile are inter-connecting waterways for good drainage. In the case of the individual noise tests with a coasting automobile, a 3 dB(A) improvement was obtained.

4.3. Histogram of Total Traffic Noise

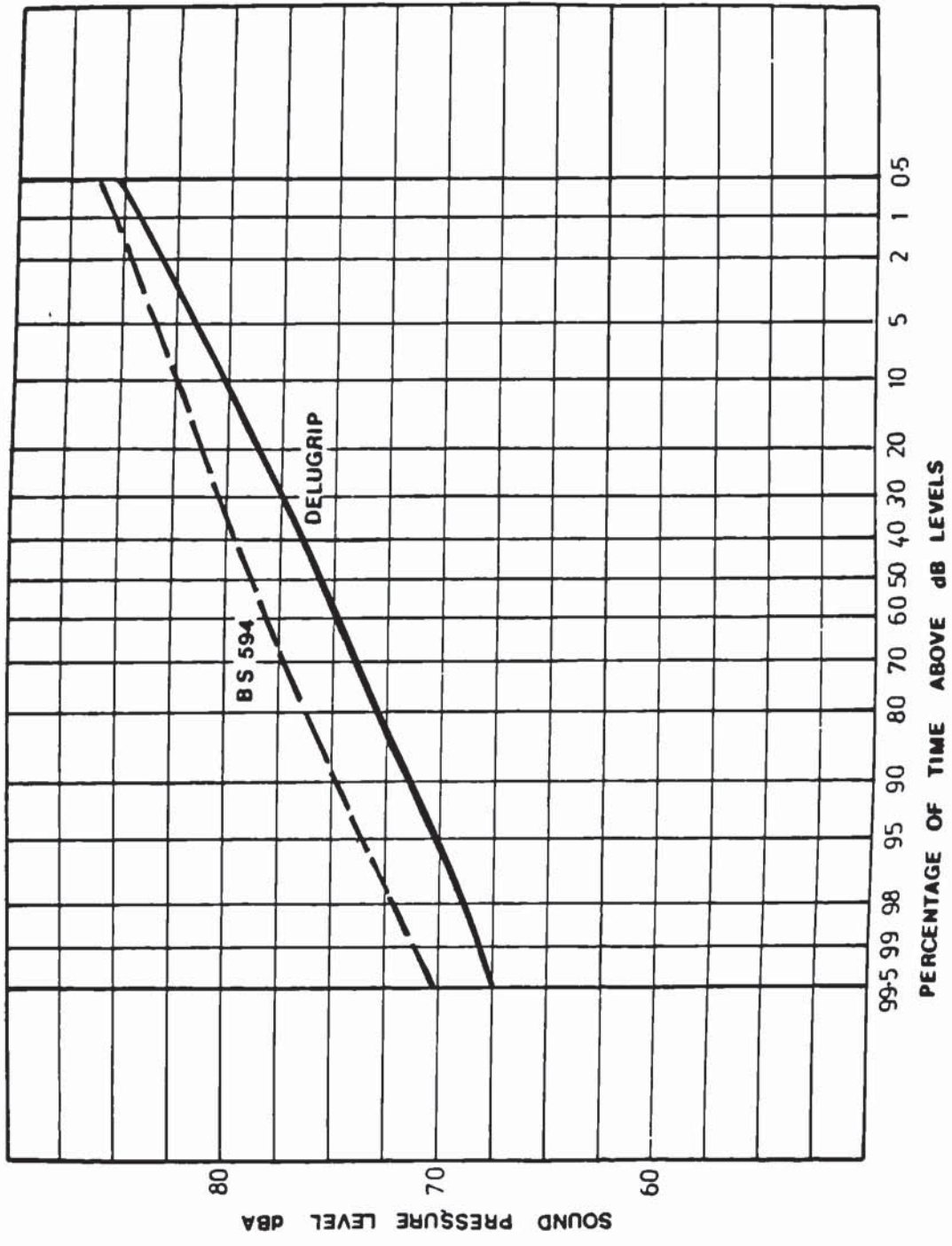
Figure 4.2. shows a distribution or histogram of the traffic noise levels for both hot rolled asphalt and the Delugrip Road Surfacing Material. The tape recording of traffic noise was fed to the Sound Level Meter which provided the input to the digital mini computer which calculated the distributions shown.

The vertical scale represents the percentage of the time that each particular dB(A) level was recorded over the total period of one hour. The horizontal scale shows increasing dB(A) levels to the right. This Delugrip type of surface is 3 - 4 dB(A) quieter than hot rolled asphalt over a large part of the distribution. The shape, the difference between the distributions, is shown more clearly in the ogives in Figure 4.3. At the noisiest end, corresponding to a noisy truck engine, the difference is much less since the engine noise dominates. However, when the quiet lorries have been produced, the quieter surface is already available.



HISTOGRAMS OF NOISE ON HAMMERSMITH FLY-OVER BEFORE AND AFTER RE-SURFACING

Figure 4.2.



DISTRIBUTION OF dB(A) LEVELS

Figure 4.3.

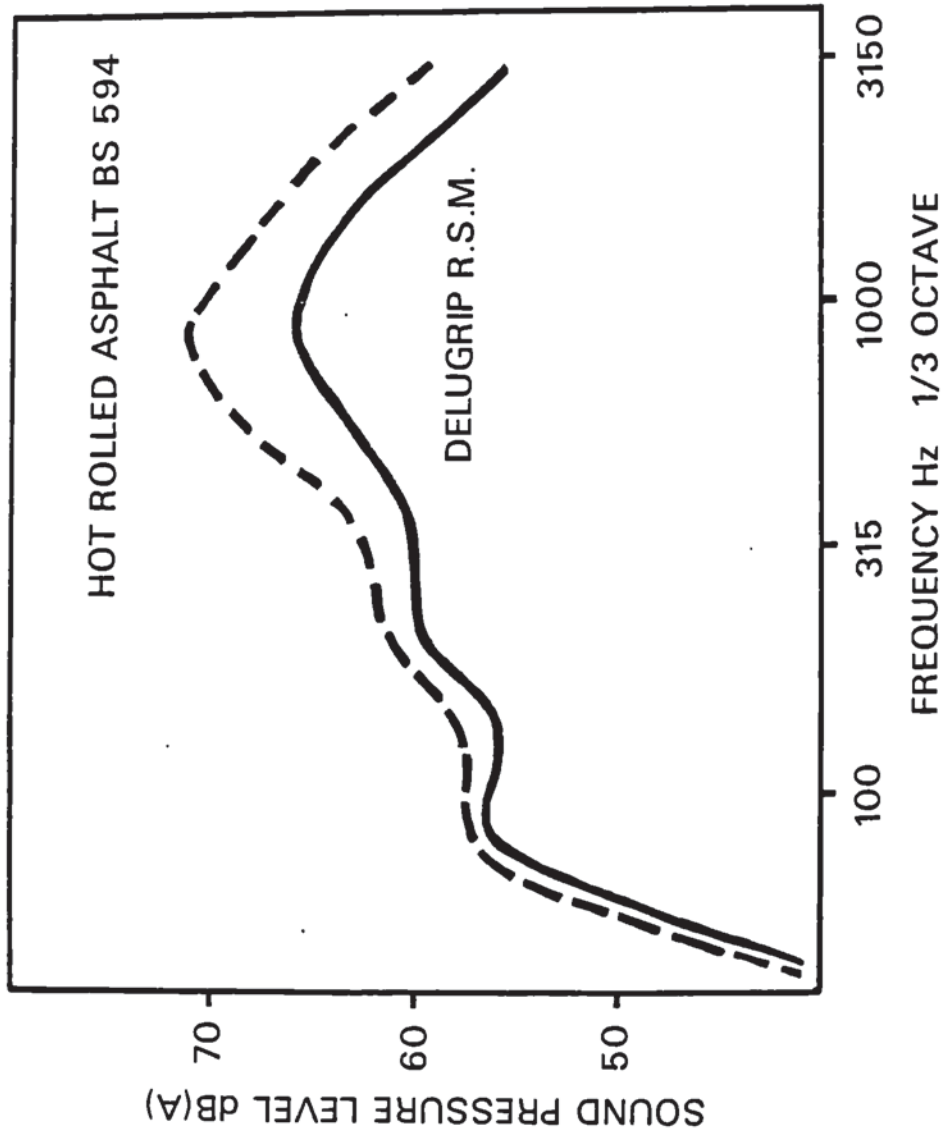


Figure 4.4.
 AVERAGE FREQUENCY SPECTRUM
 OVER TWO HALF HOUR PERIODS FOR 50% OF TIME

4.4. Total Traffic Noise - Frequency Spectrum and Probability

To investigate frequencies at which the difference between the two surfaces was greatest, the ogives were obtained from the tape recording for each of the $\frac{1}{3}$ octave bands in the range 40 Hz to 3.15 kHz. Hence frequency spectra are obtained for various percentages of time above the spectrum levels shown.

Figure 4.4. shows the spectrum for 50% of the time and is thus the median value. In this figure the various $\frac{1}{3}$ octave levels have also been weighted using the dB(A) scale in order to give a closer correspondence to that experienced by the human ear. This procedure attenuates the high intensity at the lower frequencies due to heavy goods vehicle exhausts.

It can be seen that at 1 kHz the difference between the two surfaces is 5 dB(A) thus showing that the frequency range in which the Delugrip surface is most effective is from 500 Hz to 2.0 kHz.

The hot rolled asphalt surface generates frequencies in the range 300 Hz to 2.0 kHz, whereas the Delugrip type of surface generates frequencies from 1 kHz to 5 kHz over a normal range of road speeds. Therefore the noise generation is taken out of the sensitive area around 1 kHz, where the tyre acts as a good emitter, as previously discussed in section 3.6.

4.5. Full Probability Spectrum Levels v. $\frac{1}{3}$ octave band plots

Figures 4.5. and 4.6. show the full probability plots for levels in a $\frac{1}{3}$ octave band exceeding the contour levels for the hot rolled asphalt and Delugrip Road Surfacing Material respectively. dB and not dB(A) are used.

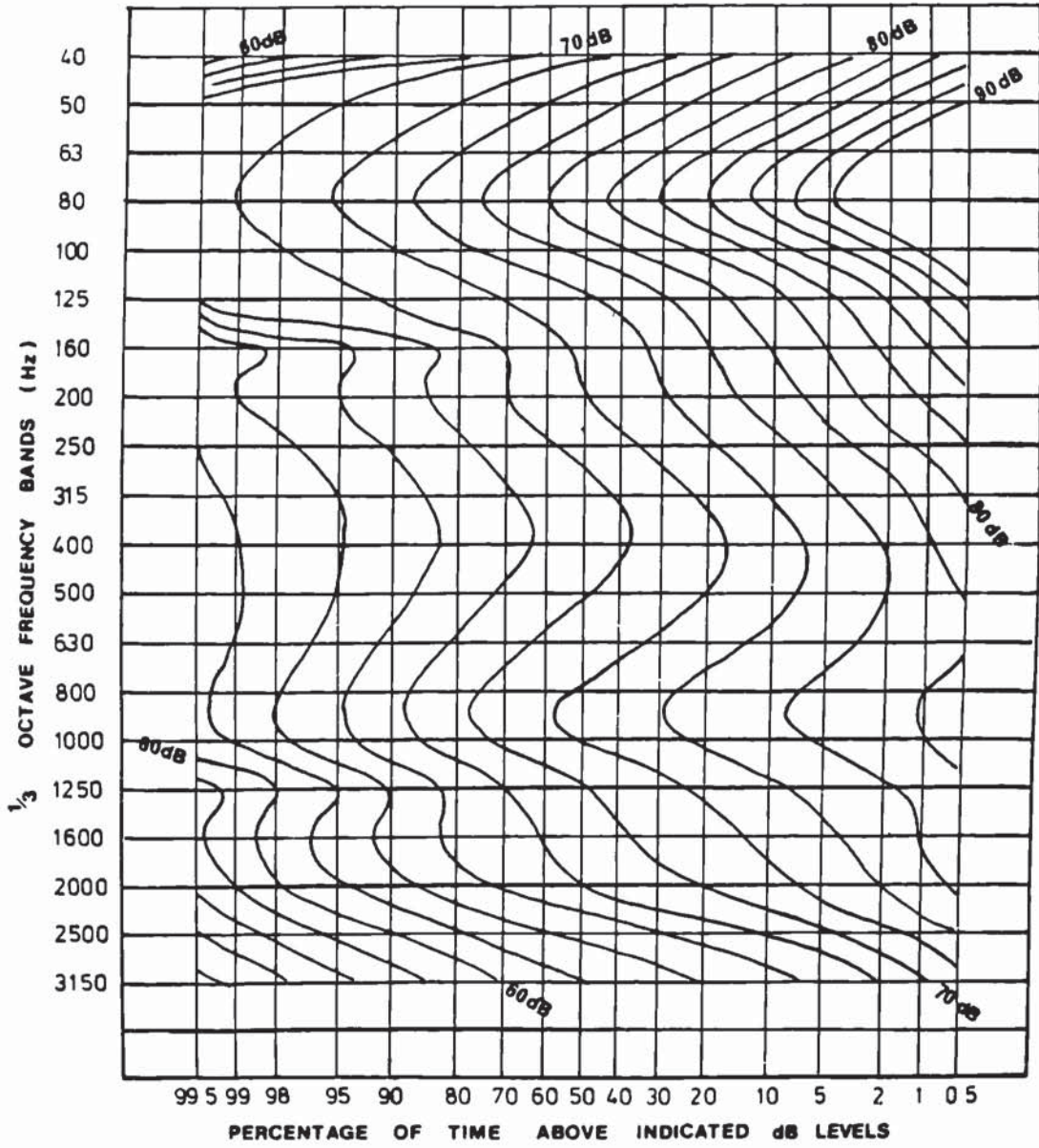
The difference between the surfaces becomes apparent in Figure 4.7. where the difference between the contours in the two previous figures is plotted superimposed on the Delugrip contours.

Figure 4.8. describes the main causes of the noise in Figure 4.7. The contours in the top half of the diagram are caused mainly by vehicle engine and exhaust noise. Those in the bottom half are caused by road/tyre and vehicle engine noise. The conditions represented by the extreme left hand edge of the diagram correspond to the infrequent periods of light traffic where the background noise, including the roar of distant traffic, is being measured.

The contour lines in Figure 4.7. show improvements due to Delugrip Road Surfacing Material in comparison with hot rolled asphalt in the range 300 - 3000 Hz with large areas of over 4 dB difference, and overall shows major benefit.

Figure 4.9. is a replot of the data showing the improvements over the full range of probability with more clarity.

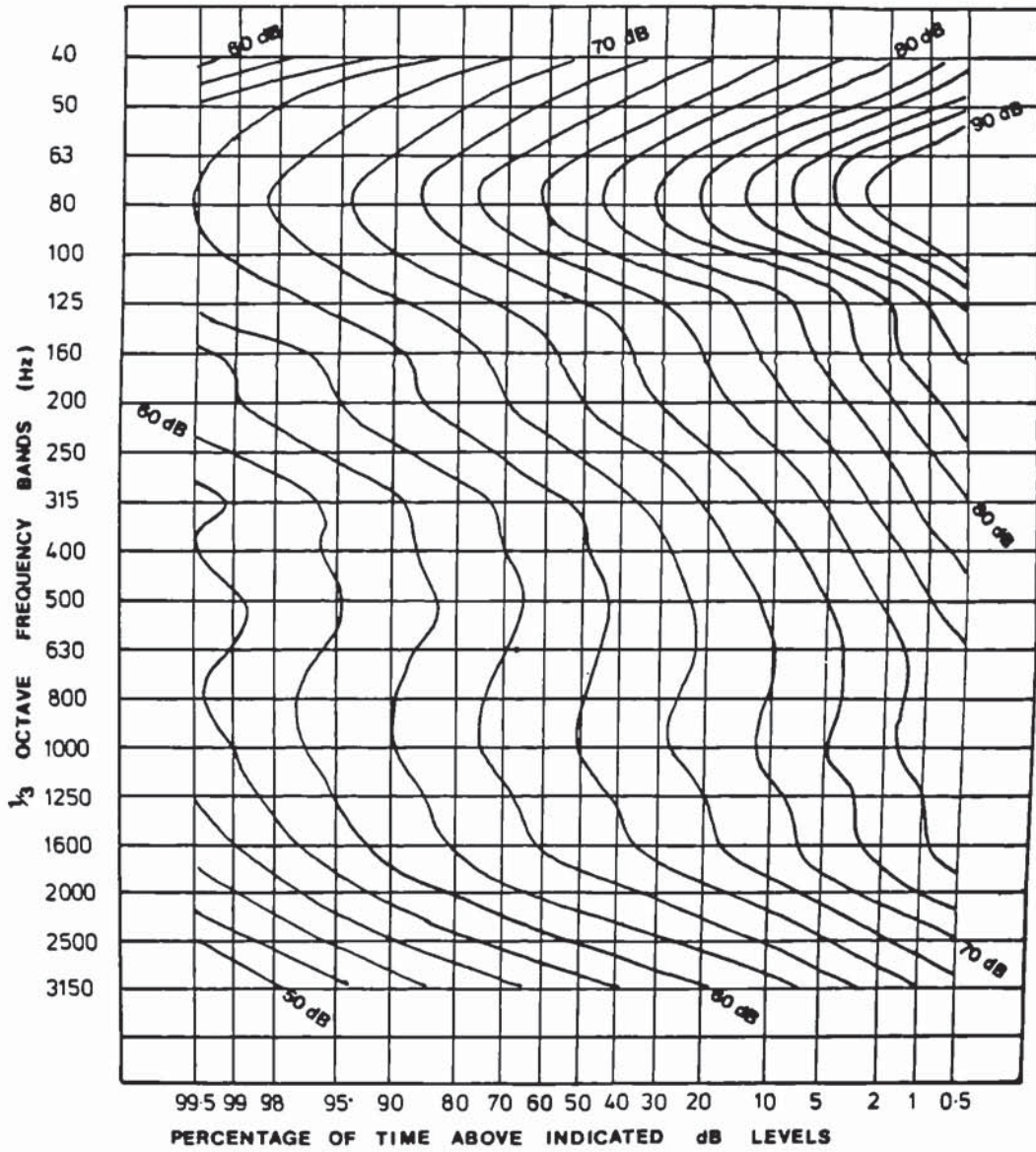
The instrument used for the tape recordings was a Philips Analog 7, operating on the FM principle, with a tape speed of 15 inches per second, giving a good frequency response up to 5 kHz. This instrument was heavy and was replaced with the Racal Store 7, which was used for later work and was much lighter.



PERCENTAGE OF TIME ABOVE INDICATED dB LEVELS IN $\frac{1}{3}$ OCTAVE BANDS FOR HOT ROLLED ASPHALT (BS 594)

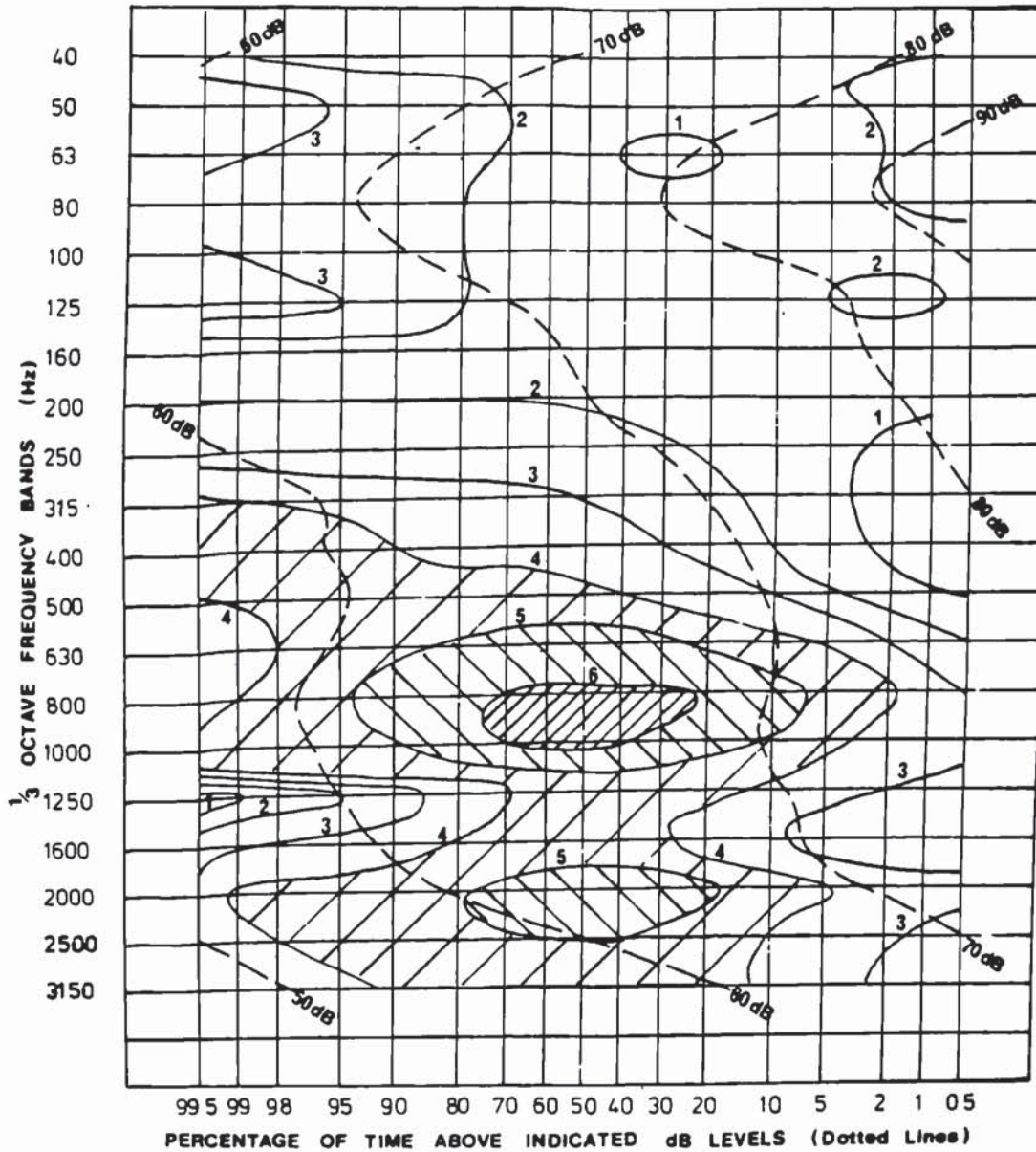
Figure 4.5.





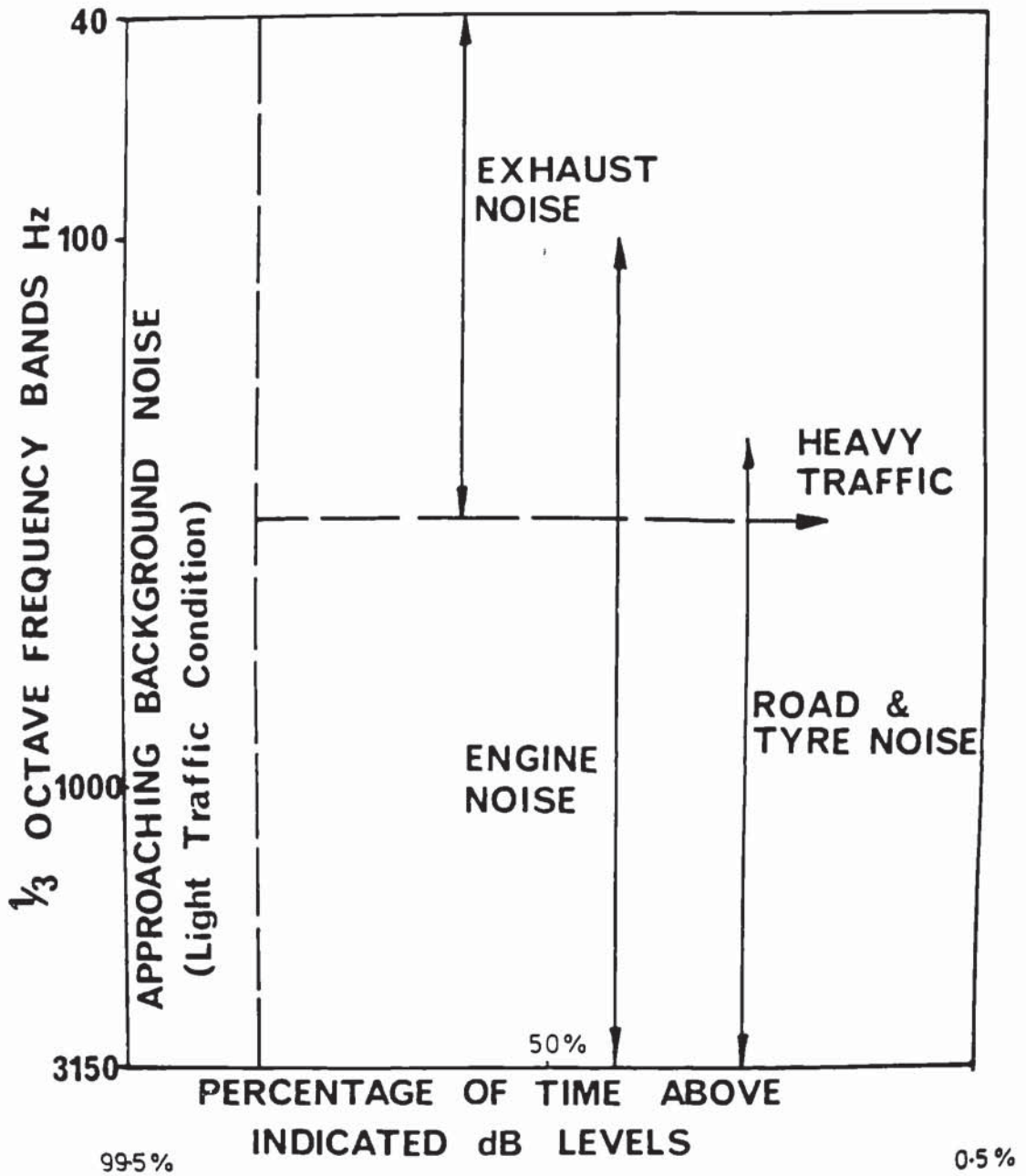
PERCENTAGE OF TIME ABOVE INDICATED dB LEVELS IN $\frac{1}{3}$ OCTAVE BANDS
FOR DELUGRIP ROAD SURFACING MATERIAL

Figure 4.6.



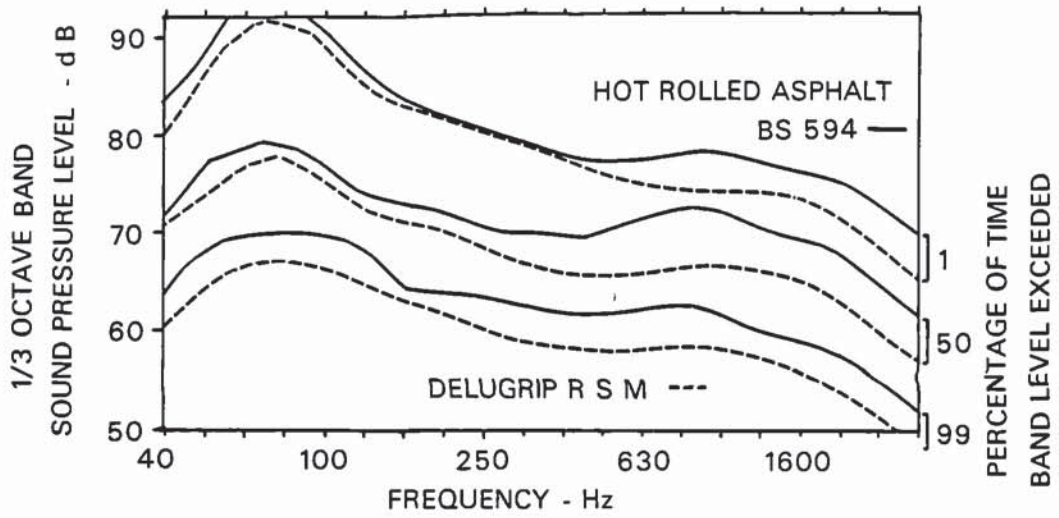
BENEFIT OF DELUGRIP (in dB) AS COMPARED WITH HOT ROLLED ASPHALT BS 594, SUPERIMPOSED ON DELUGRIP R.S.M. CURVES

Figure 4.7.

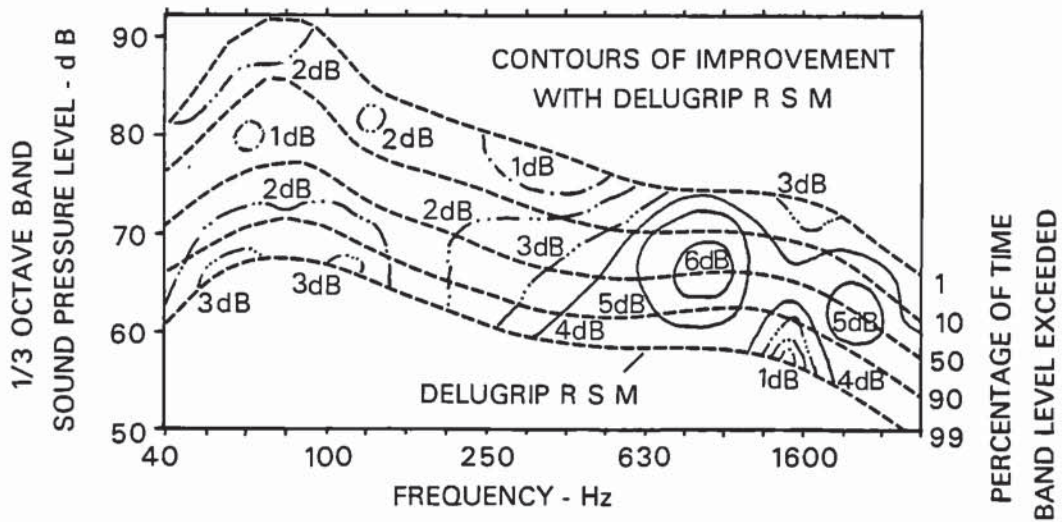


CAUSES OF THE PROBABILITY DISTRIBUTION OF NOISE WITH FREQUENCY

Figure 4.8.



1/3 OCTAVE FREQUENCY SPECTRA EXCEEDED FOR A GIVEN PERCENTAGE OF TIME



CONTOURS OF IMPROVEMENT IN 1/3 OCTAVE BAND LEVELS
OBTAINED WHEN USING DELUGRIP COMPARED WITH H.R.A. BS 594,
SUPERIMPOSED ON,
DELUGRIP R S M NOISE SPECTRA EXCEEDED FOR A GIVEN PERCENTAGE OF TIME

Figure 4.9.

CHAPTER FIVE: THE EFFECT OF DRUM SURFACE TEXTURE ON INDOOR TYRE
NOISE TESTING v. COASTING VEHICLE PASS-BY NOISE

5.1. Introduction

As referred to in Section 3.4. smooth surfaces give greater contrast between tread patterns than do normal road surfaces.

Prior to noise testing on a smooth drum surface each tyre was individually wire brushed to reduce the polishing effect.

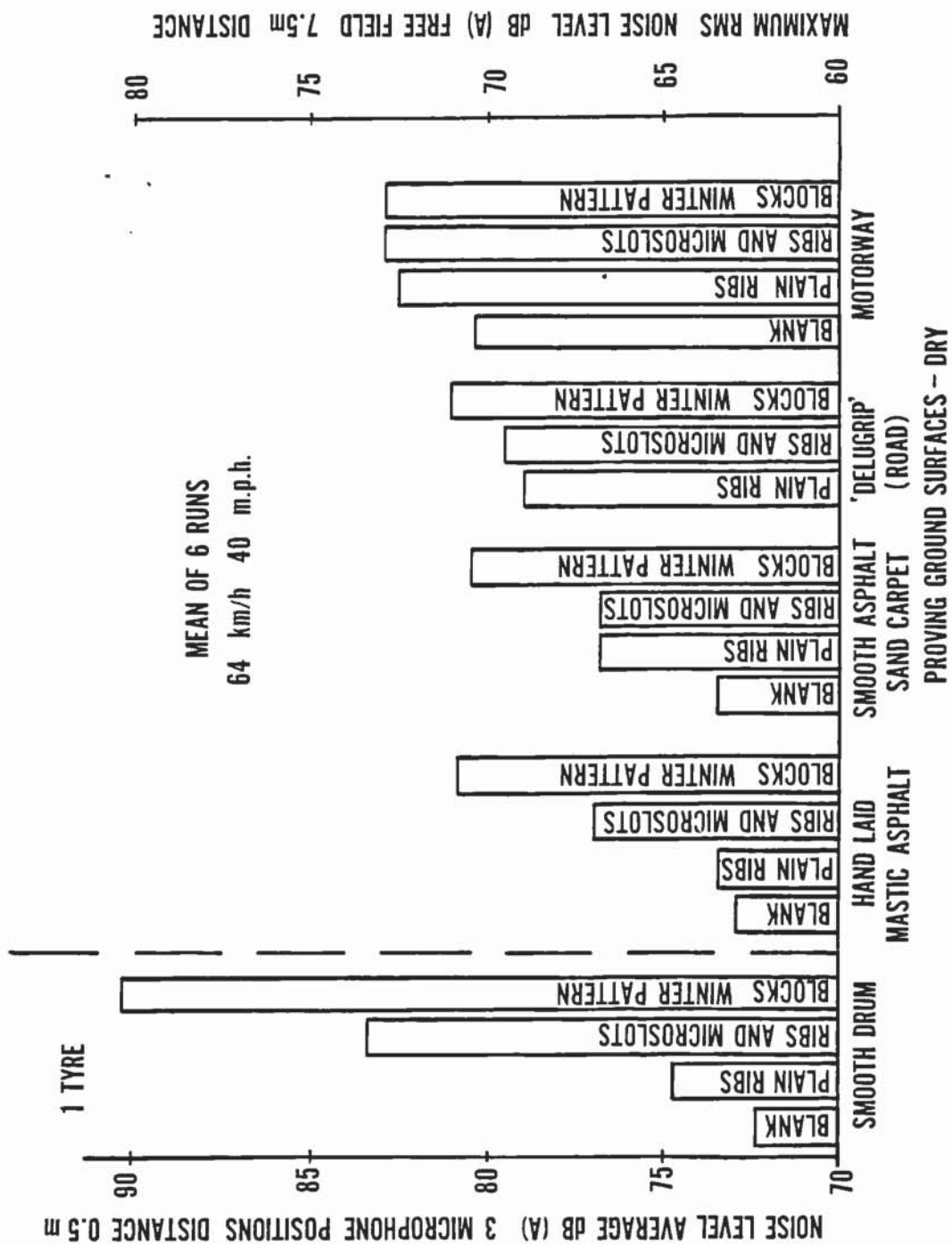
A machined steel drum surface is smoother than the smoothest road surface and gives very high contrast in the noise levels from a range of tyre patterns as shown by J C Walker and Major (1975) Figure 5.1.

A further disadvantage of a smooth drum surface is that the polishing effect is much greater than any wearing effect of the tread surface by the drum surface. This does not occur on road surfaces where the wear is adequate to prevent polishing of the tread.

The author therefore decided to cover the existing smooth drum surface with Safety Walk^R. Duralumin Shells 6.25 mm thick in three sections were bolted round the drum surface, and the 3 M Safety Walk (50 grade) was stuck to the surface. An oblique butt joint was used to minimise the effect of the joint.

5.2. Experimental Procedure

The tyres were loaded by the pneumatically loaded strut suspension to a load of 300 kg and the inflation pressure was set to 1.8 kg/cm². They were tested with zero lateral force; any lateral force built in to the tyre was offset by running it at a slight slip angle. This corresponds to normal driving attitude and minimum cornering noise.



CAR COASTING NOISE FOR VARIOUS TYRE ROAD COMBINATIONS
PROVING GROUND SURFACES - DRY

Figure 5.1.

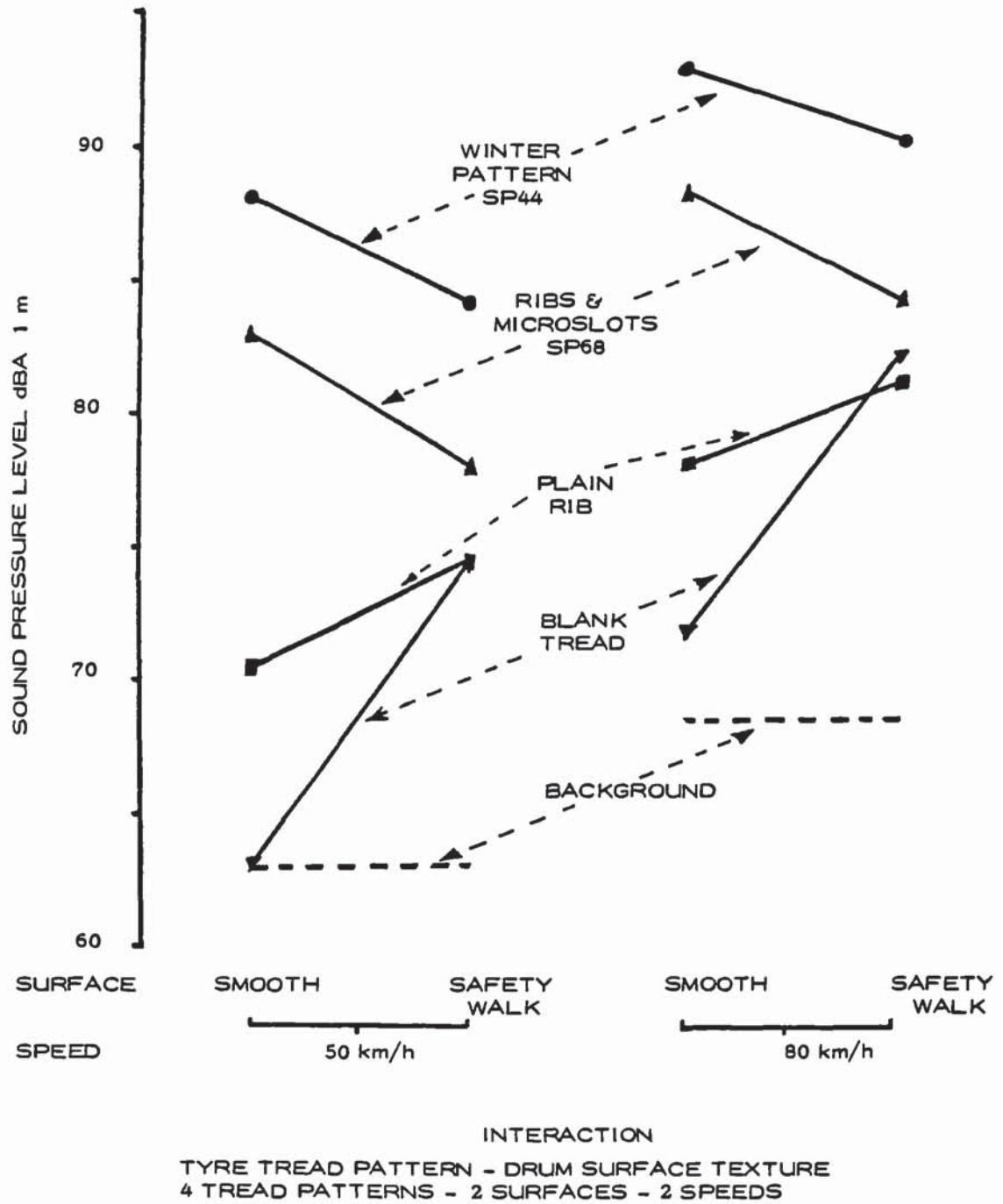


Figure 5.2.

One microphone was positioned at 450 mm from the ground plane and 800 mm from the centre of contact of the tyre and in the vertical plane containing the drum axle. The drum, of diameter 1.52 m (60 inch), protruded 3 cm through the laboratory floor which was of steel chequer plating.

Using the British Standard Test for specific room suitability, it was found that when the microphone to source distance was doubled there was more than a 5 dB drop in sound level in the frequency bands. Hence the laboratory is suitable for the type of test.

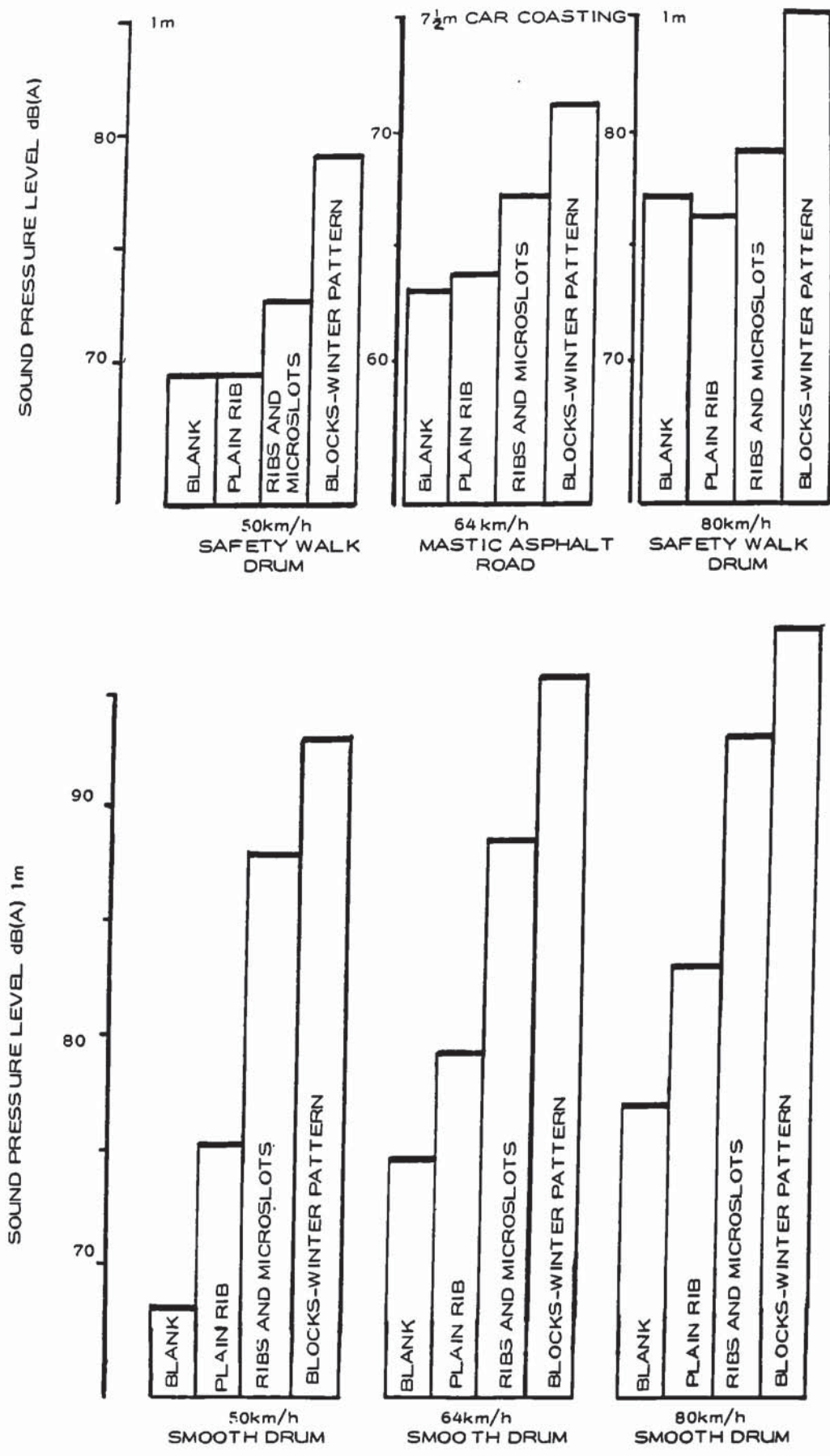
5.3. Discussion of Results

Figure 5.2. illustrates the sound pressure levels dB(A) when running tyres on Safety Walk as compared with a smooth drum surface. Four radial ply tread patterns were tested; a winter pattern, ribbed and microslotted, and a blank tread size 165-14 and a plain ribbed size 185/60-13. The levels were corrected for background level.

There was approximately 5 dB(A) increase in noise level of the plain rib over blank tread on the smooth drum. The blank tread was 9 dB(A) noisier on the Safety Walk and the plain rib was 4 dB(A) noisier.

However, the ribbed and micro-slotted tyre was 5 dB(A) quieter on Safety Walk. This is largely because the micro-slots seal and unseal on the smooth surface giving a high frequency hiss. They do not seal on the Safety Walk and are hence quieter.

The winter pattern was 4 dB(A) quieter on the Safety Walk. This tyre has a block pattern including micro-slots. A tyre with just a block pattern and no micro-slots was tested and found quieter on the Safety Walk showing that the noise reduction is not just a micro-slot effect.



A COMPARISON OF CAR COASTING NOISE WITH DRUM TESTS
 Figure 5.3.

5.4. Comparison with Vehicle Pass-by Noise

Figure 5.3. shows that the high contrast between the winter and the blank tread tyre is approximately 20 dB(A) on the smooth drum and 9 dB(A) on the Safety Walk drum. The Safety Walk results are very similar to those obtained by J C Walker and Major (1975) on mastic asphalt which also gave a contrast of 9 dB(A) between the patterns.

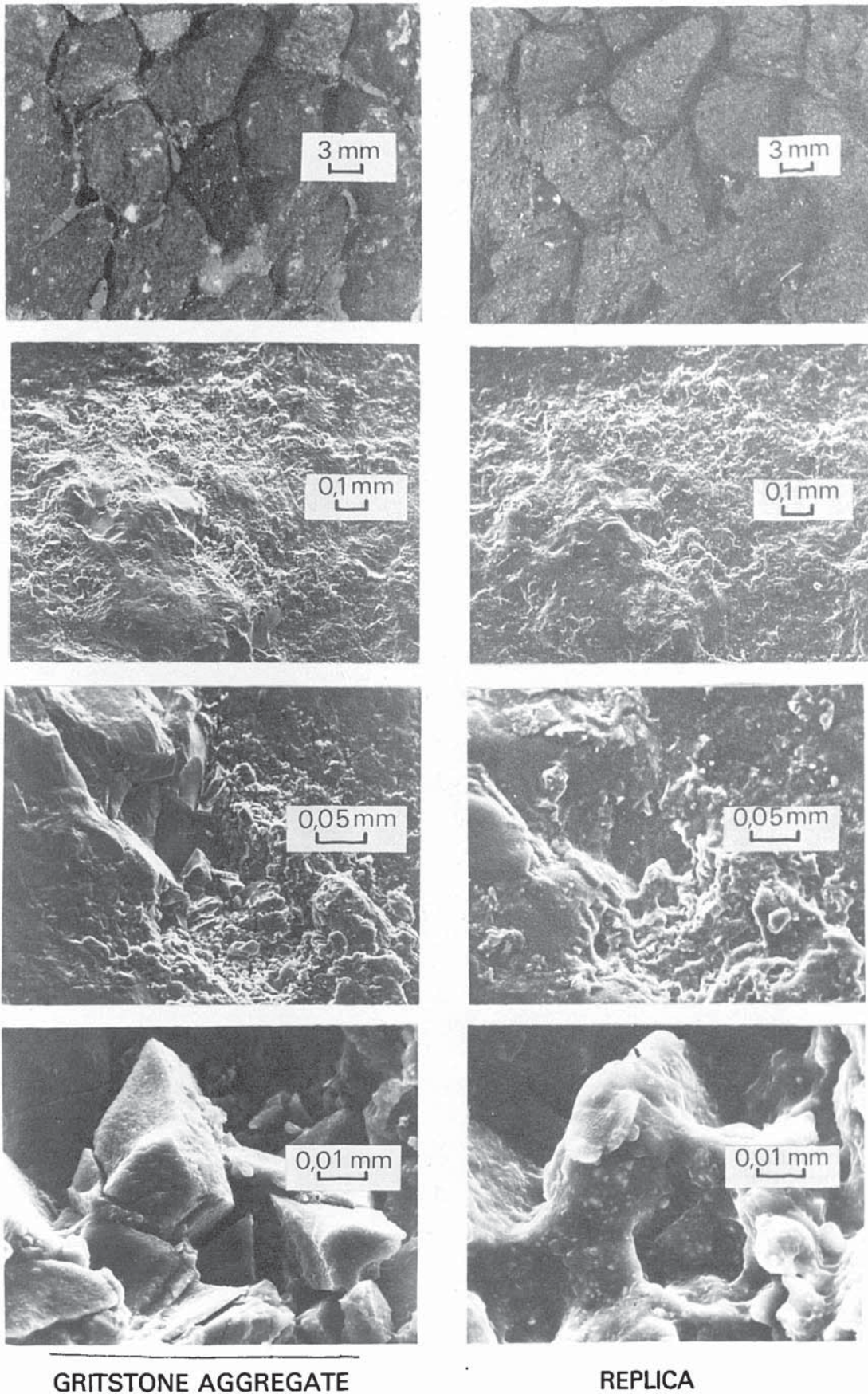
An extension of the scope of this type of work is possible with the use of replica road surface shells on drums.

5.5. Replica Road Surfaces

The following replica road surfaces were obtained by Dr A R Williams (Dunlop Limited) with a view towards investigating comfort, vibration, rolling resistance and thermographic measurements as well as noise.

Although Safety Walk is a step towards a road surface and overcomes some of the disadvantages of a polished steel drum surface, it is still non typical and abrasive. Resin surfaces have been made as exact replicas of actual road surfaces, i.e. not new and not excessively worn road surfaces. They were taken from the wheel track of road surfaces which had carried moderate to heavy traffic for a period of time. The thermal conductivity of the material is close to that of the road and gives more typical tyre temperatures. It is a simple matter to change the type of surface during a series of tests. Each surface is constructed with as few joints as possible. There is no repetition of the surface in the circumference of the drum.

A 5 metre long cast of the road surface to be replicated was taken using cold cured rubber. A cast was also taken of the drum surface. A shell was formed using these casts. The thickness of the shell was approximately 20 mm. It had an outer layer with



PHOTOMICROGRAPHS OF AGGREGATE AND REPLICA

Figure 5.4.



(2) HOT ROLLED ASPHALT BS594



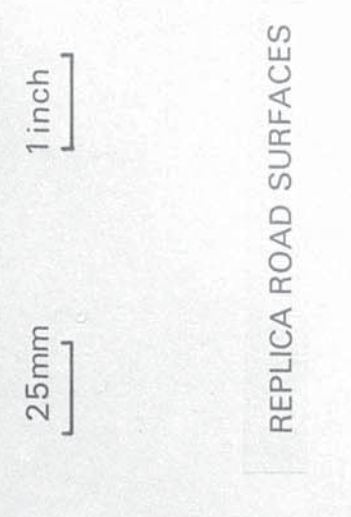
(3) SURFACE DRESSING



(4) LATERAL BRUSHED CONCRETE



(1) DELUGRIP ROAD SURFACING MATERIAL



REPLICA ROAD SURFACES

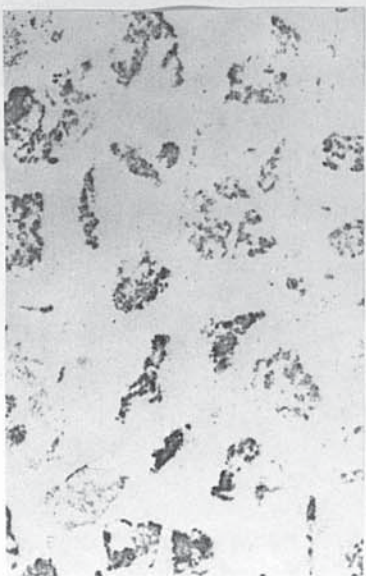
25mm

1 inch

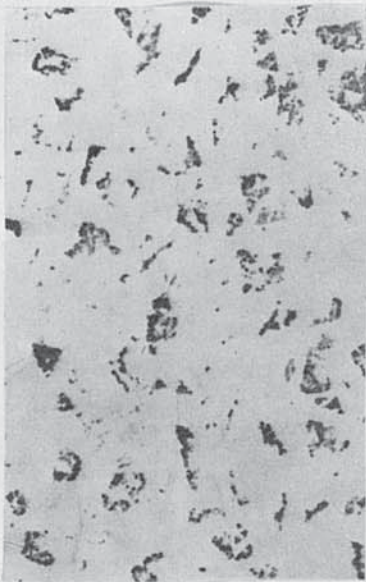


(5) LATERAL GROOVED CONCRETE

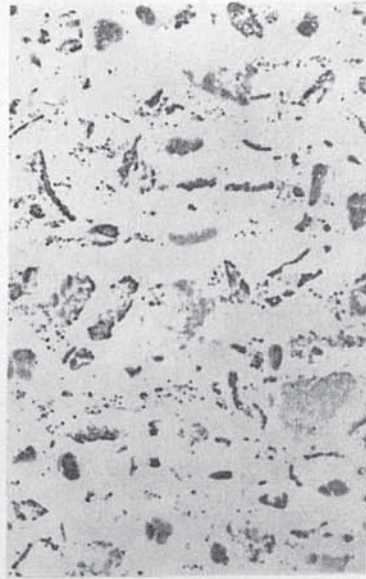
Figure 5.5.



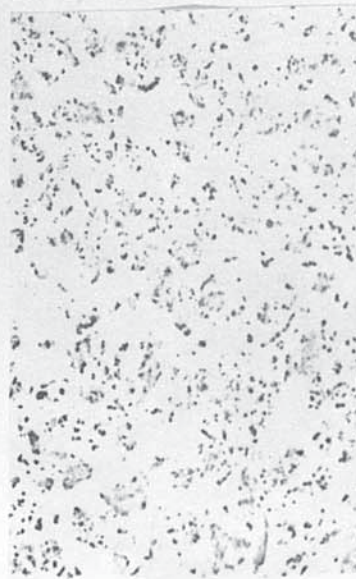
(2) HOT ROLLED ASPHALT BS 594



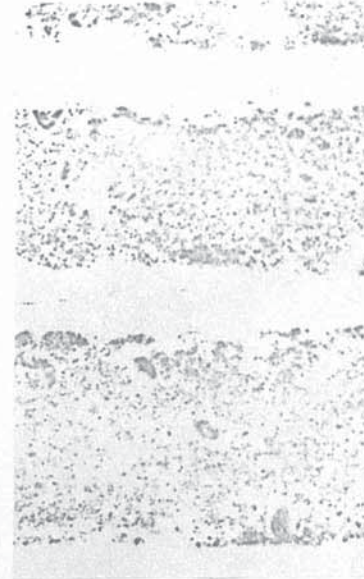
(3) SURFACE DRESSING



(4) LATERAL BRUSHED CONCRETE



(1) DELUGRIP ROAD SURFACING MATERIAL



(5) LATERAL GROOVED CONCRETE

25mm

1 inch

PLAIN TREAD TYRE

CONTACT PRINTS

ON

REPLICA ROAD SURFACES

Figure 5.6.

silicon carbide filler for high polishing resistance and inner layers of resin with glass fibre. The shell was built in three sectors round the drum and bolted down at 150 mm intervals around the circumference.

The sample of road surface and the moulded replica are shown at the top of Figure 5.4. The faithfulness of reproduction can be seen in the photomicrographs from the scanning electron microscope as the linear magnification is increased from 70 to 1500 times. The exactness of the copy of the microtexture is evident.

The replica surface has been tested for its resistance to polishing (BS 812) and gives a Polished Stone Value (P.S.V.) of 58 which is close to the value for granite.

The range of surfaces used is shown in Figure 5.5. The localised contact prints from a plain treaded tyre on each of the surfaces is shown in Figure 5.6.

The cross grooved concrete and lateral brushed concrete surfaces from which the replicas were made had been heavily worn and would be quieter than when in a less worn state.

5.6. Indoor Testing of Automobile Tyres on Replica Surfaces

Four types of tyre were tested by the author, blank tread, plain rib, ribbed and microslotted and a winter tractive block pattern. The steel breaker radial ply tyres size was 165-14.

Seven surfaces were used:

1. Smooth steel
2. Safety Walk
3. Delugrip Road Surfacing Material (R.S.M.) with maximum aggregate size of 10 mm
4. Hot rolled asphalt BS 594 with 19 mm precoated chippings

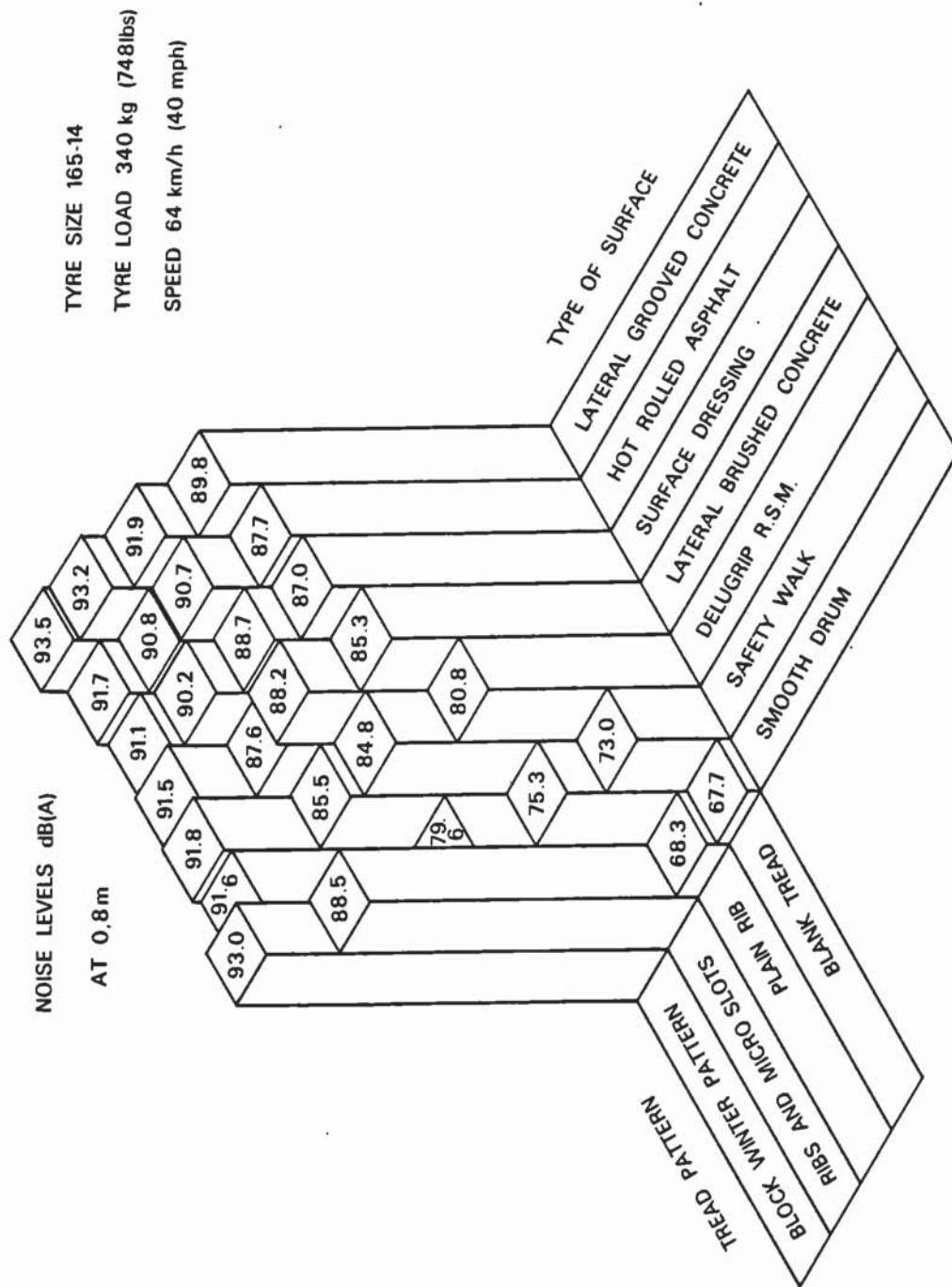


Figure 5.7.

INDOOR TESTING TYRE/ROAD NOISE ON SIMULATED ROAD SURFACES FOR VARIOUS TYRE-SURFACE COMBINATIONS

5. Surface dressing of 10 mm chippings
6. Lateral brushed concrete - brush marks 1 to 2½ mm deep and 3 to 10 mm apart (more worn than when external truck noise measurements were taken 2 years previously)
7. Lateral grooved concrete - grooves 10 mm wide and 30 to 55 mm apart, randomised but repeated every metre

The noise level results are shown in Figure 5.7.

This figure shows three distinct effects of the road surface on the tyre/road interaction noise.

(i) The Noise Excitation Effect due to Macrotecture of the Surface

This is evident when there is very little tread pattern effect, e.g. in the case of the blank tread or the plain ribbed tread which both give a similar ranking for the surfaces. The greater the texture depth the greater will be the noise excitation, but it is worse when there is cross texture like laterally brushed concrete or lateral grooved concrete. Thrasher (1976) found a 5 dB(A) reduction between cross and longitudinal brushed concrete. The excitation is less if the frequency is high enough to be above the sensitive region for the tyre. The range between minimum and maximum macrotecture excitation in this diagram is 22 dB(A).

(ii) The Break up of the Tread Pattern Excited Noise

Up to a point the greater and more pointed the macrotecture, the less the tread is in contact with the surface, then the greater is the break-up and the less will be the noise due to the tread pattern. This is shown in the block winter pattern results where the effect of the break-up dominates over the excitation effect. The reduction from smooth steel to surface dressing is 1.9 dB(A).

- (iii) The Unsealing of the Tread Pattern Microslots - Noise Reduction Effect

The macrotexture prevents the microslots sealing as they do on a smooth surface. The unsealing effect dominates the excitation effect. The reduction from smooth steel to Safety Walk is 9 dB(A).

5.6.1. Effect of Tyre Size

Tread patterns with ribs and microslots similar to that shown in Figure 5.8. are available in a wide range of textile radial ply tyres, covering a range of tyre diameters and tread widths. The tyres were tested at scheduled conditions on a range of surfaces. The noise level results are given in Figure 5.8.

These results show that the decrease in noise due to a 44% increase in tyre outside diameter more than compensates for the increase in noise due to a 71% increase in tread width.

5.6.2. Frequency Spectra

Three typical frequency spectra showing the total tyre surface noise from the blank treaded tyre are shown in Figure 5.9.

Constant bandwidth analysis of 12.5 Hz is used and averaged for 10 samples.

5.6.3. Separation of the Two Component Parts of Tyre/Road Noise

More detailed analysis has been carried out. The separation of tyre/road noise into tyre periodic noise and road excited periodic noise was shown by Pope (1976) (1978) on a Safety Walk surface. With a replica road surface on a drum, similar analyses can be carried out for actual worn road surfaces.

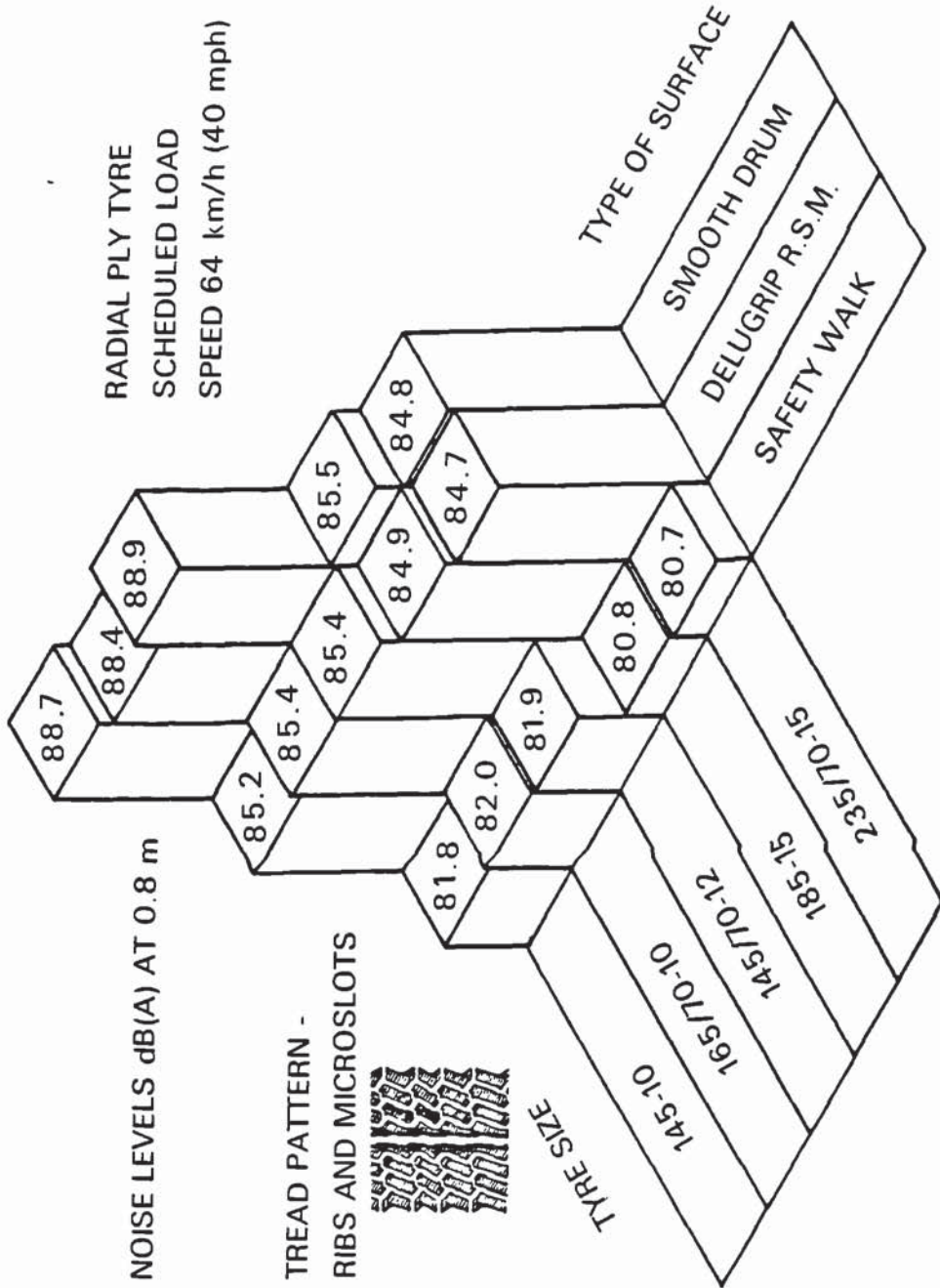
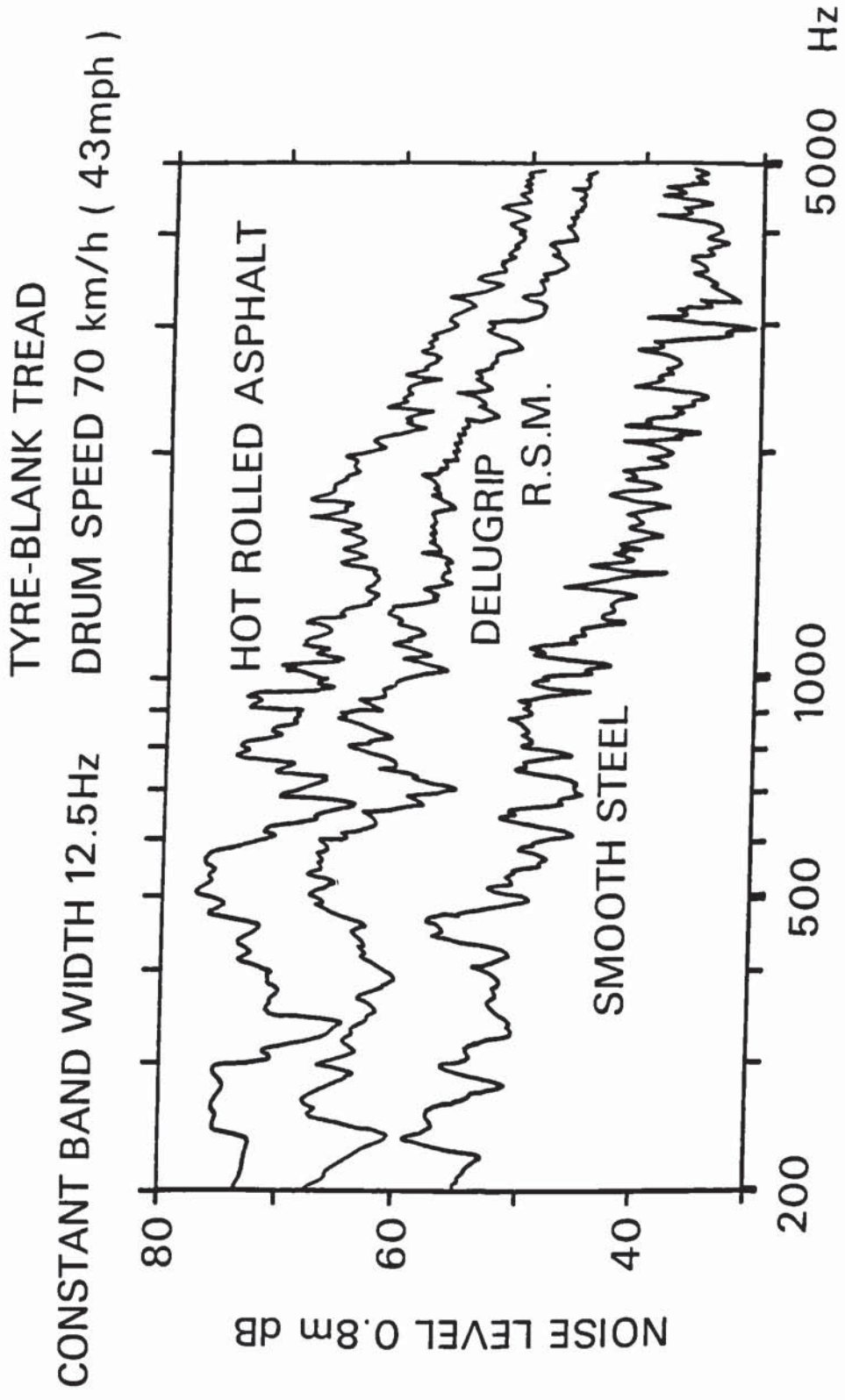


Figure 5.8. INDOOR TESTING TYRE/ROAD NOISE ON SIMULATED ROAD SURFACES FOR A RANGE OF TYRE SIZES



FREQUENCY SPECTRA OF NOISE FROM
BLANK TREAD TYRE ON REPLICA SURFACES

Figure 5.9.

A real time spectrum analyser was used, triggered by a pulse from the drum to take in the sound wave for 0.08 seconds. This was repeated for each revolution of the drum and sound waves averaged until the 256th average was reached. In order to correct for any small drifts in speed, for example 0.1 kmh, the signal from a 144 pulse per revolution source on the drum shaft was multiplied with the tracking adapter (phase locked) to provide the timing control for the real time analyser. Nicolet equipment was used for this.

As can be seen on the left-hand side of Figure 5.10, the plain treaded tyre periodic noise, obtained with the triggering pulse once per revolution of the tyre assembly, is very small. The replica surface noise is substantially nonperiodic with respect to the tyre pulse and will therefore average away leaving tyre periodic noise.

On the right hand side of the figure the respective constituent spectra are shown. Hence the total noise is separable into its constituent parts arising from tyre and road surface excitation.

The progressive stages of the synchronously averaged waveform for the periodic noise excited by the Delugrip surface and the blank tread, at a speed of 64 km/h are shown in Figure 5.11., and the corresponding synchronous dB(A) levels are given in Figure 5.12. The Sound Level Meter was used on the (A) scale to process the signal for these tests.

The dominant wave approaches its stable final value fairly rapidly but a much longer time is required to carry out considerable averaging down of a random wave to obtain a small amplitude wave. The synchronous blank tread excited noise is approximately 12 dB(A) below the level for a blank tyre on a smooth drum as shown in Figure 5.7.

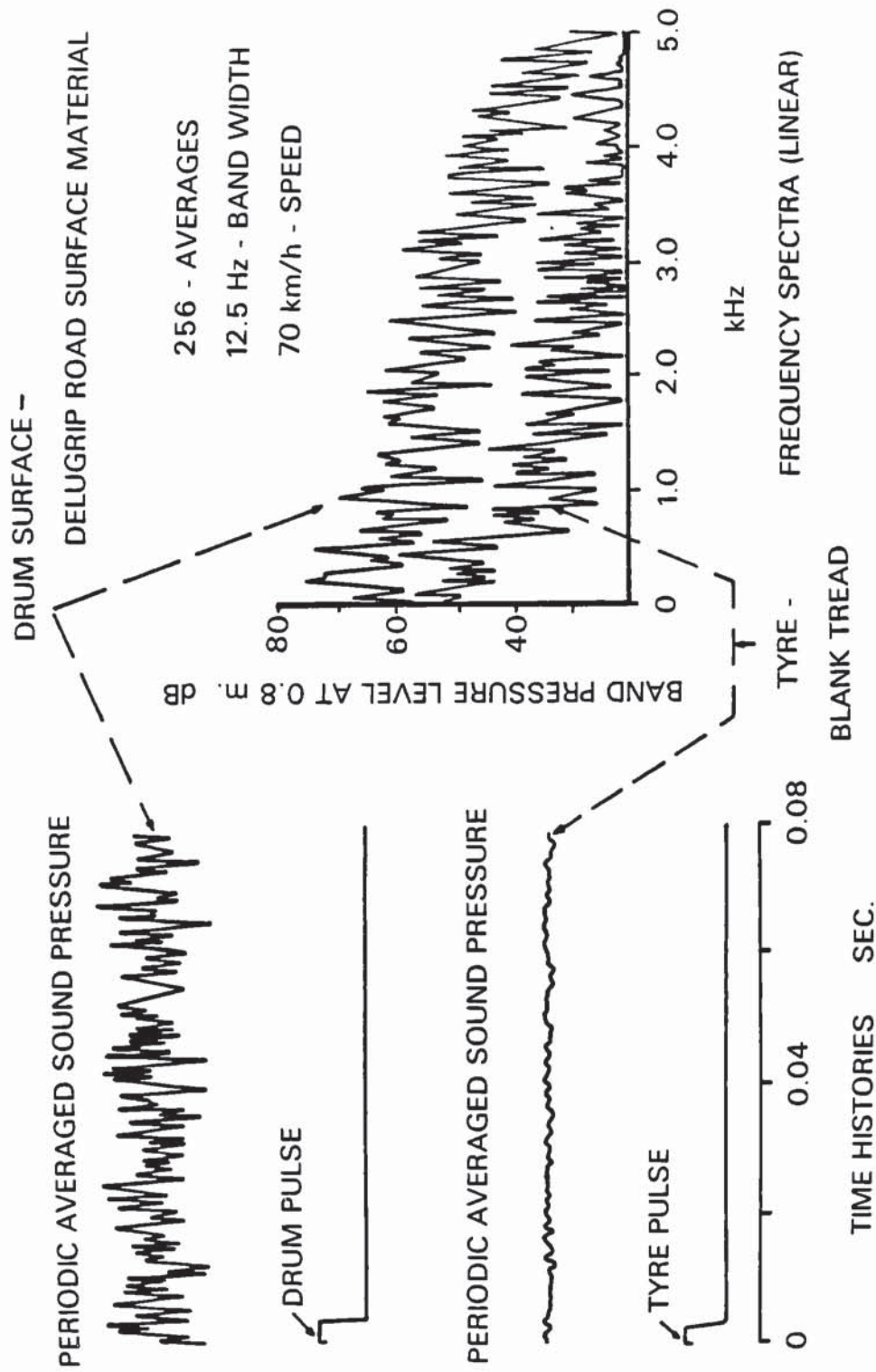
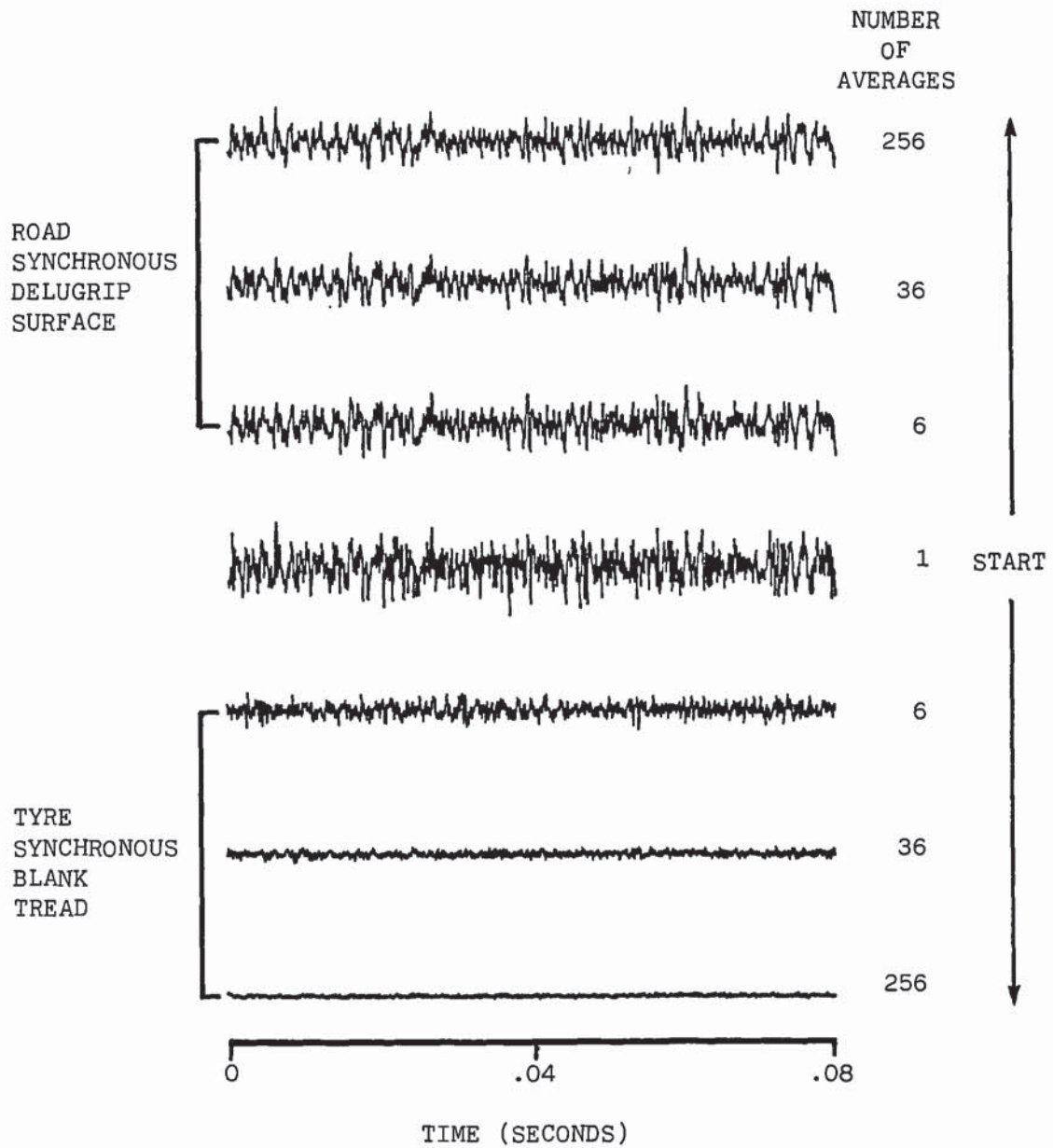


Figure 5.10.

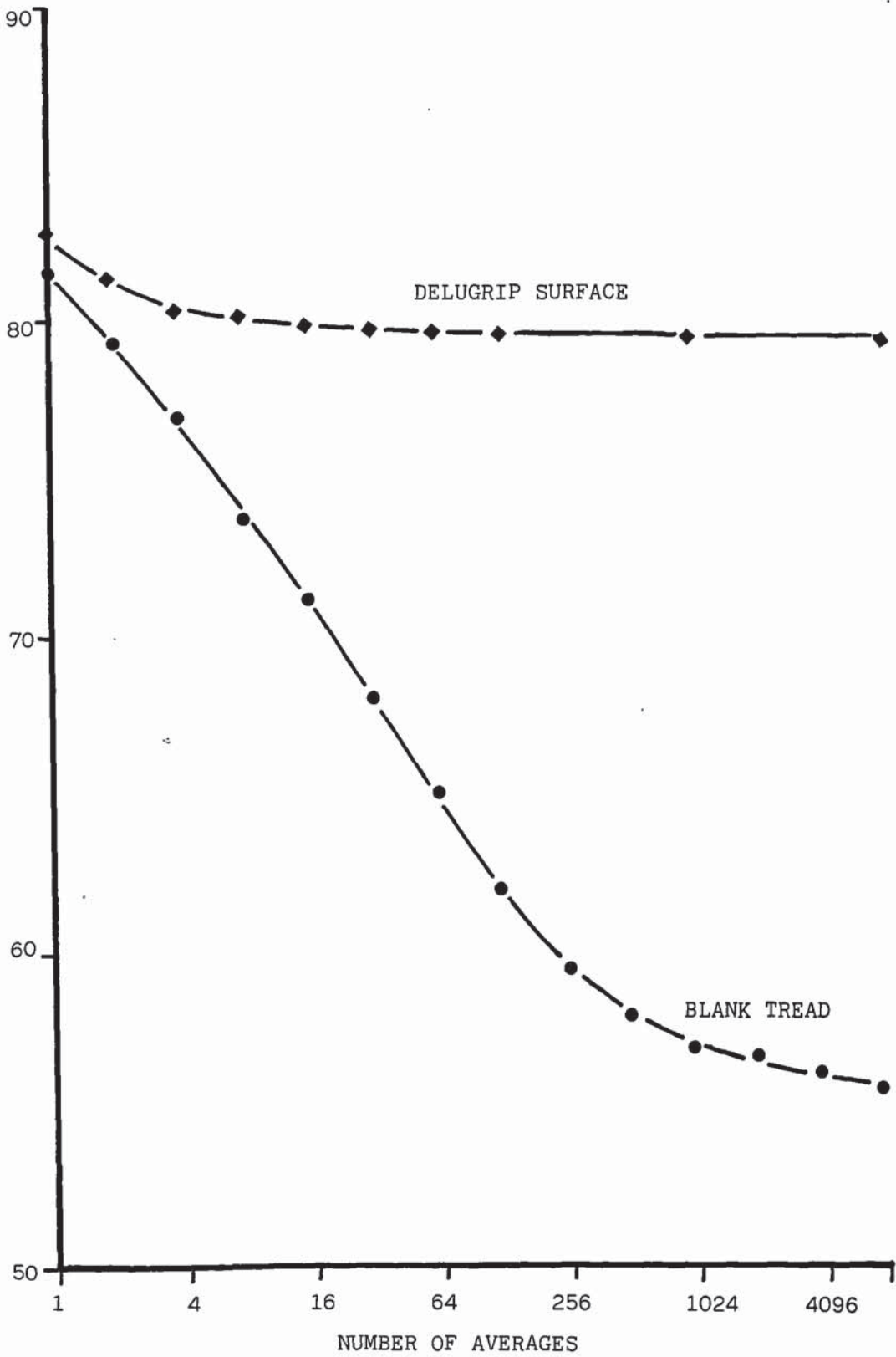
DECOMPOSITION OF THE TOTAL TYRE/ROAD NOISE INTO TYRE PERIODIC NOISE AND
DRUM SURFACE PERIODIC NOISE WITH A PLAIN TREAD TYRE AND THE DELUGRIP REPLICA SURFACE



THE STAGES OF AVERAGING, SHOWING THE PROGRESSIVE ISOLATION OF THE SYNCHRONOUS NOISE WAVES EXCITED BY THE DELUGRIP SURFACE AND THE BLANK TREAD

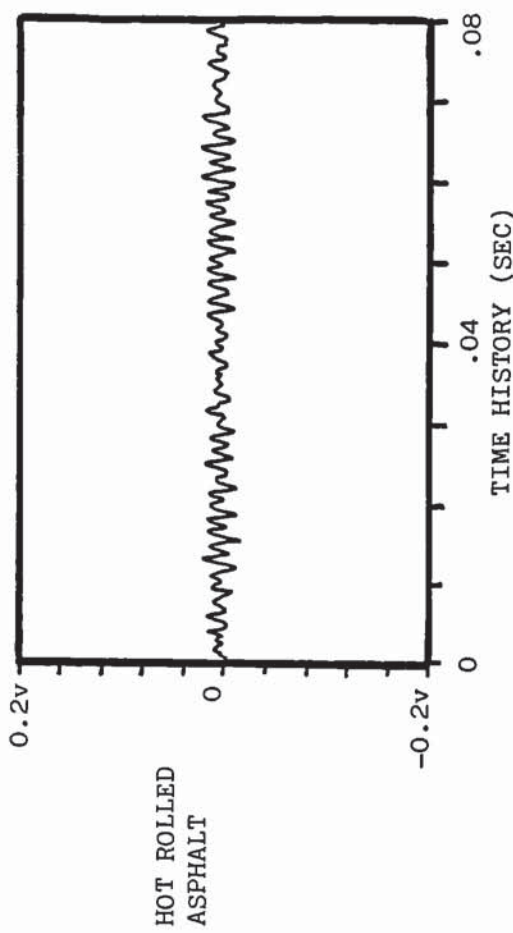
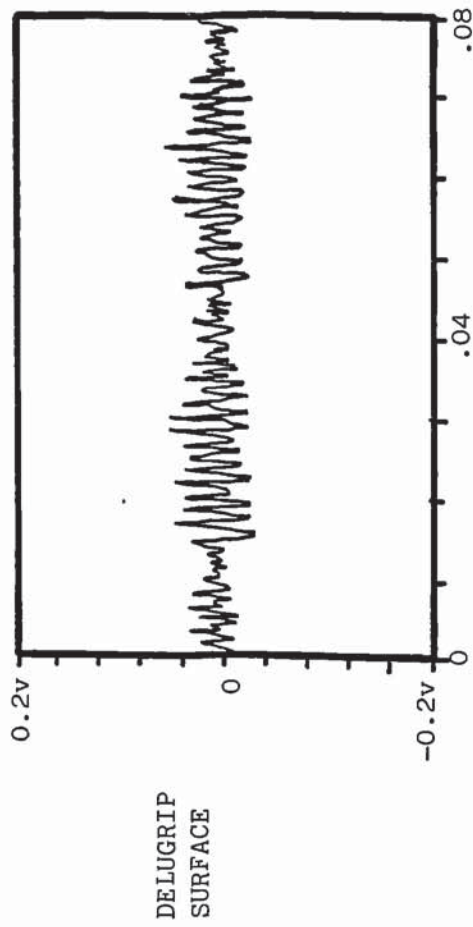
Figure 5.11.

SYNCHRONOUS
NOISE LEVEL dB(A)

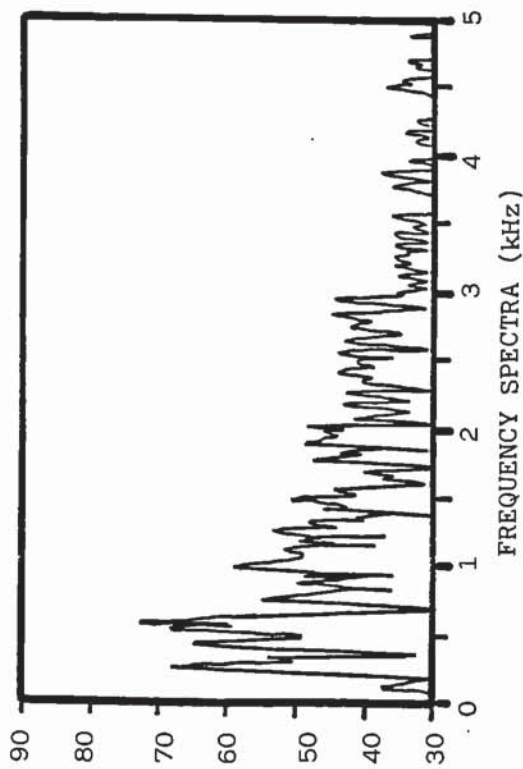
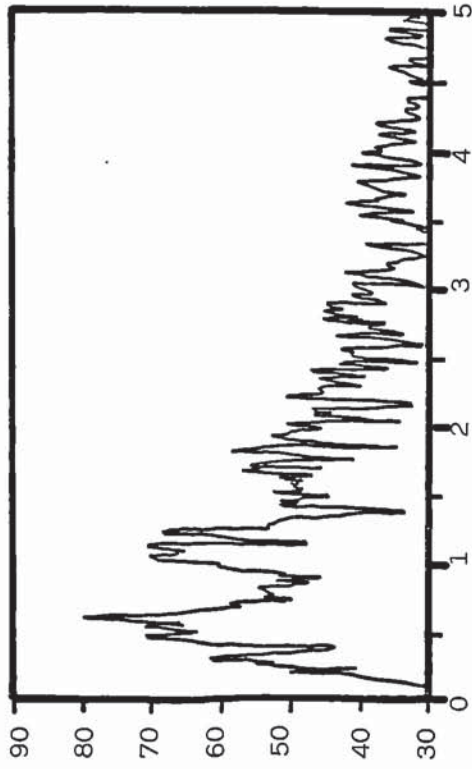


PROGRESSIVE ISOLATION, UNTIL THE VALUE STABILISES, OF THE SYNCHRONOUS NOISE LEVEL EXCITED BY THE DELUGRIP SURFACE AND THE BLANK TREAD

Figure 5.12.



BAND PRESSURE LEVEL DB A WEIGHTED AT 0.8 m



WINTER PATTERN TYRE SYNCHRONOUS NOISE ON THE HOT ROLLED ASPHALT AND DELUGRIP REPLICA SURFACES - SPEED 64 km/h

Figure 5.13.

Results from a winter pattern tyre are given in Figure 5.13. The synchronous tyre noise is reduced from 83.7 dB(A) to 76.7 dB(A), that is a reduction of 6 dB(A) when on the hot rolled asphalt as compared with the Delugrip surface. This reduction in amplitude of the synchronous wave is easily seen in the time histories on the left hand side of the figure. It is due to the fact that the tread block contact is more broken up by the coarse hot rolled asphalt surface. The hot rolled asphalt synchronous noise is 86.9 dB(A) which is 10 dB(A) greater than that for the winter tyre. This technique is useful for investigating how tyre pattern and road surface texture excited noise combine.

For example the periodic noise of a ribbed and microslot tread pattern tyre was $13\frac{1}{2} \pm 2$ dB(A) greater than a blank tread tyre on both a Delugrip and a Safety Walk surface.

Conversely the Delugrip surface which is a very quiet practical road surface had a periodic noise of 9 ± 1.7 dB(A) greater than a Safety Walk surface with both a ribbed and microslot tread pattern tyre and a blank tread tyre.

This shows that tyre excited noise can be determined over a small range of surface types and the effect of the surface on the results may be considerably reduced by this technique.

This example also shows that road/tyre interaction is somewhat more complex than simple addition of tyre and road excitation.

5.6.4. Correlation - External Automobile Coasting Noise v. Indoor Testing on Replica Surfaces

The indoor testing dB(A) levels (Figure 5.7) are plotted against external car coasting dB(A) levels at the same speed 64 km/h (Figure 5.1. and 3.6.) in Figure 5.14.

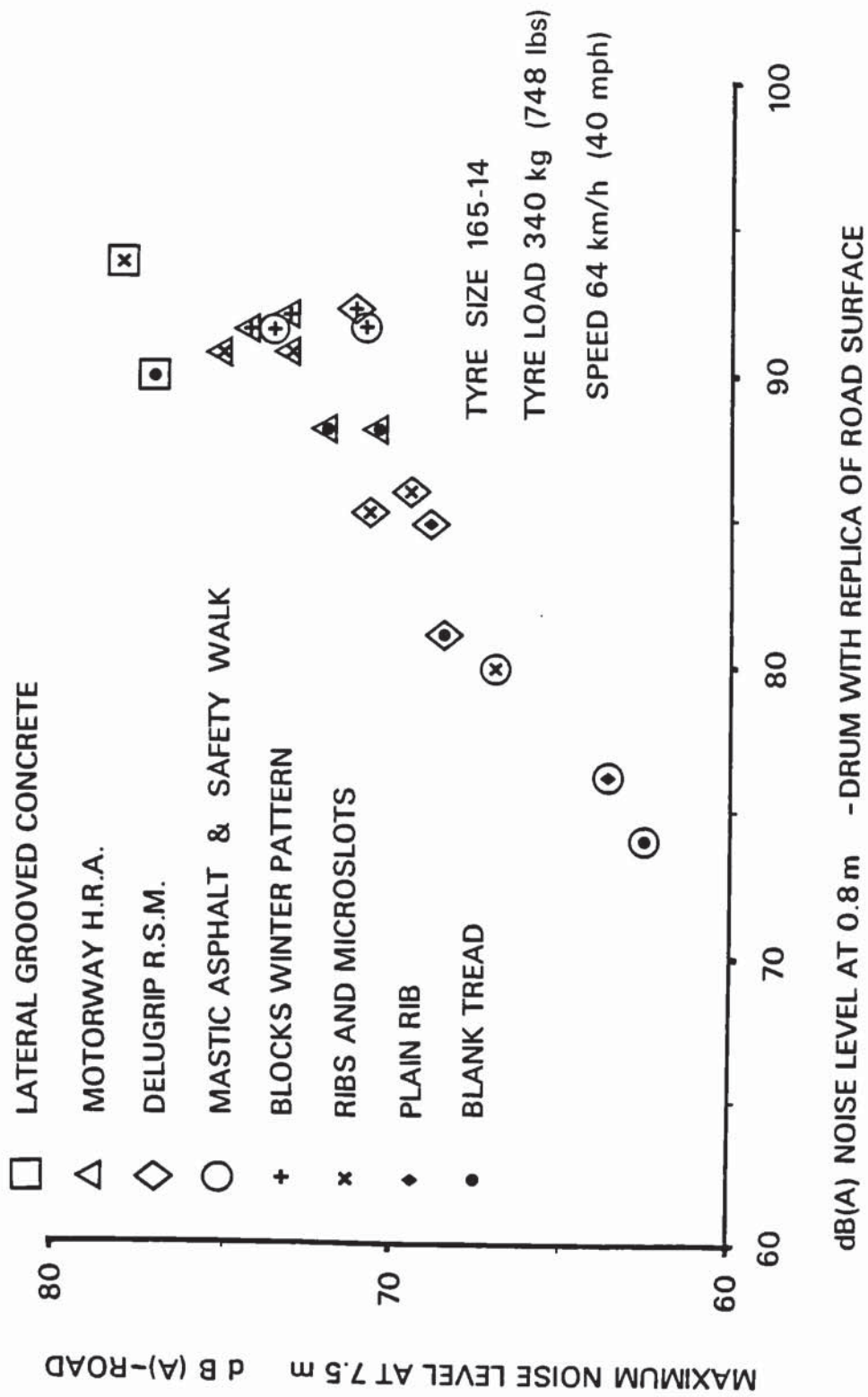


Figure 5.14. AUTOMOBILE COASTING NOISE GENERATION ON DISSIMILAR SURFACES CORRELATED WITH INDOOR DRUM TESTS USING REPLICAS OF THE SURFACES

There is a reasonable correlation, and an approximation may be estimated for the difference between the single tyre indoor figures at 0.8 m and the automobile coasting figures at 7.5 m. The decrease from the indoor noise level at 0.8 m, allowing for the inverse square law, would be -18.6 dB(A) at 6.8 m on the near side of the automobile, and -20.2 dB(A) at 8.2 m on the far side of the automobile. 3 dB(A) is added for the second nearside tyre and 1½ dB(A) is added for the far side tyres.

$-18.6 + 3 + 1\frac{1}{2} = -14.1$ dB(A). This compares with -16 dB(A) from Figure 5.14.

The correlation is more than adequate for tyre tread pattern development purposes, when aiming to keep within certain dB(A) limits and experience is showing that the frequency spectra and the subjective ratings also correlate.

5.6.4.1. Factors Influencing Correlation

(1) State of wear of Road Surfaces

It would be expected that if the outdoor tests and indoor tests were performed on the same stretches of road surface at the same state of road wear then the correlation would be closer.

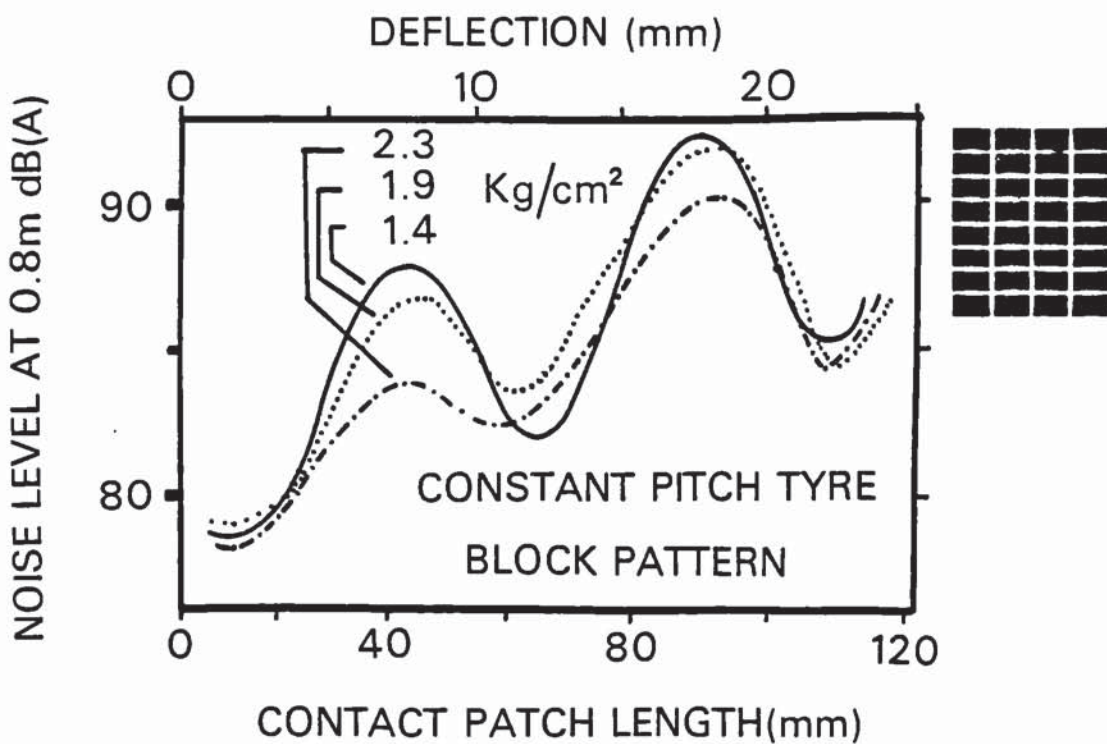
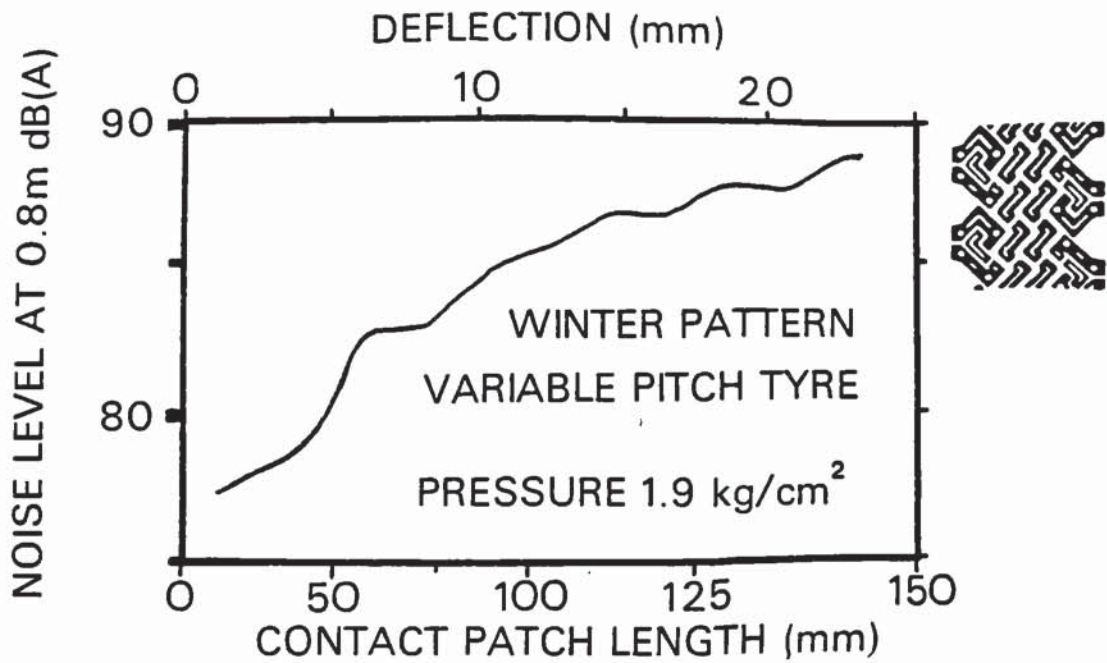
(2) Effect of Contact Patch Length of Tyre

At constant load, a tyre on a curved drum surface has a greater maximum deflection and a shorter contact length, Krempf (1967). If the load applied to the tyre on the drum is decreased to give the same maximum deflection then the contact length is further shortened. The importance of contact patch length has been noted by Samuels (1976).

The author obtained the following experimental results on the

effect of contact patch length, which demonstrate an interesting facet of tyre noise generation. The effect of patch length is shown in Figure 5.15. for a constant pitch block tread tyre. In the lower half of the figure, as deflection is increased, the level goes through peaks and troughs with approximately 9 dB(A) difference. This must be due to reinforcement and partial cancellation of the noise from the front and rear of the contact patch. At this low speed the first harmonic of the block frequency dominated the frequency spectra.

In the case of a tyre with a variable pitch tread block pattern, in the upper half of the figure, there is no such constancy of phase between the excitation at the front and the rear of the contact patch and hence the noise increases with very small variations as the deflection is increased.



EFFECT OF CONTACT PATCH LENGTH ON NOISE LEVEL FROM TYRES ON A SMOOTH DRUM

Figure 5.15.

CHAPTER SIX: THE EFFECT OF SINUSOIDAL MODULATION OF TREAD SEGMENT LENGTHS ON DOMINANT TONES (CONSTANT MODULATING FREQUENCY, f_s)

6.1. Mechanical Frequency Modulation (MFM)

Forty years ago car tyres were made with their tread segments at irregular pitches to break-up any dominant noise frequencies. However, with the application of computer techniques, further improvements in sequences are possible. Kryter and Pearson (1965) showed that band limited random noise is perceived to be less noisy than sound composed of pure tone superimposed on bandwidth limited noise, if the overall sound pressure levels are the same. Hence the sound consisting of a pure tone superimposed on random background noise can be made to sound less noisy by dispersing the energy of the tone over a number of discrete frequencies.

With this in mind, Varterasian (1969) presented a computer method of doing this, making use of rectangular unit impulses with spacing proportional to that of the tread segment spacing round the periphery of the tyre and a Fourier analysis of the resulting wave. The method is iterative, allowing successive approximation to better sequences, with manual input to change the sequence for each approximation. However, this does not ensure the best sequence since the process is analogous to finding the lowest spot in the ocean bed, and depending on where a start is made, successive approximations may merely lead to the lowest spot in a minor pocket.

Vorih (1971) simplified the waveform for a tread segment to a zero width pulse, in this type of program. This was also used by Willett (1975), who correlated the results with tyre drum tests, using simple experimental tread patterns with transverse grooves. Mechanical frequency modulation results were correlated with cross bar truck tyre vehicle boom microphone tests by Eberhardt (1975).

The ensuing discussion in this Chapter provides the basis of the

author's work in reducing dominant tones in tyre noise.

6.2. Mathematical Basis of Frequency Modulation Tones

An early step before developing the computer model is the examination of the reduction of the amplitude and the spread of the bandwidth of frequency modulation tones. The following analysis is composed from the work of Terman (1943), Reiter (1973) and Ewald (1971). The symbols used in the analysis are as follows:

α_0	average tread segment spacing angle
N	number of segments around the circumference
p	revolutions per second of the tyre
f_0	average segment frequency
ω_0	average segment angular frequency
$\Delta\alpha$	tread segment spacing angle variation amplitude
Δf	frequency deviation amplitude
$\Delta\omega$	angular frequency deviation amplitude
m	number of modulations around the tyre
f_s	modulation frequency
ω_s	modulation angular frequency
$\Delta\phi$	phase modulation amplitude
β	modulation index
θ_i	i-th segment position in an equi spaced segment arrangement
θ'_i	i-th segment position after rearranging the segments
$\Delta\theta$	angle change amplitude

$$f_0 = \frac{\omega_0}{2\pi} = Np \quad 6.1.$$

$$f_s = \frac{\omega_s}{2\pi} = mp \quad 6.2.$$

from 6.1. and 6.2.

$$\frac{f_s}{f_0} = \frac{\omega_s}{\omega_0} = \frac{m}{N} \quad 6.3.$$

$$N = \frac{2\pi}{\alpha_0} \quad 6.4$$

$$\Delta f = \frac{-\Delta\alpha}{\alpha_0} \times N \times p \quad 6.5$$

$$\beta = \frac{|\Delta f|}{f_s} = \frac{|\Delta\omega|}{\omega_s} \quad 6.6$$

Substituting from 6.2 and 6.5

$$\beta = \frac{\Delta\alpha}{\alpha_0} \times \frac{N \times p}{m \times p} = \frac{\Delta\alpha}{\alpha_0} \times \frac{N}{m} \quad 6.7$$

$$\Delta\phi = N\Delta\theta \quad 6.8$$

$$\theta_1 = 2\pi pt \quad \frac{-\Delta\alpha}{\alpha_0} = \frac{\Delta\omega}{\omega_0} \quad 6.9$$

These equations are used for the analysis in the following section.

6.2.1. Phase Modulation Amplitude

Ewald et al (1971) considered frequency modulation effects of the spacing of fan blades. The analysis is just as applicable to tyre tread segment spacing.

If the tread segments are the same length then there is a set of

segment positions around the circumference of the tyre as in the top half of Figure 6.1. When there is modulation of the spacing, there is a segment e.g. the x th, which has a maximum angle change $\Delta\theta$ relative to the x th segment position in the fixed segment length tyre as in the lower half of Figure 6.1. The phase modulation amplitude is $\Delta\phi$ i.e. the angle change related to one mean segment spacing angle, rather than to one revolution as in the case of $\Delta\theta$ ($\Delta\phi = N\Delta\theta$).

The modulated positions are described by:

$$\theta'_i = \theta_i + \Delta\theta \sin (m \theta_i) \quad 6.10$$

Substituting 6.9 in 6.10.

$$\theta'_i = 2\pi pt + \Delta\theta \sin (m \cdot 2\pi pt)$$

For N segments

$$N\theta'_i = 2\pi Npt + N\Delta\theta \sin (2\pi mpt)$$

Substituting from 6.1, 6.2 and 6.8.

$$N\theta'_i = \omega_o t + \Delta\phi \sin \omega_s t$$

The instantaneous signal

$$e = A \sin (\omega_o t + \Delta\phi \sin \omega_s t) \quad 6.11$$

An alternative approach has been made to this by Reiter (1973) following the work of Terman (1943) on the frequency modulation of radio carrier signals. This shows the modulation index $\beta =$ the phase modulation amplitude $\Delta\phi$.



Figure 6.1.

(Ewald, 1971)

Equation (6.11) can be expressed using Bessel coefficients of the first kind and the nth order with argument $\Delta\phi$.

$$\begin{aligned}
 e = A & \left(\begin{aligned} & J_0(\Delta\phi) \left(\sin \omega_0 t \right) \\ & + J_1(\Delta\phi) \left(\sin(\omega_0 + \omega_s)t - \sin(\omega_0 - \omega_s)t \right) \\ & + J_2(\Delta\phi) \left(\sin(\omega_0 + 2\omega_s)t + \sin(\omega_0 - 2\omega_s)t \right) \\ & + J_3(\Delta\phi) \left(\sin(\omega_0 + 3\omega_s)t - \sin(\omega_0 - 3\omega_s)t \right) \\ & + \dots \dots \dots \end{aligned} \right)
 \end{aligned}$$

6.12

As seen in the set of Bessel coefficients in Figure 6.2 $\Delta\phi$ controls the amplitude and bandwidth of the dominant harmonics.

A trial value is chosen for $\Delta\phi$. Then a vertical line is drawn through the trial value of $\Delta\phi$. The intersection of the $J_n(\Delta\phi)$ curves indicates the relative amplitudes of the resulting components at frequencies $f_0 \pm n f_s$ where n is an integer multiple. The amplitudes are symmetrical about the centre frequency. The resulting spectra is given to the right of the graph. Note that absolute values are plotted on the frequency spectrum. The dashed lines indicate the normalised amplitude of the fundamental segment passing frequency tone for a tyre with evenly spaced segments.

In Figure 6.2 $N = 22 \quad \Delta\theta = .175 \text{ radians}$

$$\Delta\phi = N\Delta\theta = 22 \times .175 = 3.85 \text{ radians}$$



Figure 6.2. BESSEL COEFFICIENTS VERSUS MAXIMUM PHASE DEVIATION $\Delta\phi$ AND FREQUENCY SPECTRUM FOR $\Delta\phi = 3.85$ (EWALD 1971)

also
$$\frac{\Delta \alpha}{\alpha_0} = 0.175 \beta = \frac{\Delta \alpha}{\alpha_0} \times \frac{N}{m} = .175 \times 22 = 3.85$$

When considering the case of higher harmonics, that is multiples of f_0 , then the appropriate phase modulation amplitude is $n\Delta\phi$ for the frequency nf_0 . Hence higher harmonics are more dispersed than f_0 for a given value of $\Delta\phi$.

6.2.2. Modulation Index

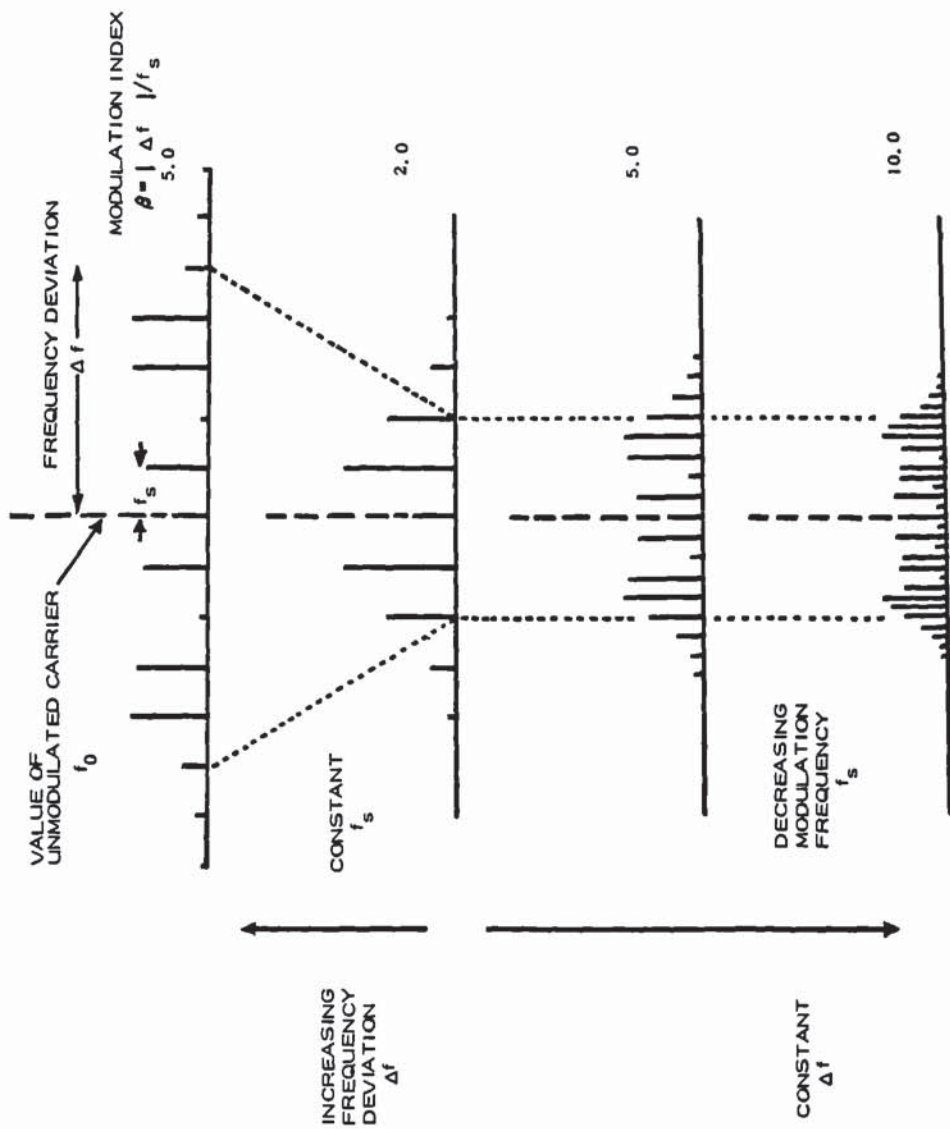
As a general guide, important spectral components are generally found in a bandwidth centred on the carrier frequency, given by twice the sum of the frequency deviation (Δf) and the modulation frequency (f_s) according to Reiter (1973). Frequency spectra for various values of the modulation index (β) are shown in Figure 6.3.

To obtain a wider bandwidth, the frequency deviation is increased and the modulating frequency kept constant as in the upper half of the figure. This increases the modulation index (β) and reduces the amplitude of the dominant frequencies.

For a fixed frequency deviation (Δf) the modulation frequency (f_s) controls the spacing of the frequencies as in the lower half of the figure. Decreasing the modulation frequency (f_s) increases the modulation index (β) and reduces the amplitude of the dominant frequencies.

In order to obtain a bandwidth of significance, the modulation index (β) must be greater than 1.

The author feels that it is worth expressing the results in a single diagram. Figure 6.4. shows the value of (β) calculated from equation 6.7. for a range of values of, the number of segments (N) from 30 to 80, the modulation frequency 4 to 8, and the fractional deviation from mean pitch 0 to 0.25.



EFFECT ON FREQUENCY SPECTRA OF INCREASING MODULATION INDEX $\Delta f/f_s$ BY:

- 1) INCREASING FREQUENCY DEVIATION Δf AT CONSTANT f_s
- 2) DECREASING MODULATION FREQUENCY f_s AT CONSTANT Δf

Figure 6.3.

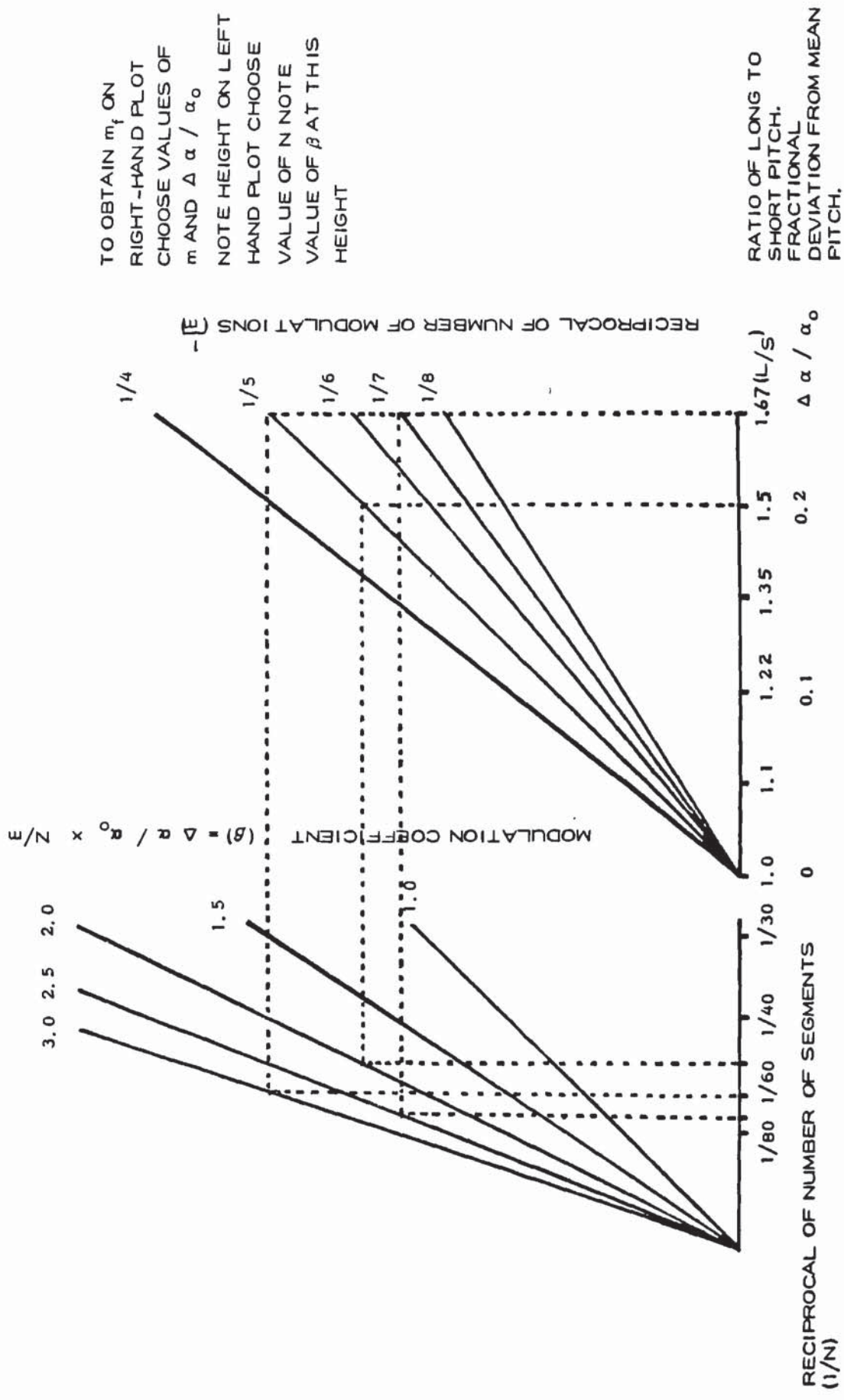


Figure 6.4. TO OBTAIN β FROM N , m , and $\Delta \alpha / \alpha_0$

Figure 6.5. shows a simpler plot relating the modulation index (β) to the ratio (N/m) from 6 to 14 and the fractional deviation from the mean pitch $\frac{\Delta \alpha}{\alpha_0}$ from 0 to 0.25. In practice, larger tyres have a higher N and a higher m , N/m tends to be constant keeping β constant for a given pitch ratio.

The modulation index for the sequences associated with the frequency spectra shown in later figures is calculated as follows:

$$\beta = \frac{\text{fractional change in tread spacing } \frac{d \alpha}{\alpha_0} \times \text{number of segments (N)}}{\text{Number of modulations per revolution (m)}}$$

Figure 7.2 initial spectra (drum tests) $\beta = 0.10 \times \frac{36}{7}$

$$\beta = 0.10 \times 5.2 = 0.52$$

Modified tyre $\beta = 0.10 \times \frac{36}{4}$

$$\beta = 0.10 \times 9 = 0.90$$

Figure 7.4. at 140:100:60 ratio (computed harmonics) $\beta = 0.4 \times \frac{62}{8}$

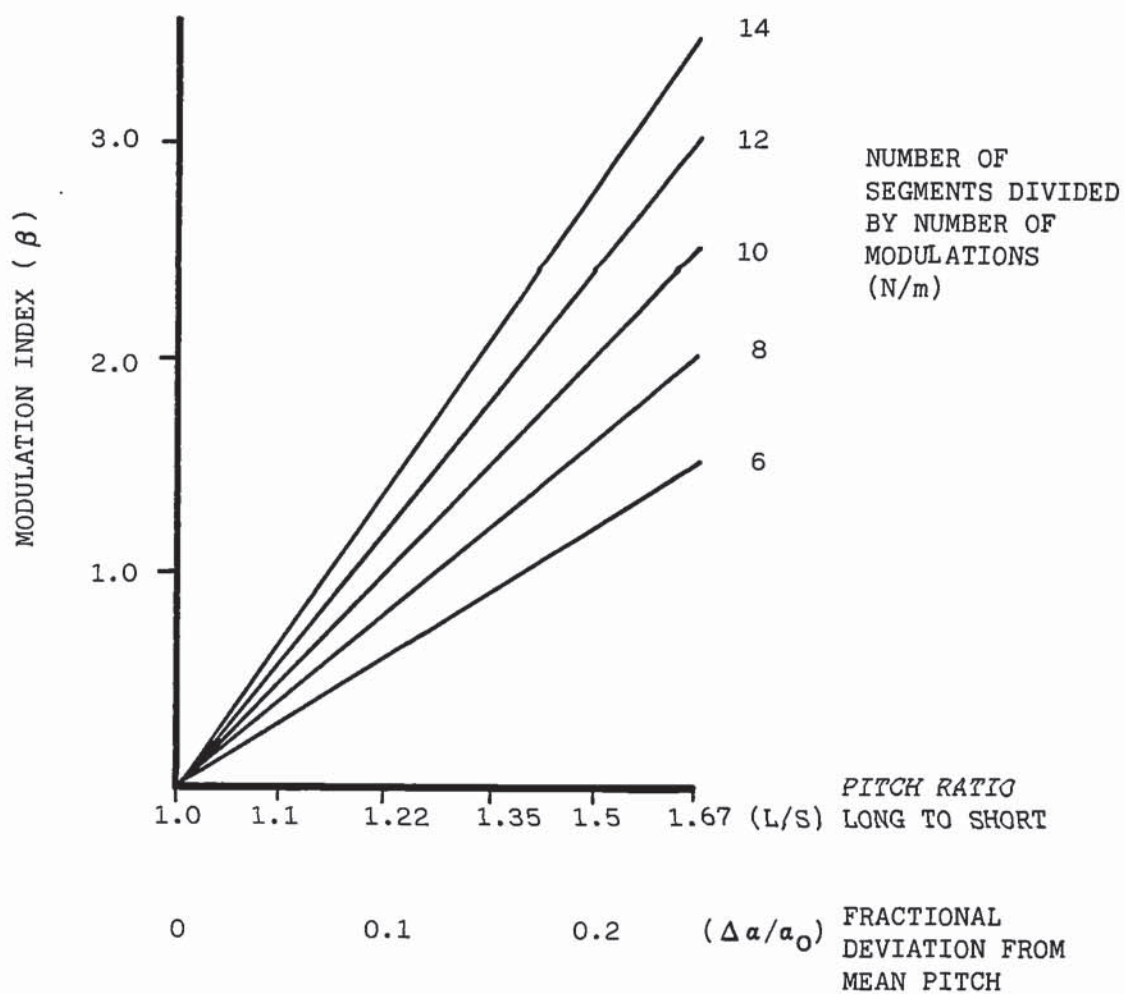
$$= 0.4 \times 7.75 = 3.1$$

As the value of β increases, the dominant frequencies decrease in amplitude as seen in the corresponding figures.

If the tread spacings do not vary sinusoidally, but vary in a more complex fashion, then a more complex spectrum is obtained.

However, the bandwidth containing the major spectral components does not enlarge and is determined by the modulation index.

The preceding analyses apply to sinusoidal modulation of constant wavelength. In order to investigate more complex types of modulation a computer program has been developed.



TO OBTAIN MODULATION INDEX FROM N/m AND $\Delta a/a_0$

Figure 6.5.

6.3. Constraints in Actual Tyre Design Modulation

By taking the case of one cycle of sinusoidal modulation around the tread circumference, and a fractional change in mean segment length of 0.25, then for 60 segments the modulation index will be $0.25 \times 60 = 15$, and for 30 segments will be 7.5.

Although this would give a good reduction in dominant tones it would also cause a warbling effect. Tyre noise becomes noticeable at speeds above 48 km/h (30 mph) and for warbling to be too rapid to be noticeable at this speed, there would need to be approximately a minimum of five cycles of modulation around the circumference of a large car tyre. This reduces the modulation index for 60 segments to 3.0.

Tyre moulds can be made at lower cost with three segment lengths, since using a greater number of segment lengths involves greater cost.

CHAPTER SEVEN: THE EFFECT OF NON SINUSOIDAL MODULATION OF TREAD
SEGMENT LENGTH AND VARIABLE MODULATING FREQUENCY
ON DOMINANT TONES

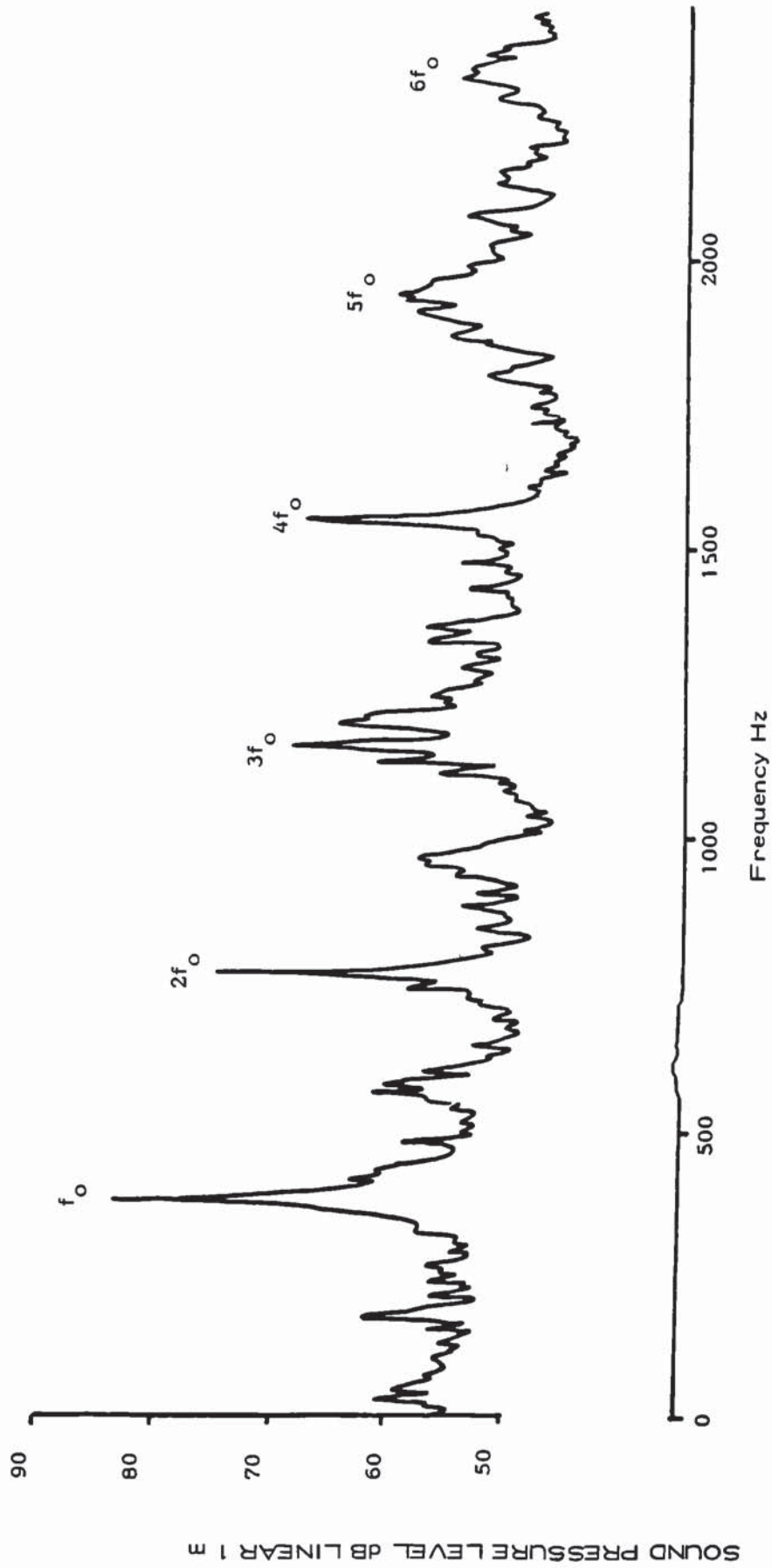
7.1. The Approach to the Investigation

As has been stated in Chapter 6 non sinusoidal modulation is not susceptible to mathematical analysis. There are three possible approaches to this investigation.

1. Experimental sequences may be cut in blank tread tyres. A blank tread is of full tread thickness but has no tread pattern. This method is costly and slow for investigation purposes, but it is useful to test a tread pattern before it is put into production.
2. An Analogue System. The tread pattern may be printed in a drum and detected by a line of photocells across the tread pattern with the optical signal being converted to audio output. This is less costly and quicker than method (1), but in its simple form does not take into account, tread contact pressure distribution effects, tread radius, breaker construction and pattern depth. This type of simulator was described by Mukai (1974).
3. Digital Computer Method. This has the advantages of quick input and flexibility for increased sophistication as further insight is gained into the mechanisms of tyre noise generation.

7.1.1. Introduction to a Digital Computer Method of Tyre Noise Simulation

Figure 7.1. shows the frequency spectrum of a simple constant pitch block pattern tyre tested by the author on a drum in the laboratory. The experimental procedure was described in Chapter 5.2. The tyre had 51 pitches and was rotating at 7.54 Hz.



DOMINANT HARMONICS - DRUM TEST - CONSTANT PITCH BLOCK PATTERN

Figure 7.1.

The spectra shows the block frequency $f_0 = 385$ Hz and higher harmonics of descending magnitude. Hence a wave to represent the effect of a single block in a computer model would need to have higher harmonic content. Two possibilities are discussed.

7.1.2. The Waveform used to Represent the Effect of a Tread Segment

Varterasian (1969) used a wave of unit impulse height, and of width $2\pi K$. On Fourier Analysis this gives:-

$$y = 1. \left(K + \frac{2}{\pi} \left(\begin{array}{l} \sin K\pi \cos \omega t \\ + \frac{1}{2} \sin 2K\pi \cos 2\omega t \\ + \frac{1}{3} \sin 3K\pi \cos 3\omega t \\ \vdots \\ + \frac{1}{n} \sin nK\pi \cos n\omega t \end{array} \right) \right)$$

therefore

The coefficients of $\cos n\omega t$ are proportional to $\frac{\sin nK\pi}{n\pi}$

when K is very small $= \frac{nK\pi}{n\pi} = K$

i.e. the coefficients are constant. This means that all the lower harmonics up to the 10th have substantially the same amplitude as the fundamental.

While the use of a narrow pulse is economical on computer storage, it is however considered to represent the practical situation poorly. The experimentally derived spectrum in Figure 7.1. shows decreasing higher order harmonics. This suggests that a sawtooth is a much closer representation of the practical waveform.

$$y = \frac{2}{\pi} 1. \left(\begin{array}{l} \sin \omega t \\ - \frac{1}{2} \sin 2\omega t \\ + \frac{1}{3} \sin 3\omega t \end{array} \right)$$

$$\begin{aligned}
 & - \frac{1}{4} \sin 4 \omega t \\
 & + \dots\dots\dots)
 \end{aligned}$$

This series contains both odd and even harmonics with decreasing amplitudes as the harmonic order rises.

A comparison of the rate of reduction in amplitude as the harmonic order rises is given on the following page.

TABLE 7.1. RELATIVE POWER RATIOS OF HARMONIC ORDERS.
EXPERIMENTAL VERSUS SAWTOOTH WAVE

Harmonic Order	Experimental from Figure 4.1. Power Ratio	Sawtooth Power Ratio
1	1	1
2	1/3	1/4
3	1/5	1/9
4	1/6	1/16
5	1/14	1/25
6	1/27	1/36

The waveform of the noise from the tyre varies considerably with speed due to tyre resonance effects, as indicated by J C Walker and Major (1975), and also due to any standing waves. This will alter the relative amplitude of the different harmonics.

Nevertheless, the experimental wave is better represented by a sawtooth wave than by a narrow pulse wave. A more accurate representation at this tyre speed would be a sawtooth with rounded corners.

7.2.1. Introduction - The Program

In the approach to investigate different sequences, Dr D J Osborne

(Dunlop Limited) developed a program for the IBM 370 originally on similar lines to that used by Varterasian. A sawtooth wave form is used to represent the noise from a tyre tread segment.

The length of the sawtooth is proportional to the length of the corresponding tread segment. The whole tyre circumference is built up from sawtooth waves and the resultant wave is Fourier analysed in the computer. The results are printed out, or punched tape output can be obtained to feed to a mini-computer. This feeds to a loudspeaker or to a tape recorder. A frequency spectrum can be obtained on A4 size paper using the fast Fourier transform (FFT) program in the mini-computer. The input to the IBM program is very simple as it requires the lengths and order of the segments only. A typical run takes 9.04 secs C.P.U. and the program operates within the 100 K partition of the IBM 370. The storage for the program is 16 K bytes. The program input is further described in the Appendix in Section 1. The following studies using this program were carried out by the author.

7.2.2. Correlation between Frequencies Predicted by the Program and Tyre Drum Test Results

In the simplest case, a tyre with for example, 36 equal length segments would give a 36th dominant harmonic tone, i.e. its frequency is 36 times the revolutions per second of the tyre. The upper part of Figure 7.2. shows the frequency analysis of the noise from a tyre tested on a smooth drum, of 1525 mm (60 inch) diameter, in a fairly large laboratory with non parallel walls. The dominant frequencies simulated by the computer, shown by arrows, agree well with the actual measured results. As mentioned in Section 6.2.2. β is only 0.52, which is very low. Such a poor sequence would not be used with present knowledge. The tread pattern of this tyre is shown in Figure 7.3. which has been drawn by the computer drafting machine with standard programs.

In the lower part of Figure 7.2. there is again good agreement.



TREAD PATTERN - COMPUTER DRAFTED - 185/70HR13 D1 TYRE
Figure 7.3.

This spectrum is better than the previous one since the small number of dominant tones are now split into more tones of lower intensity. As calculated in Section 6.2.2. β is 0.90 which is better than the previous case. The harmonics noted, reading from left to right correspond to L, M, S, $2L + m$, $2M$, $2M - m$, $2S$ where L:M:S are long: medium: short segment harmonics and m corresponds to the modulation, which is 4 per revolution in this case. This is as expected from the Frequency Modulation Theory.

7.3. The Effect of Segment Length Ratio on Dominant Tones

Figure 7.4. shows the intensity of the dominant harmonics for a typical traditional sequence. The segment length ratio changes from 100/100/100 to 135/100/65. At 100/100/100 the strong 62nd harmonic corresponds to the number of segments around the tyre circumference. As the ratio increases, the energy is taken from the 62nd harmonic and appears in the 54th and then the 50th at a lower level, giving a maximum reduction of approximately 10 dB.

In this construction the tread is divided into eight blocks or modulation cycles. All of these contain short, medium and long segments arranged so that the short elements are at the end of a block, and the long elements are near the centre of a block, with the medium elements between short and long. The blocks can contain any number of segments between 5 and 10. The sequence with the block configuration is shown at the top of Figure 7.4.

Thus a pronounced frequency will be the harmonic of the wheel revolution frequency, represented by the difference between the mean segment frequency and the modulation or block frequency i.e. $62 - 8 = 54$ th harmonic.

The shape of the curves has considerable similarity to the Bessel coefficient curves in Figure 6.2. which showed a drop from 1.0 to 0.3. i.e. 10 dB in P.S.D. to be the maximum drop. However, the

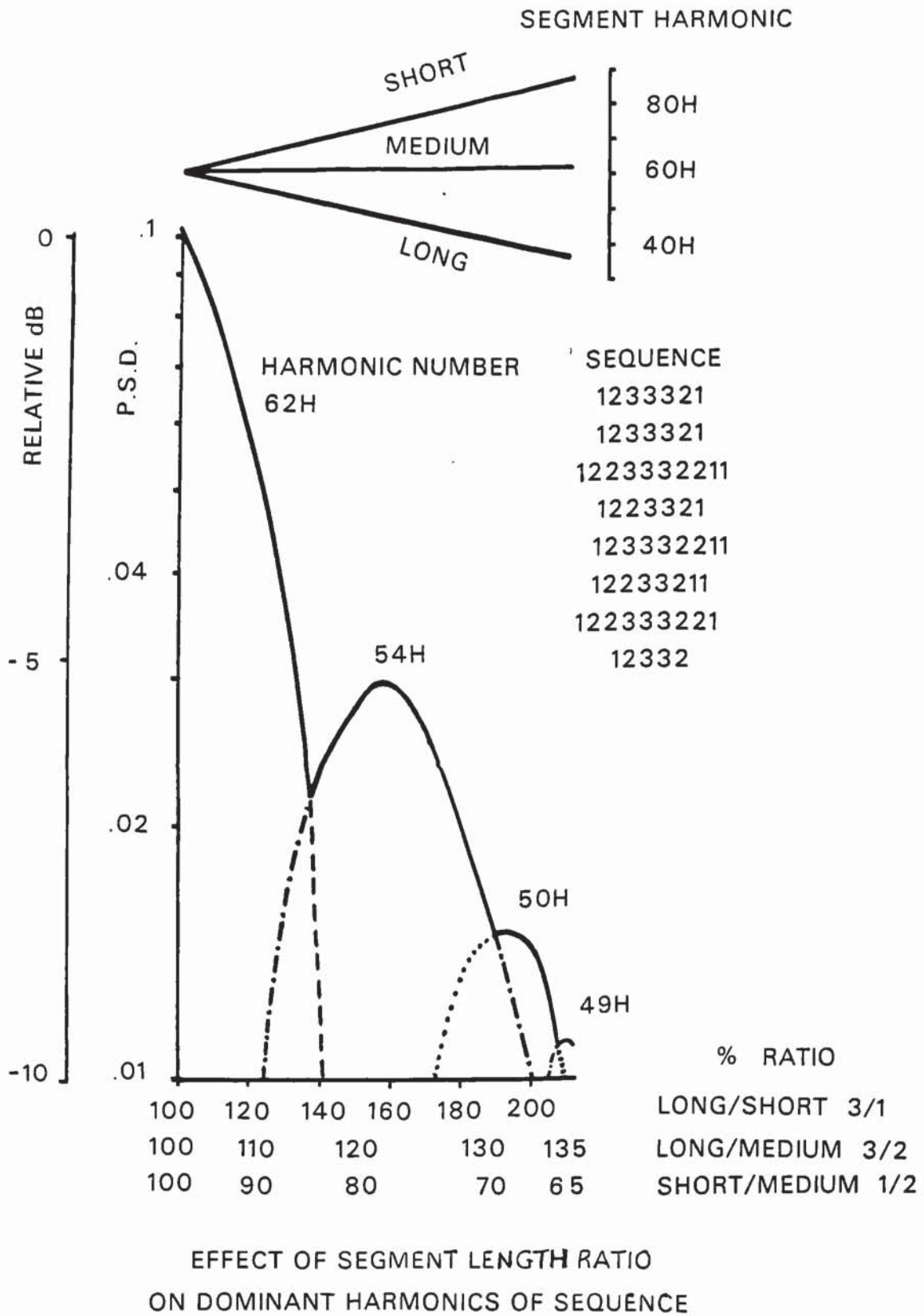


Figure 7.4.

non sinusoidal modulation gives a somewhat more rapid decrease in the dominant harmonic as the segment length ratio is increased. P.S.D. is the power per Hz bandwidth and has traditionally been used.

The harmonics corresponding to the segment lengths are shown at the top of the diagram, but none of these harmonics are dominant in the spectra below, as they would be if a greater number of identical adjacent segments occurred in the sequence.

To take account of different values for the medium segment length, contour plots may be derived to relate the independent variables $2/1$, $3/2$ and the P.S.D.

7.4. The Best Sequence

The previous figure showed the effect of segment length on a given sequence. The next variable to investigate is the effect of altering the sequence. To permute the order of all the segments is prohibitive in magnitude of calculation. However one way of altering the sequence is to permute the order of the blocks of segments in the sequence, *retaining the order within each block*. The program was modified to do this. Figure 7.5. shows the intensity of the dominant tones for each permutation which are ranked from worst to best. The details of the sequence are included on the figure. Also a permutation of a 2 pitch sequence is given.

The program contains $6!$ permutations (720 maximum). However 40 permutations are usually adequate to get close to the best sequence.

7.5. The Effect of the Maximum Number of Identical Length Adjacent Segments (Long and Short)

Figure 7.6. shows the number of adjacent long segments required

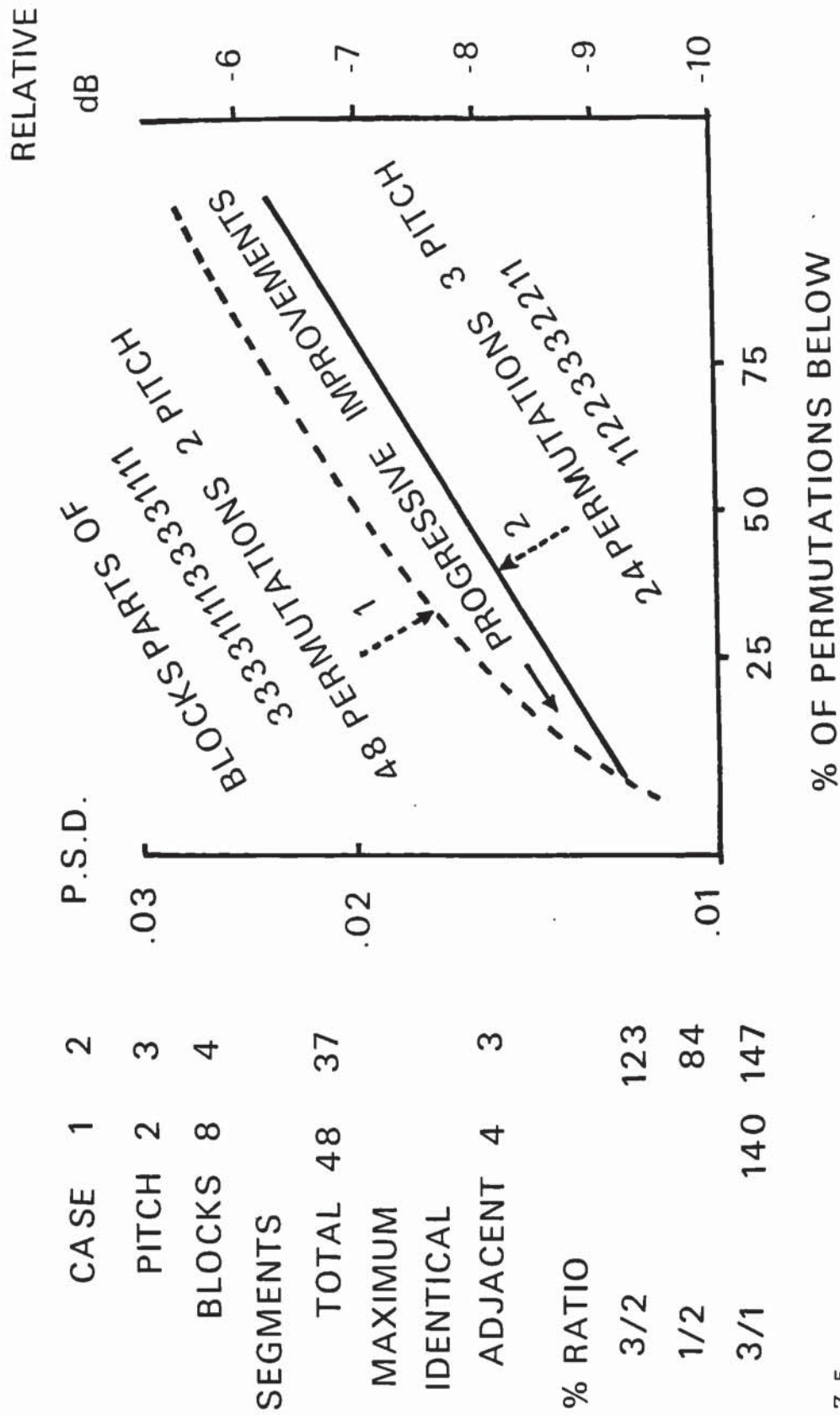
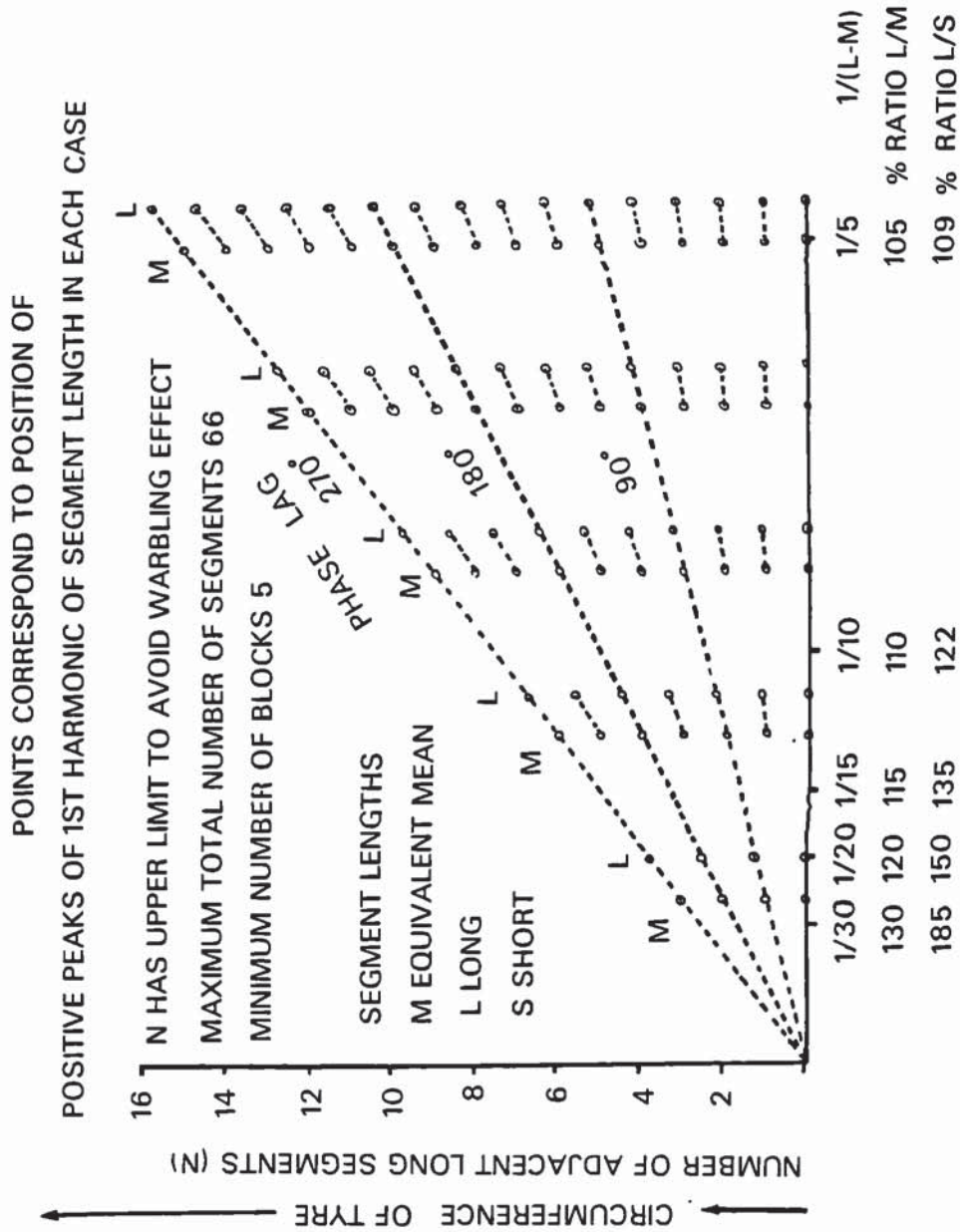


Figure 7.5.

DISTRIBUTION OF DOMINANT TONE INTENSITY AFTER MANY PERMUTATIONS



NUMBER OF ADJACENT LONG SEGMENTS
REQUIRED AT DIFFERENT RATIOS TO GET L OUT OF PHASE WITH M
AND MINIMISE THIS DOMINANT HARMONIC

Figure 7.6.

at different ratios to get the long segment out of phase with the mean segment length. They start in phase at the bottom of the diagram and this is in effect the $\Delta\phi$ referred to in section 6.2.1. The 90° , 180° and 270° phase lag lines are shown. The advantage of having more than 2 identical length adjacent segments is that the higher this number is ($\Delta\phi$ not above π radians) and within the limit for excessive warbling, then the more will the segment get out of phase with the equivalent mean segment length wave which is the dominant wave at small ratios. Thus the intensity of this harmonic will be reduced. The segment length to be considered for any sequence is the one, either long or short, in which the maximum number of adjacent identical length segments is the lesser, since this will degrade the value of the sequence.

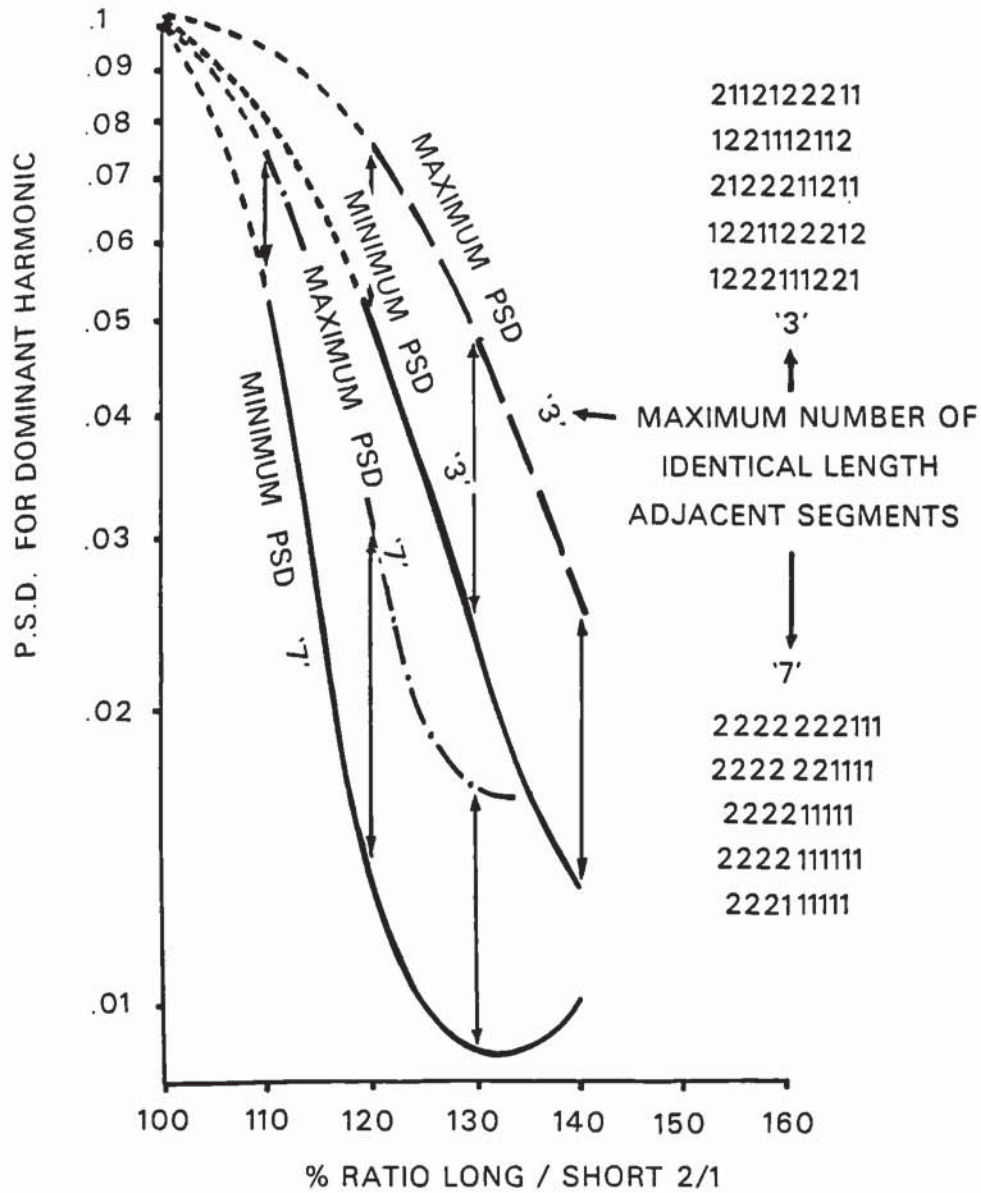
7.6. The Combined Effect of Segment Length, Number of Identical Length Adjacent Segments, and Permutations of the Order of Blocks of Segments, on the Dominant Harmonics of Two Pitch Sequences

Figure 7.7. shows a sequence with up to three adjacent identical length segments, the best and worst P.S.D. from the permutations. The P.S.D. values for the sequence with seven adjacent identical length segments are much better. Both sequences are shown for a range of long/short ratios.

The danger of having too many identical length adjacent segments is that an undesirable warble will appear in the noise. The values for tyres previously discussed fall logically into place in Figures 7.6. and 7.7.

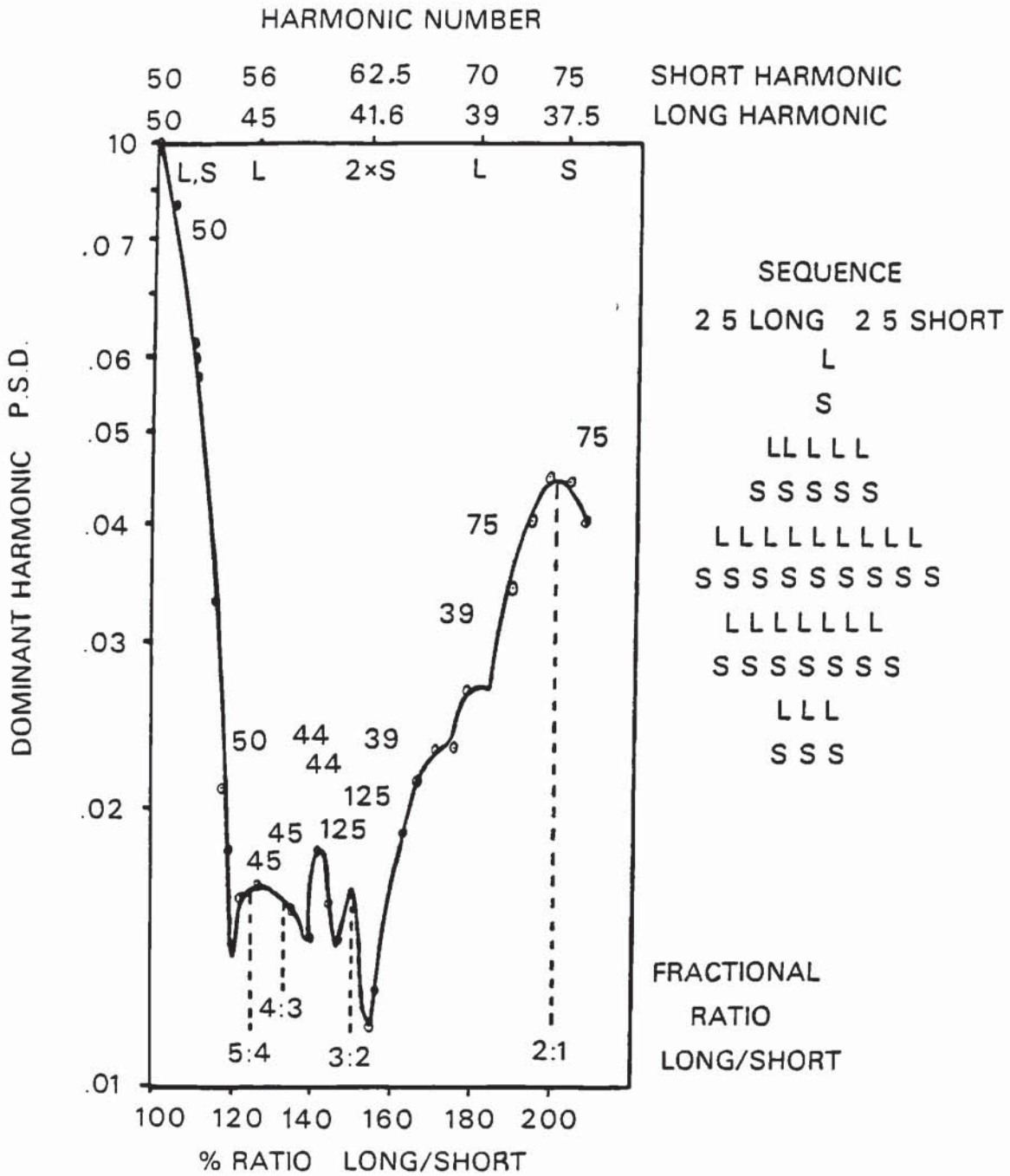
7.7. Ratio of Segment Lengths (2 Pitch)

In Figure 7.8., as the ratio is increased a considerable improvement occurs. This shows that the dominant frequencies over a large part of the frequency range correspond to those produced by the long and short segments. They are listed at the top of the figure.



- THE EFFECT ON THE DOMINANT HARMONIC OF 2 PITCH SEQUENCES:
1. PERMUTING ORDER OF BLOCKS OF SEGMENTS
(MAXIMUM AND MINIMUM PSD AFTER MANY PERMUTATIONS)
 2. % RATIO LONG TO SHORT SEGMENT LENGTH
 3. MAXIMUM NUMBER OF IDENTICAL LENGTH ADJACENT SEGMENTS

Figure 7.7.



THE EFFECT ON THE DOMINANT HARMONIC OF THE SEGMENT LENGTH RATIO. 2 PITCH

Figure 7.8.

They tend to be worse with a ratio of low adjacent integers, e.g. 1:1, 2:1, 3:2, 4:3, 5:4. In the case of the 3:2 ratio, the third harmonic of the long segment and the second harmonic of the short segment are the same frequency and will add, leading to a dominant tone of relatively higher intensity at this ratio.

7.8. 3 Pitch Sequence with fewer Identical Length Adjacent Segments v. 2 Pitch Sequence with more Identical Length Adjacent Segments

Figure 7.4. shows the general improvement trend as the three pitch ratios are widened up to 200% L/S ratio. Modulation frequencies dominate and the individual segment length frequencies are not dominant.

Figure 7.8. shows that as the two pitch ratio is widened, a very rapid improvement occurs at small ratios up to 120% and then segment length frequencies dominate especially at fractional ratios of low adjacent numbers, getting much worse as 200% is approached.

7.9. Test of the Effect of Phase of the Sawtooth Wave within the Segment

Computer tests were made on a sequence 23321 11223 32112 33322 11122 33322 11233 21122 33322 112333 221112 with segment lengths 1:2:3 - 27.53: 32.86: 40.60 mm.

A P.S.D. of the dominant harmonic 0.02087 at the 51st harmonic was obtained with the steep front of the sawtooth at the start of the segment and 0.02112 at the 51st harmonic with the steep front of the sawtooth wave half way along the segment.

The two results are within 1% of each other, hence the effect of phase within the segment is very small.

The next stage in development of the program is to include the influence of different tread patterns.

CHAPTER EIGHT: THE MODELLING OF THE EFFECT OF TREAD PATTERN ON
DOMINANT TONES

8.1. Analytical modelling

As referred to in Chapter 2, Reiter (1973) modelled the tyre noise of two simple tread patterns, a simple cross bar pattern and a ribbed pattern.

8.1.1. Cross Bar Pattern

He regarded the noise as being generated by the series of damped parallelopipeds on a rigid foundation. There is compression of the element during contact and a sudden release as it comes out of contact. He derives the sound power (W_n) for a single element at one frequency at a specific time (T_s).

$$W_n = \frac{\rho_o \cdot a_o \cdot k_n^2 \cdot A^2}{\pi^5 n^4} (h - h_o)^2 \cdot 4 \cdot \omega_n^2 \cdot e^{-n\omega_n T_s}$$

The symbols used in the analysis are as follows:

ρ_o	= density of air
a_o	= speed of sound in air
k_n	= wave number associated with nth mode = $\frac{\omega_n}{c_L}$
c_L	= longitudinal wave speed
A	= cross bar tread element area
$h-h_o$	= initial radial compression
ω_n	= natural frequency of nth mode
T_s	= specific time

8.1.2. Ribbed Pattern

He modelled this pattern as a flexible string, representing the tread band, embedded in an elastic foundation, accounted for by the sidewalls and the internal pressure. A transverse wave generated on the tyre by the road surface interaction will be damped out in a distance less than the tyre circumference.

The radiated noise power W = the radiation resistance $R_{\text{rad}} \times$ the mean squared velocity $\langle v^2 \rangle$

where

$$R_{\text{rad}} = A \rho_o a_o \left(\frac{k_a}{k_b}\right)^2 \left(\frac{1}{k_a \ell}\right) \left\{ \frac{[2 - (\frac{k_a}{k_b})^2]}{[1 - (\frac{k_a}{k_b})^2]^{3/2}} \right\}$$

$$\langle v^2 \rangle = \frac{1 \left[\frac{F_o}{T}\right]^2 \pi^2 v^2}{40 s^2} \frac{1}{\left[\left(\frac{\omega}{c}\right)^2 - \frac{k}{T}\right] \left[1 - \left(\frac{v}{c}\right)^2\right]}$$

Further symbols used in the analysis are:

A = beam area

k_a = acoustic wave number = $\frac{\omega}{a_o}$

k_b = structural wave number = $\frac{\omega}{c_b}$

ℓ = equivalent beam length in radiation resistance

T = tension in string

S	=	distance on road for repetition of force cycle
$\frac{\omega}{c}$	=	wave speed of the string
k	=	foundation stiffness
F ₀	=	transverse force proportional to tyre load
V	=	vehicle speed

However as Reiter stated "The complexity of tyre geometry and construction can easily be used to generate a problem that is mathematically intractable."

8.2. Finite Element Modelling

Although finite element techniques are well advanced, computer stores are at present too small to deal with the degree of complexity required and the complexity of the change of input would be considerable when a tread pattern is changed.

8.3. Simple Digital Simulation

This work by the author is based on the analogue modelling system for tyre noise from complex tread patterns, already referred to in Chapter 7.1.

8.3.1. Simple Analogue model

The tread pattern segment is drawn as in Figure 8.1. with grooves and microslots black, and tread rubber white. The different length segments are stuck in appropriate order for the sequence to be used on the inside of a drum approximately 600 mm in diameter. The segments are illuminated and a line of photo diodes across the tread pattern pick up an optical signal as the drum is rotated. The outputs are averaged and amplified to give audio output.

8.3.2. Digital Equivalent of Simple Analogue Model

This analogue system may be simulated digitally. The simulated noise wave from a tread segment is the variation along the segment of the groove width across the tread. Hence in the previous program referred to in Section 7.2.1. the sawtooth wave is replaced by the tread segment wave just described. As previously, the program builds up the simulated noise wave for the whole tyre circumference and the frequency spectrum is produced.

Three types of tread pattern were tested both with digital simulation and also noise testing of the tyres on smooth drums. The results for the dominant harmonics are shown in Figure 8.2. and give fair agreement between simulation and practical measurements at speeds of 50 km/h and 80 km/h. The comparison of the spectra of the D1 pattern is shown in Figure 8.3. The spectra are shown as harmonics of the wheel rotation frequency to aid the clarity of the comparison at different speeds. Again the comparison is fair.

However it was realised that this simple simulation could have its scope of application extended.

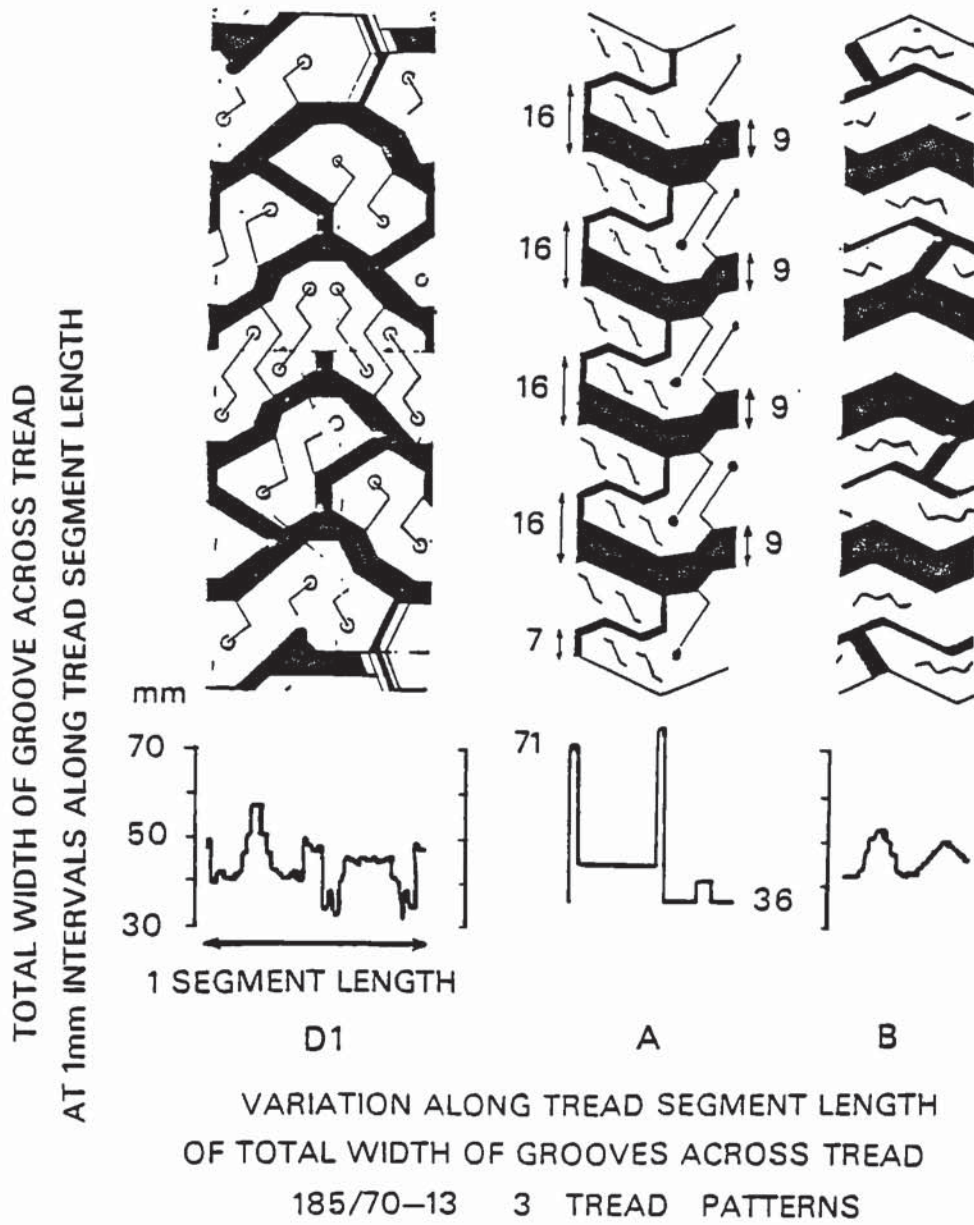
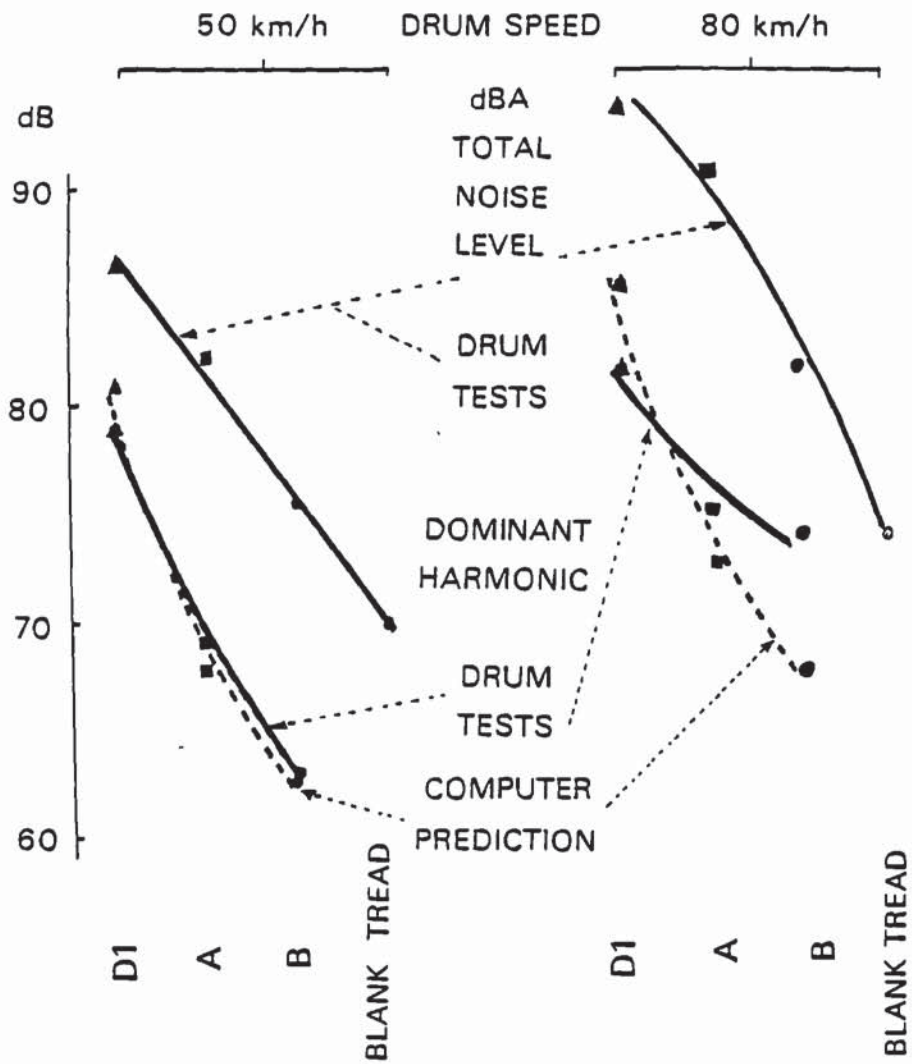
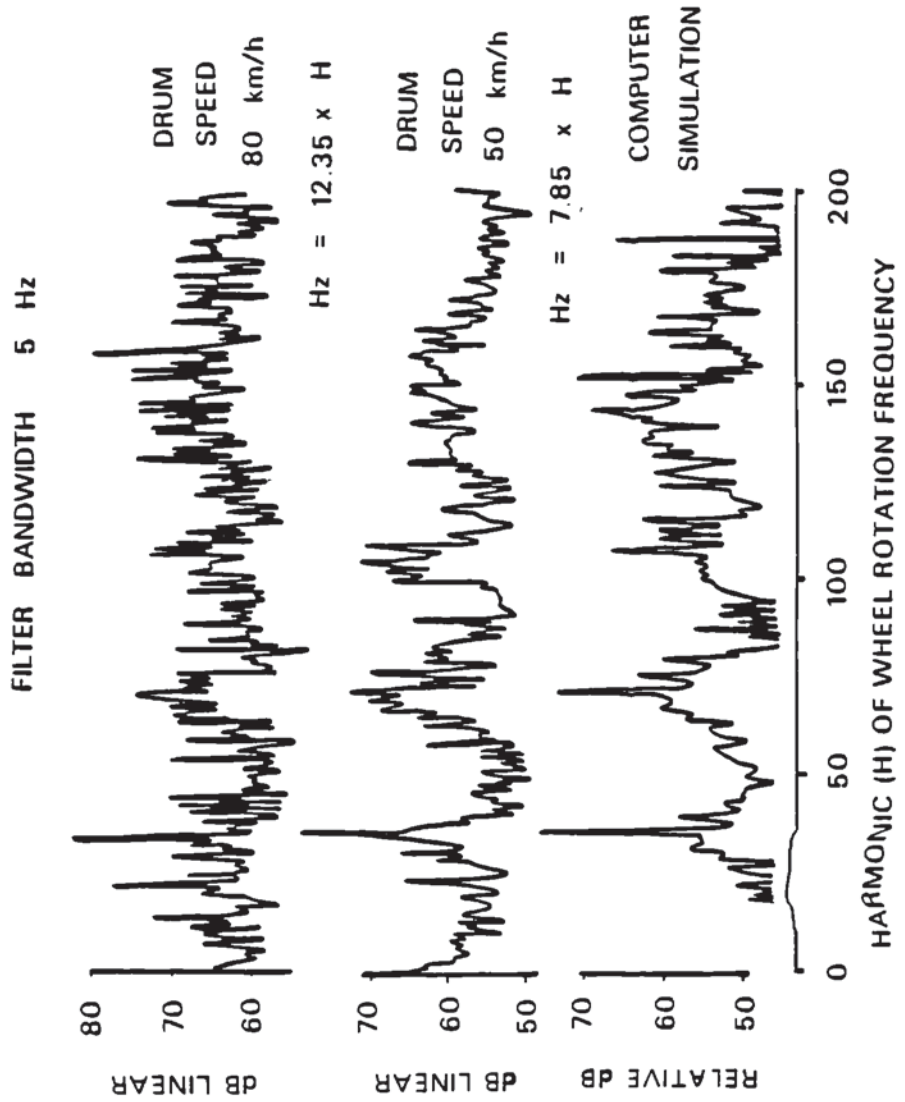


Figure 8.1.



COMPUTER PREDICTION V DRUM TESTS DOMINANT HARMONIC
3 TREAD PATTERNS-2 DRUM SPEEDS

Figure 8.2.



TYRE NOISE ON SMOOTH DRUM v COMPUTER SIMULATED TREAD PATTERN NOISE
 HARMONIC SPECTRA 185/70HR13 D1

Figure 8.3.

CHAPTER NINE: THE EXTENSION OF THE MODEL TO INCLUDE THE EFFECTS OF MICROPHONE POSITION, TYRE SPEED AND CONTACT PATCH SHAPE

9.1. Introduction

The tread pattern noise simulation program, referred to in Chapter 8, used as input, "the variation along a segment of the total width of grooves across the tread" and gave fairly realistic simulation for many tread patterns. However, it was realised that certain basic pattern types having this variation zero, such as antiphase blocks and a case of diagonal grooves, could "fool" the program. Plain tread tyres were cut with these patterns and the scope of the program was extended to simulate these. In addition, errors to which digital spectral analysis is susceptible, were reduced.

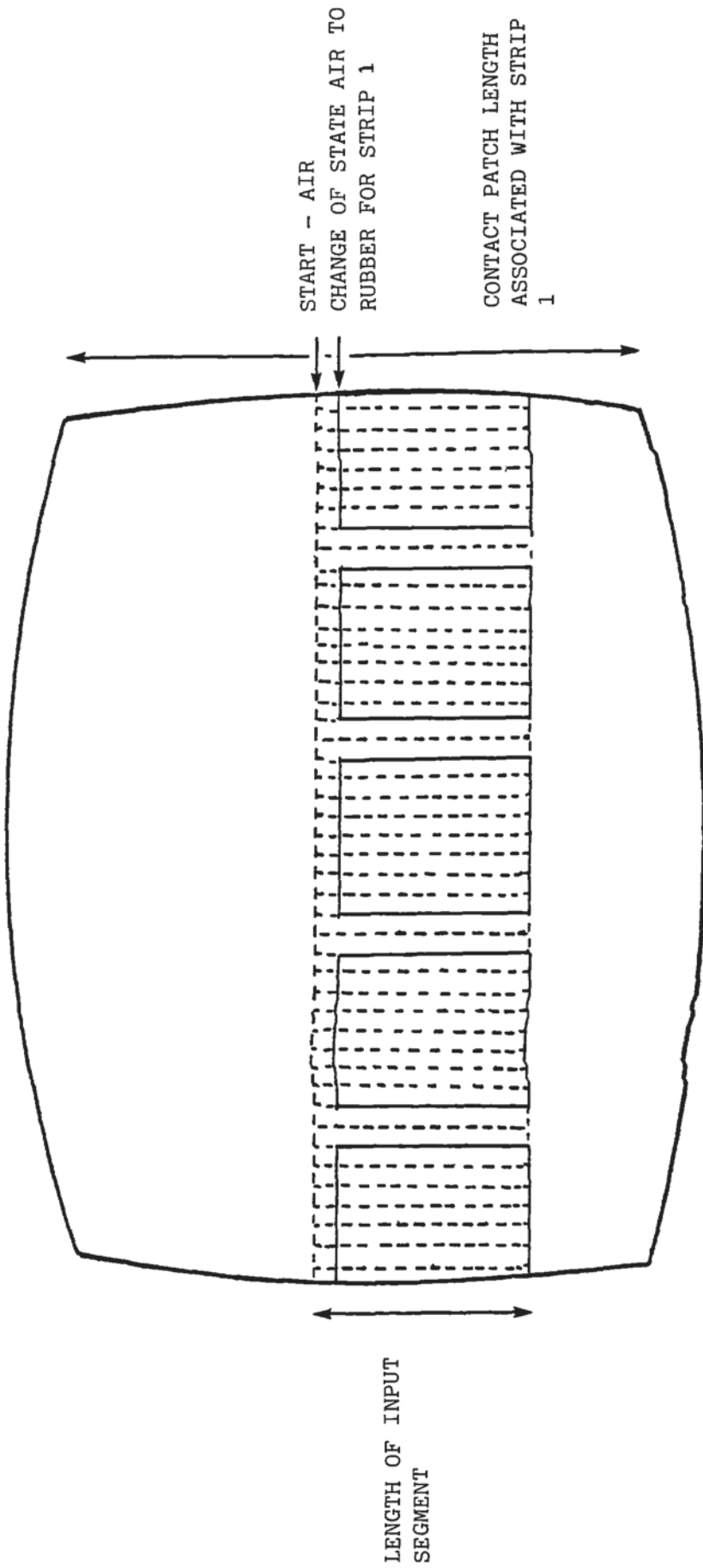
9.2. Tread Pattern Input

The tread pattern input is now more detailed. Circumferential strips e.g. 2 mm wide are taken along a segment and the positions of the changes from land to sea are noted along each strip, as shown in Figure 9.1. The contact patch length is also noted for each strip position. Hence the input now has the nature of two dimension information, rather than one dimension as in the previous model. A typical input is shown in Appendix section 2. The initial sequence of variable pitch segments is also entered as previously.

9.3. Program Scheme

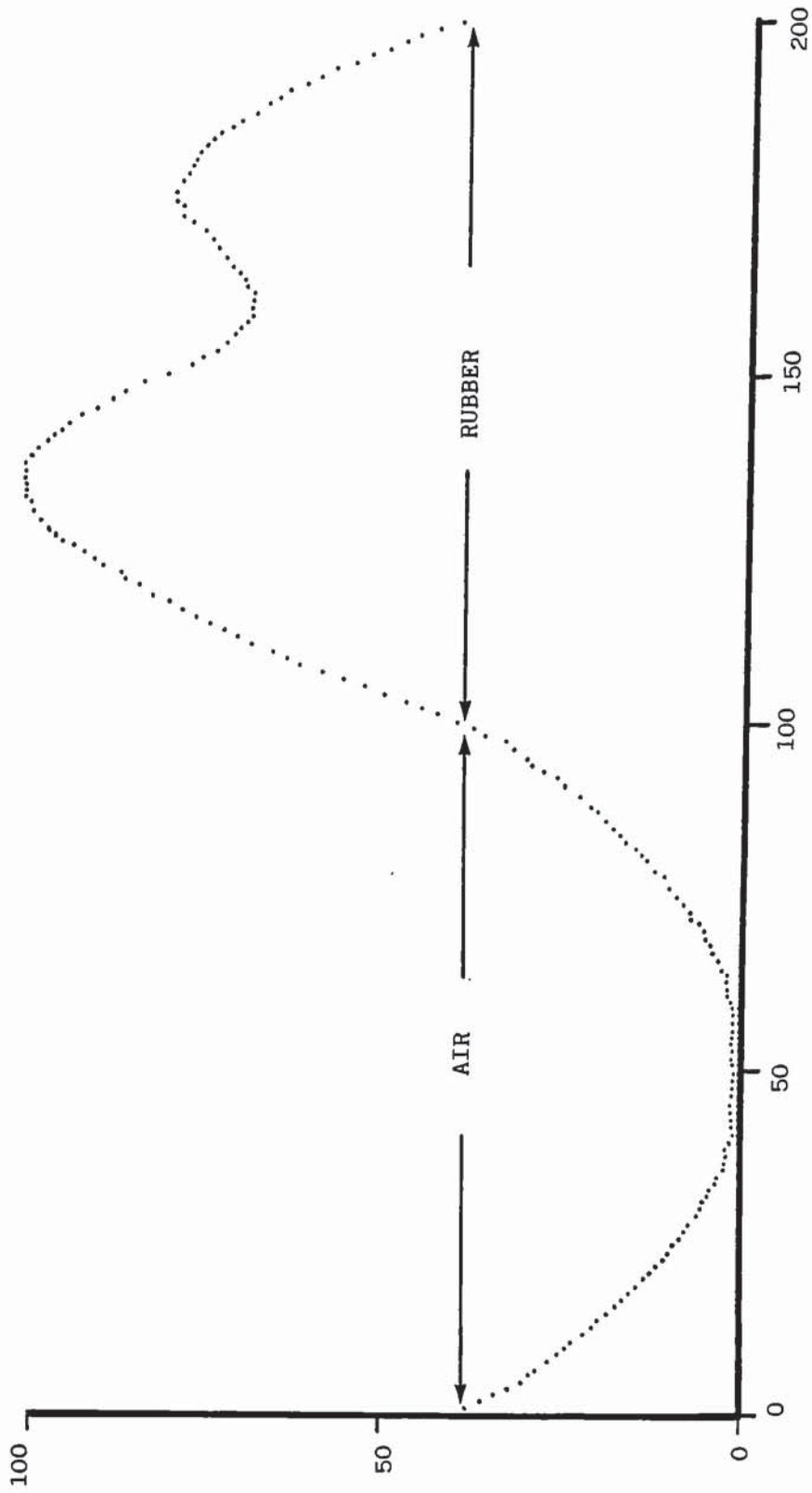
Starting at a strip along a segment at the edge of the tread, a change from land to sea and sea to land brings in a basic noise waveform, as shown in Figure 9.2. The program then generates the wave for the whole tyre circumference. The waves from the front and back of the contact are combined.

The waves for adjacent strips are then added to take in the full



TYPICAL INPUT FOR SIMULATION PROGRAM FROM THE TYRE CONTACT PATCH AND ONE TREAD SEGMENT

Figure 9.1.



THE ELEMENTAL SIMULATED NOISE WAVE

(GENERATED AT RUBBER/AIR AND AIR/RUBBER CHANGES ALONG A THIN STRIP DOWN THE LENGTH OF A TREAD SEGMENT)

Figure 9.2.

contact width of the tread. Small delays in adding the strips are included to predict the noise at the side microphone position.

The basic simulated noise waveforms from land to sea and sea to land have been empirically determined to give a good match with the anti-phase block pattern automobile tyre for a side microphone position and also with a view to reducing aliasing effects.

The program uses a tapering window to minimise leakage type effects. The window is stepped round the tyre circumference so that undue emphasis is not given to any particular portion of the circumference.

The fast Fourier transform results are susceptible to two types of error:-

1. Aliasing as discussed in Appendix Section 3.2.
2. Leakage as described in Appendix Section 3.3.

9.3.1. Program Details

The input is entered as described in the input data and as shown for a typical example in Appendix Section 2.1. The program reads the input data and proceeds in the following steps.

9.3.1.1. To Generate a Simulated Tread Pattern Noise Waveform suitable for the Fast Fourier Transform

9.3.1.1.1. Generation of the Waveform due to a Single Circumferential Strip around the Tyre Circumference at 1024 Points

For the right hand strip of the first tread segment as shown in Figure 9.1. a waveform is generated using the elemental waveform given in Figure 9.2.

The 'air' wave is scaled in length to fit the gap portions of the strip and similarly the 'rubber' wave is scaled in length to fit the rubber portions of the strip. This is continued for all the segments round the circumference of the tyre. The tread segment joints do not effect the wave. A continuous strip of air or rubber around the whole circumference is simulated by a steady value for the function.

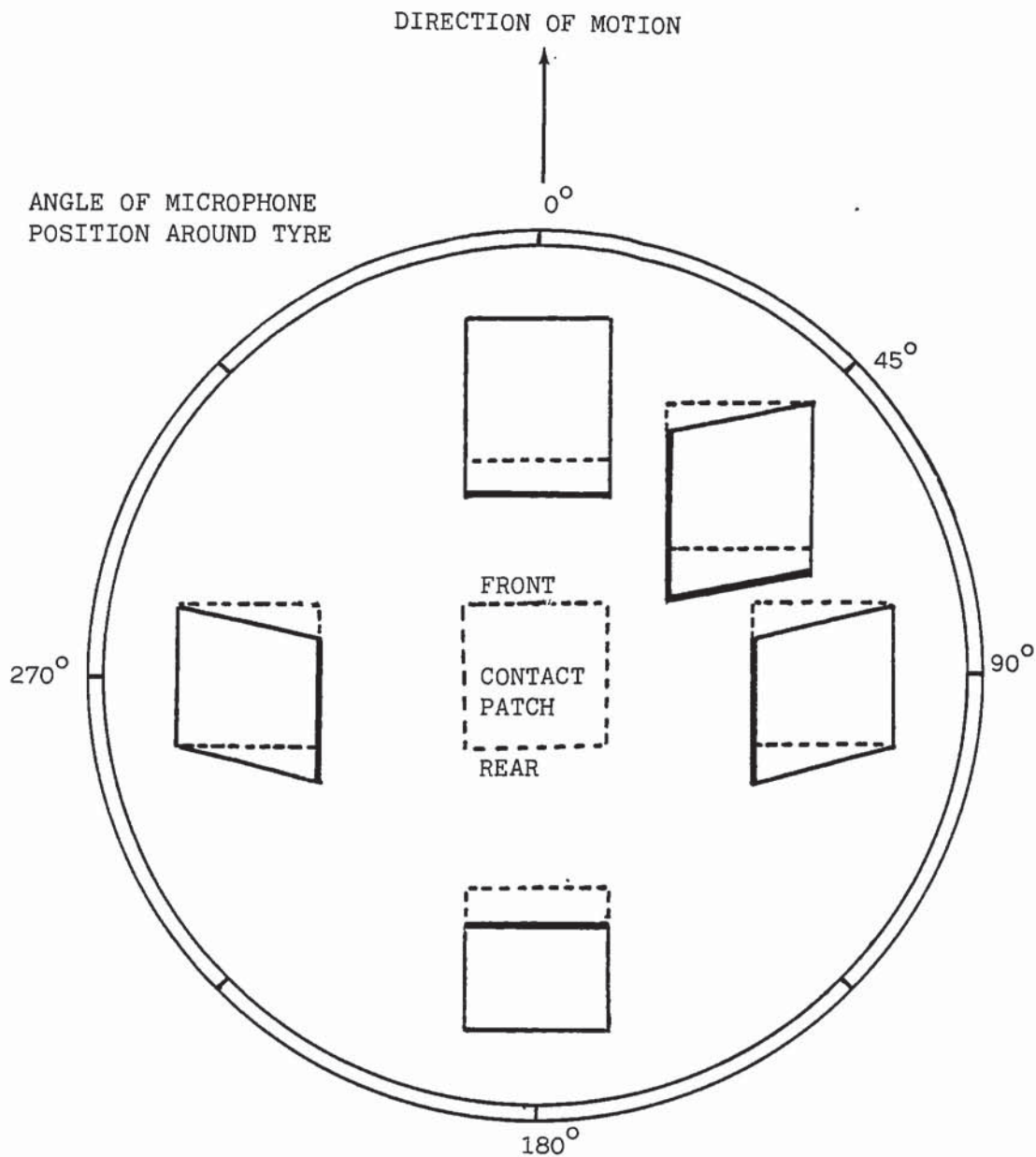
In order to allow for the effects of the width of the strip and its speed, the ordinates of the 1024 point strip waveform are multiplied by the width of the strip and by (speed)²; thus doubling the speed raises the noise level by approximately 12dB.

9.3.1.1.2. Accounting for the Contact Patch Geometry and the Microphone Position Angle

To obtain the simulated noise wave for the first strip, half of the magnitude of the strip waveform described in 1.1., the wave at the rear of the contact, is subtracted from the full magnitude of wave taken at the front of the contact. The experimental relationship between the sound wave at the front of the contact patch, and that at the rear, was determined using probe microphone sound time histories. The resultant wave is stored for each of 1024 points around the circumference of the tyre.

Similarly the information for the next strip is added into the store, allowing for the small delay in sound travelling across the tyre at the speed concerned. This is continued until the waves from all the strips have been added.

In order to predict the noise for different microphone positions, the delays for the sides of the tyre away from the microphone position are taken into account as shown in Figure 9.3. They are proportional to the velocity of the tyre. As well as accounting for delays, some screening attenuation in noise is also allowed for, due to the dominance of the side of the tyre



DOTTED FIGURES SHOW HOW SOUND WOULD REACH MICROPHONE AT VERY LOW TYRE SPEED.

SOLID FIGURES SHOW HOW MICROPHONE SEES TIME DISTORTION IN CONTACT PATCH AT DIFFERENT MICROPHONE ANGULAR POSITIONS FOR HIGHER TYRE SPEEDS.

SIMULATION OF NOISE FOR DIFFERENT ANGLES OF MICROPHONE POSITION - SCHEMATIC DIAGRAM SHOWING COMPENSATION FOR ACOUSTIC LAGS ON EDGE OF TYRE FURTHEST FROM MICROPHONE AT SPEED (v).

Figure 9.3.

near the microphone.

9.3.2. Obtaining the Frequency Spectra

The simulated noise wave is:

1. Stored for audio output (for the best sequence)
2. Windowed with the centre of the window at four equi-spaced positions around the circumference of the tyre. Windowing is discussed in Appendix Section 3.3. The output for each position of the window is input to the fast Fourier transform, the output of which is averaged for the four positions. This prevents undue emphasis of any portion of the tyre circumference. The frequency and dB level of the dominant frequency is stored. The spectrum is plotted on the line printer and is available for output to the digital plotter (for the best sequence).

9.3.3. To Determine the Optimum Sequence of Groups of Tread Segments

The permutation files are stored as referred to in Appendix Section 2.1. The number of permutations required is entered as input. The initial order of segments is as entered. The frequency spectra of the simulated noise is determined, then the order of the groups of segments is changed to that for the first permutation. The stages 1.1., 1.2. and 2. are repeated. The cycle is repeated and the spectrum with the lowest amplitude dominant frequency is stored until it is superseded by a better one.

9.4. Tread Pattern Noise Tests - Experimental

Three types of simple basic tread patterns, at constant pitch, were cut and run on a Safety Walk surface to validate the program:

1. In phase blocks

2. Out of phase blocks
3. In phase cross grooves

In addition a well sequenced diagonal block tread pattern was tested to provide an example of a quiet pattern with minimised dominant harmonics.

The indoor tests were normally at two speeds, 50 and 80 km/h, with the side microphone position.

9.4.1. Tread Pattern Noise Tests - Simulated

The spectra for the above tyres were simulated using 1024 points around the tyre circumference and the Blackman window. Windowing is discussed in the Appendix Section 3.3. The subroutine is as used by Ackroyd (1973). The tread width was divided into 3 mm wide strips.

9.4.2. Comparison Between Simulated and Experimental Noise Spectra - Tread Patterns, Basic Constant Pitch and well Sequenced Variable Pitch

Figures 9.4 to 9.12 show the tread patterns and their respective experimental and simulated spectra and Table 9.1 gives the summarised results.

The left hand side of Figures 9.7 and 9.8 show that this program is a considerable advance in the simulation of the shape of the spectrum from the out of phase block pattern tyre.

The right hand side of Figures 9.7 and 9.8 show how the intensity of the block frequency is reduced relative to that of the second harmonic of the block frequency with the microphone in front of the tyre both in the experimental and simulated spectra.

TABLE 9.1. COMPARISON BETWEEN EXPERIMENTAL AND SIMULATED NOISE

Sequence	Constant Pitch						Optimum Sequence
	Tread Element	Blocks		Cross Grooves		Diagonal Blocks	
Phasing Across Tread		In Phase	Out of Phase	In Phase	In Phase		
Speed km/h	50	80	50	80	50	80	50 80
<u>Experimental Results</u> Maximum PSD. of Dominant Harmonic	88.0	93.8	86.4	90.3	84.9	89.0	71.0 85.0
Sound Pressure Level dB(A)	88.5	99.0	85.5	99.0	83.0	91.0	79.0 86.0
<u>Simulated Results</u> Relative Maximum PSD. of Dominant Harmonic	79.1	87.2	72.6	81.2	73.3	81.0	51.7 62.1

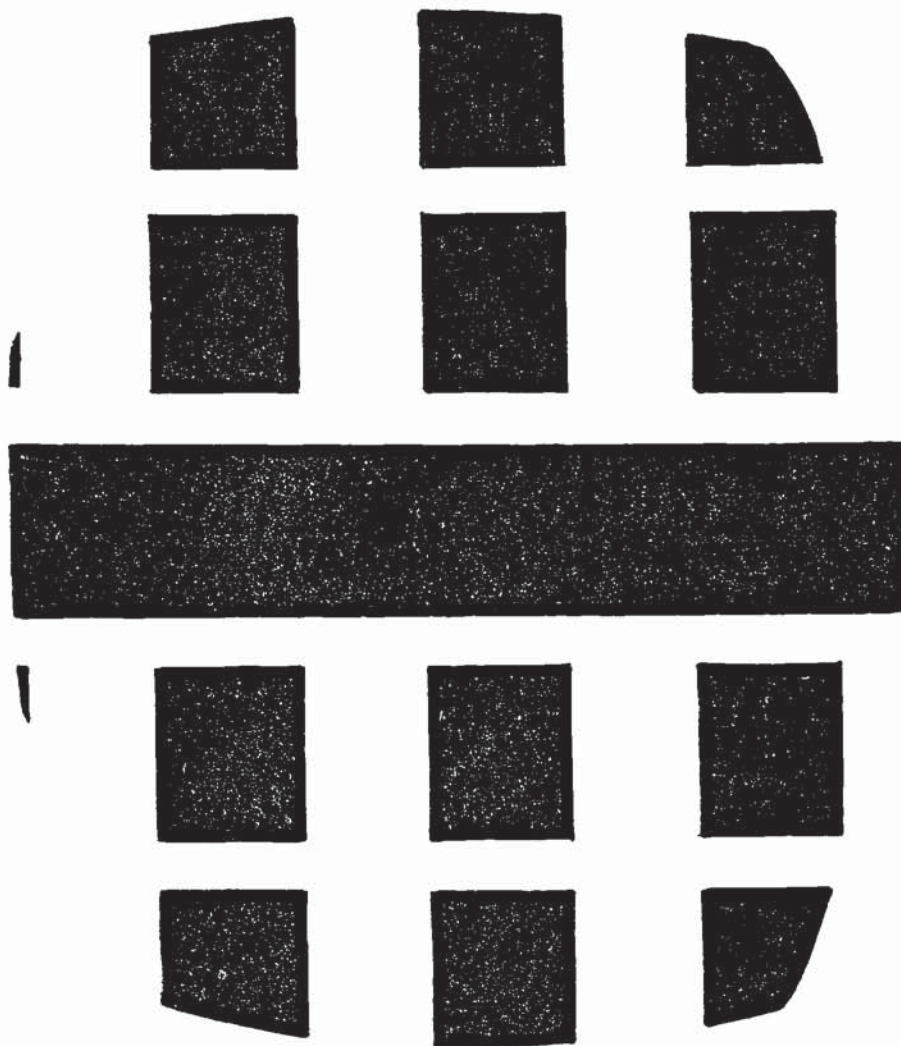
The decrease in spectrum peaks occurring with the narrow cross grooves is evident from Figure 9.9 and 9.10 for both types of spectra.

Stacked experimental spectra are shown over a wide speed range for the in phase cross groove pattern in Figure 9.11, and for the in phase block pattern in Figure 9.12, which shows some evidence of resonances.

As a comparison with the basic fixed sequence block type tread patterns, the following results correspond to a very well sequenced pattern. The tread pattern is shown in Figure 9.13 and the respective simulated and experimental frequency spectra are shown in Figures 9.14 to 9.16 including stacked spectra over a wide speed range.

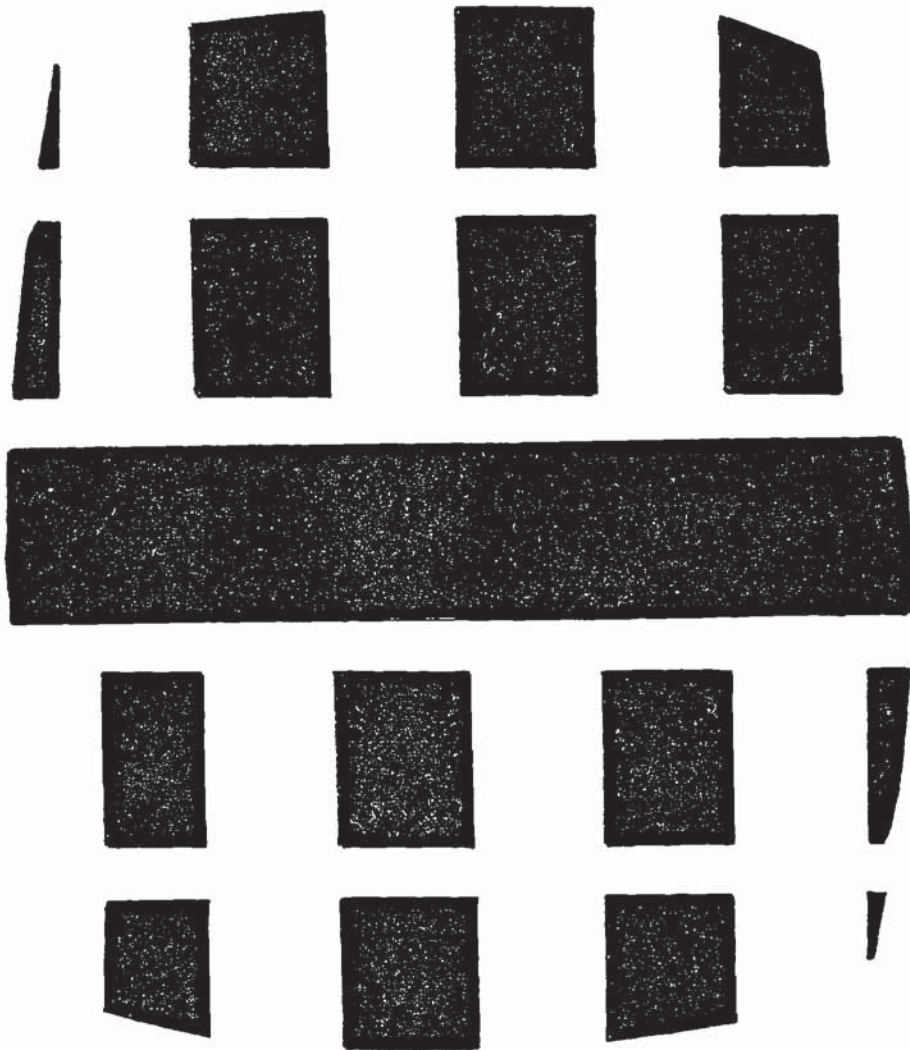
The sequence of tread segments as shown in Figure 9.14 is a good example of random modulation of the three tread pitch lengths. Dominant tones have been considerably reduced. The pattern is directional, the noise is 3dB(A) greater if the tyre is rotated in the reverse direction, which is consistent with the discussion in Section 2.1.2.1.1. The pattern has best wet grip in the direction of rotation which gives best noise. The effect on noise of the microslots in the tread blocks is to soften the blocks and reduce the noise by 1.5dB(A).

The simulated spectra agree fairly well with the experimental spectra. There is a departure at low frequencies. The experimental spectra are greater at frequencies below 50 Hz due to low frequency ambient noise in the laboratory, and at frequencies between 50 Hz and 150 Hz due to the Safety Walk excited tyre noise. The most important region of the spectrum is in the region of the mean pitch frequency.



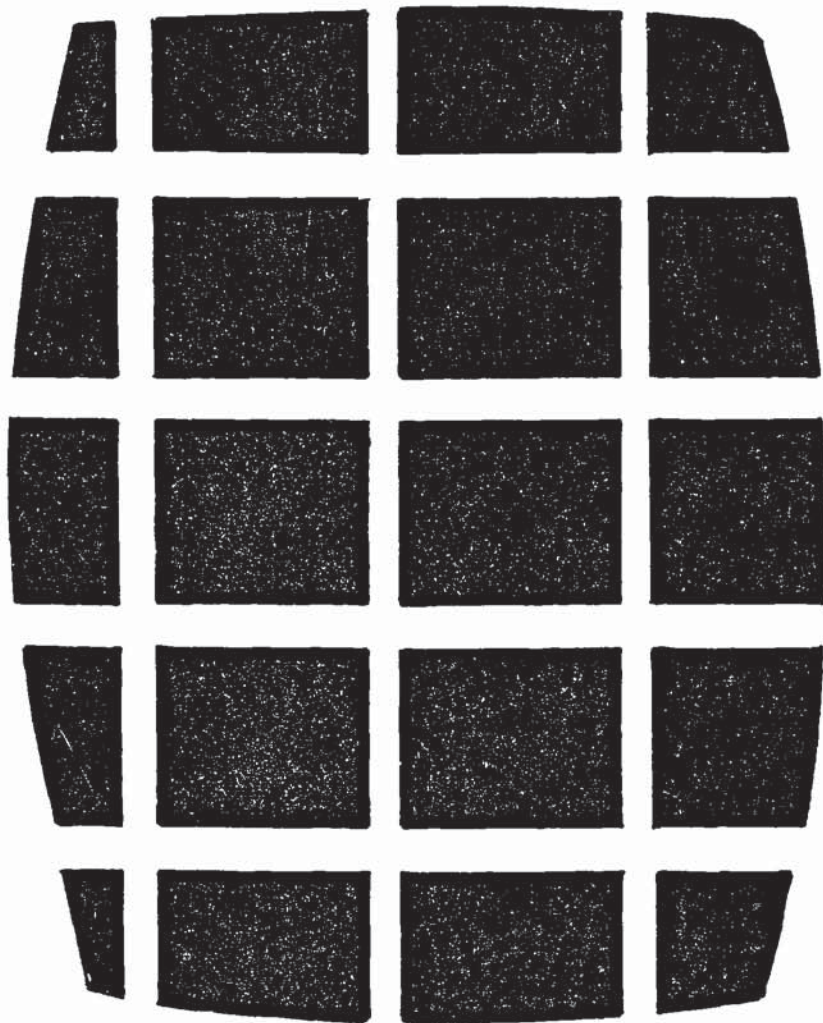
TREAD PATTERN
IN PHASE BLOCKS
CONTACT PATCH

Figure 9.4.



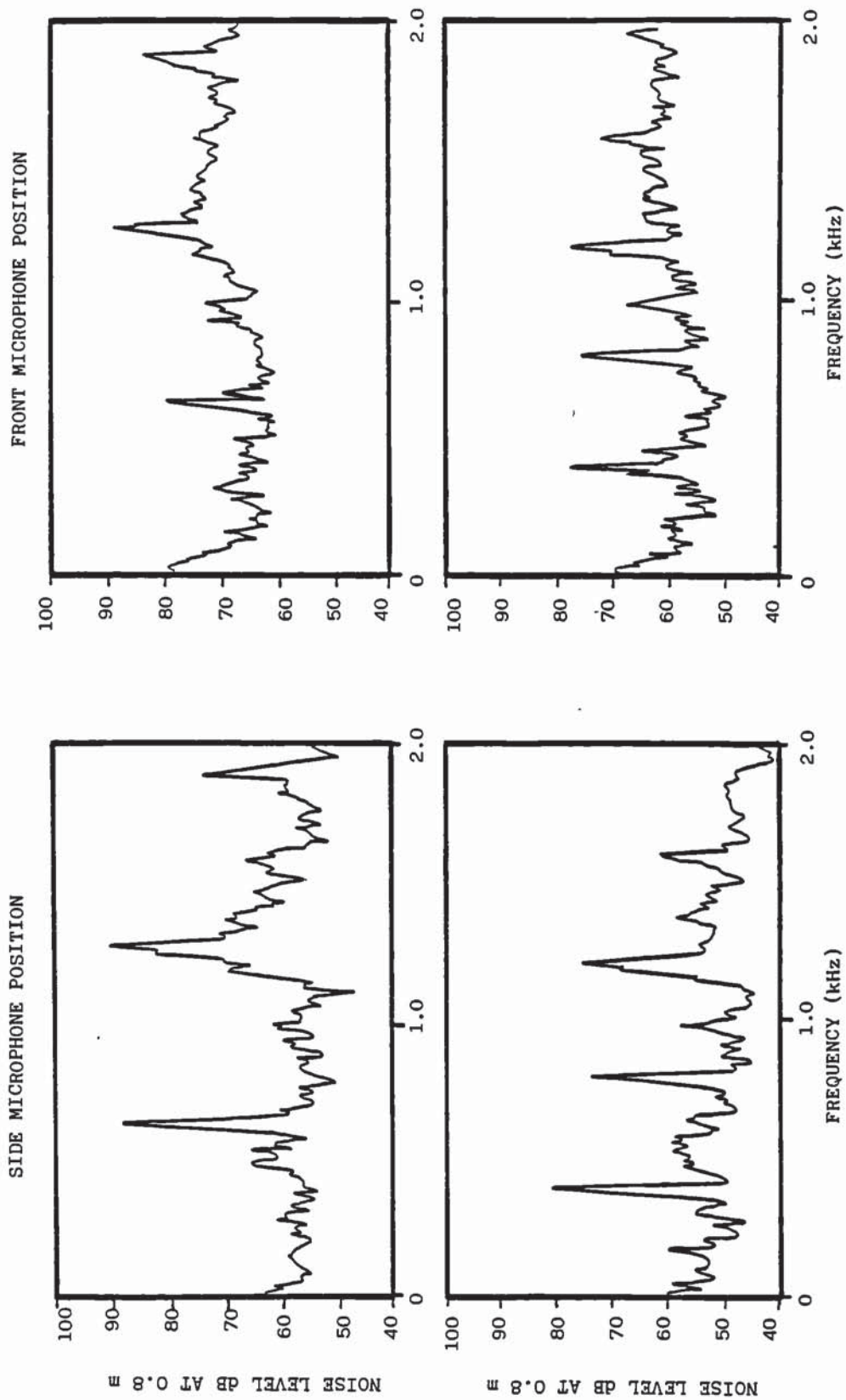
TREAD PATTERN
OUT OF PHASE BLOCKS
CONTACT PATCH

Figure 9.5.



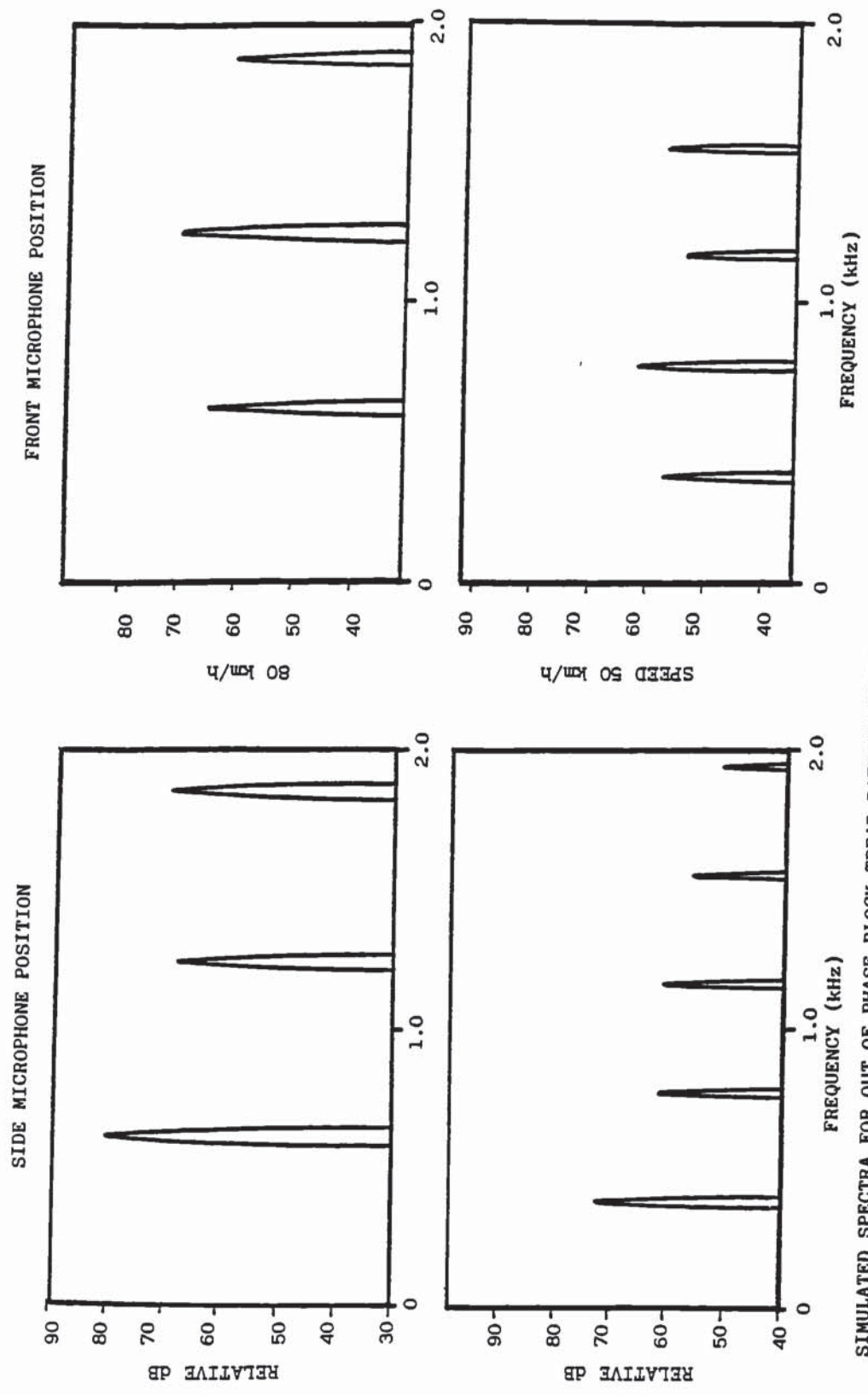
TREAD PATTERN
IN PHASE CROSS GROOVES
CONTACT PATCH

Figure 9.6.

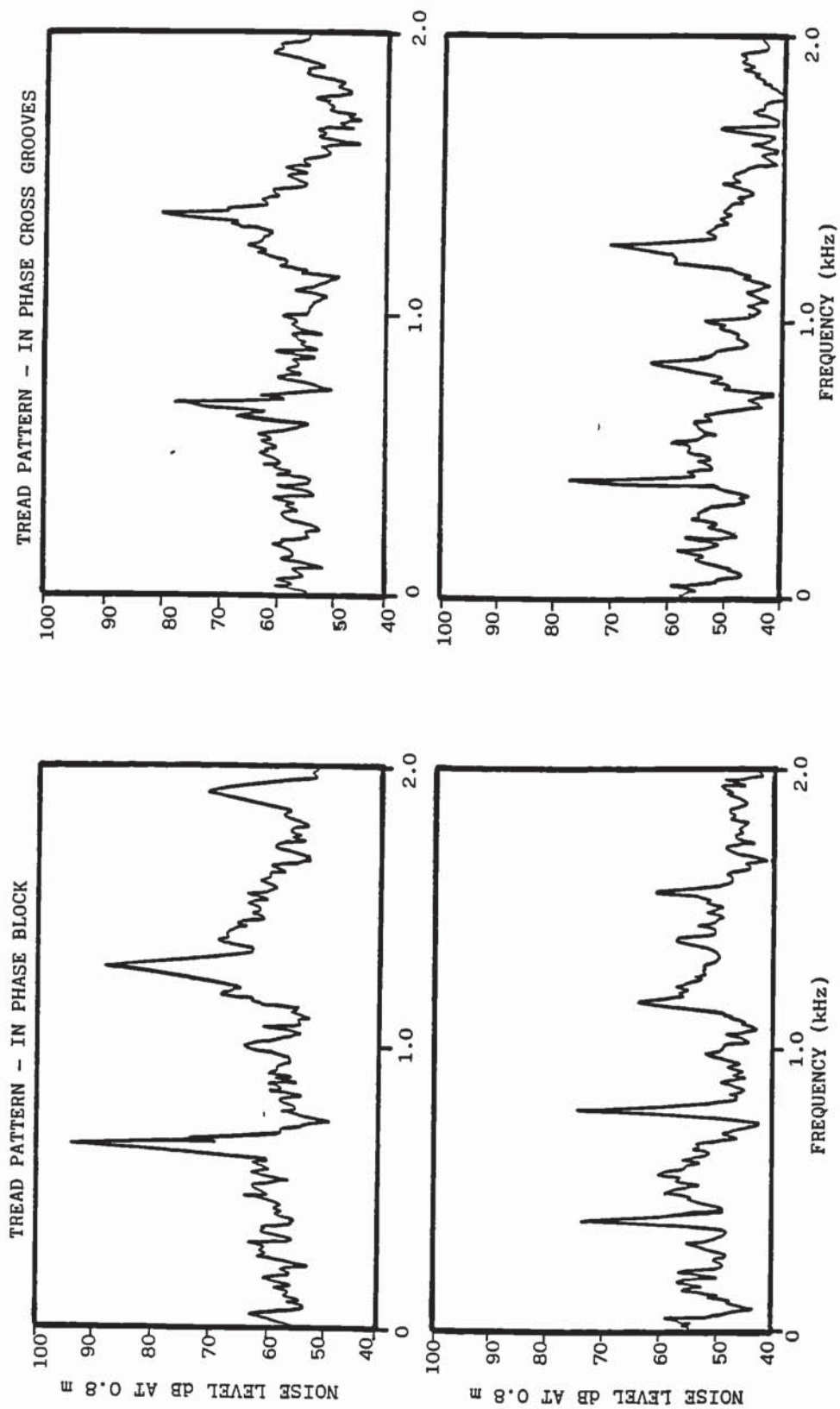


EXPERIMENTAL SPECTRA FOR OUT OF PHASE BLOCK TREAD PATTERN COMPARING SIDE AND FRONT MICROPHONE POSITIONS

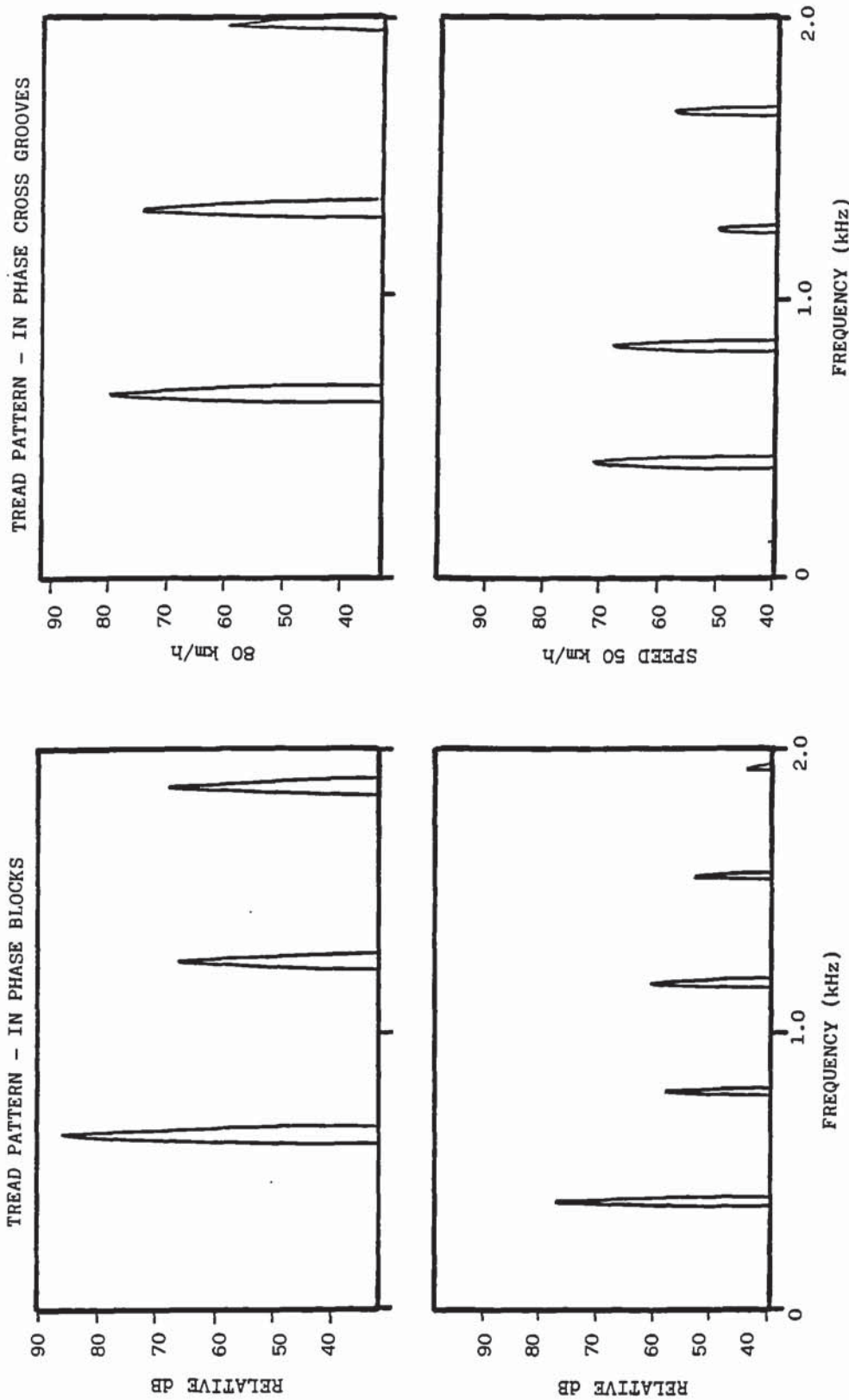
Figure 9.7.



SIMULATED SPECTRA FOR OUT OF PHASE BLOCK TREAD PATTERN COMPARING SIDE AND FRONT MICROPHONE POSITIONS
 Figure 9.8.

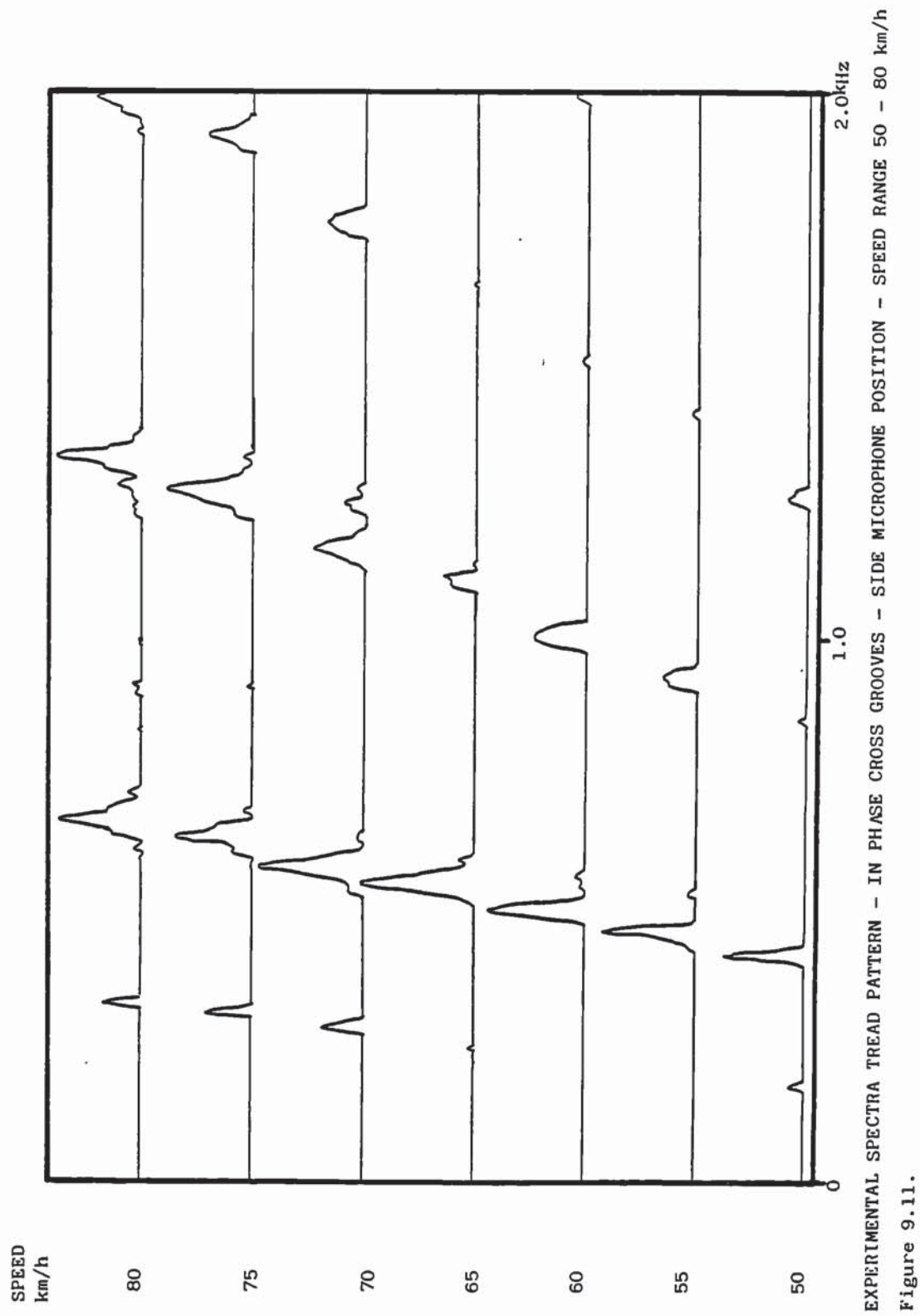


EXPERIMENTAL SPECTRA FOR SIDE MICROPHONE POSITION COMPARING IN PHASE BLOCK WITH IN PHASE CROSS GROOVE TREAD PATTERNS
 Figure 9.9.

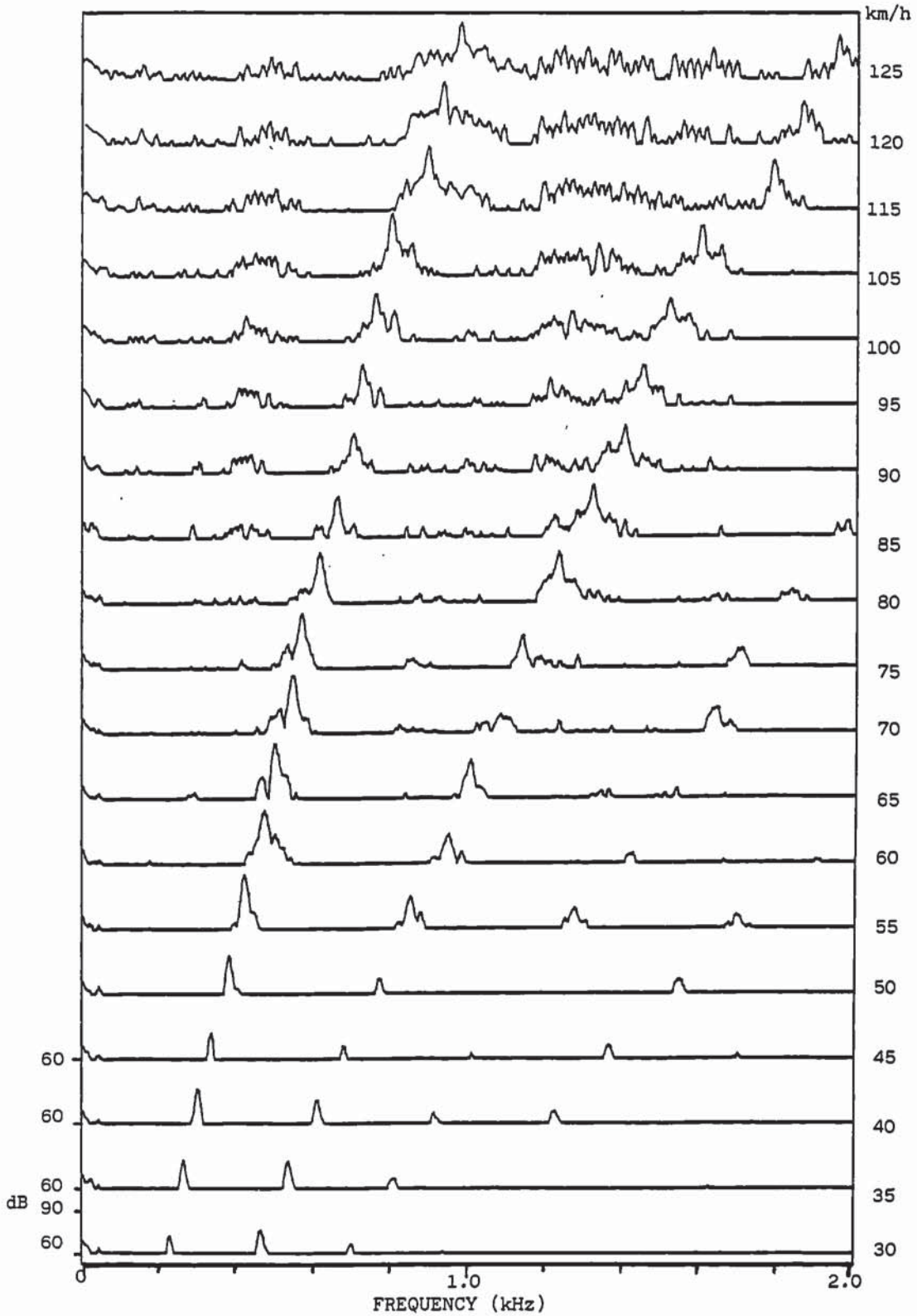


SIMULATED SPECTRA FOR SIDE MICROPHONE POSITION COMPARING IN PHASE BLOCKS WITH IN PHASE CROSS GROOVE TREAD PATTERNS

Figure 9.10.



EXPERIMENTAL SPECTRA TREAD PATTERN - IN PHASE CROSS GROOVES - SIDE MICROPHONE POSITION - SPEED RANGE 50 - 80 km/h
 Figure 9.11.



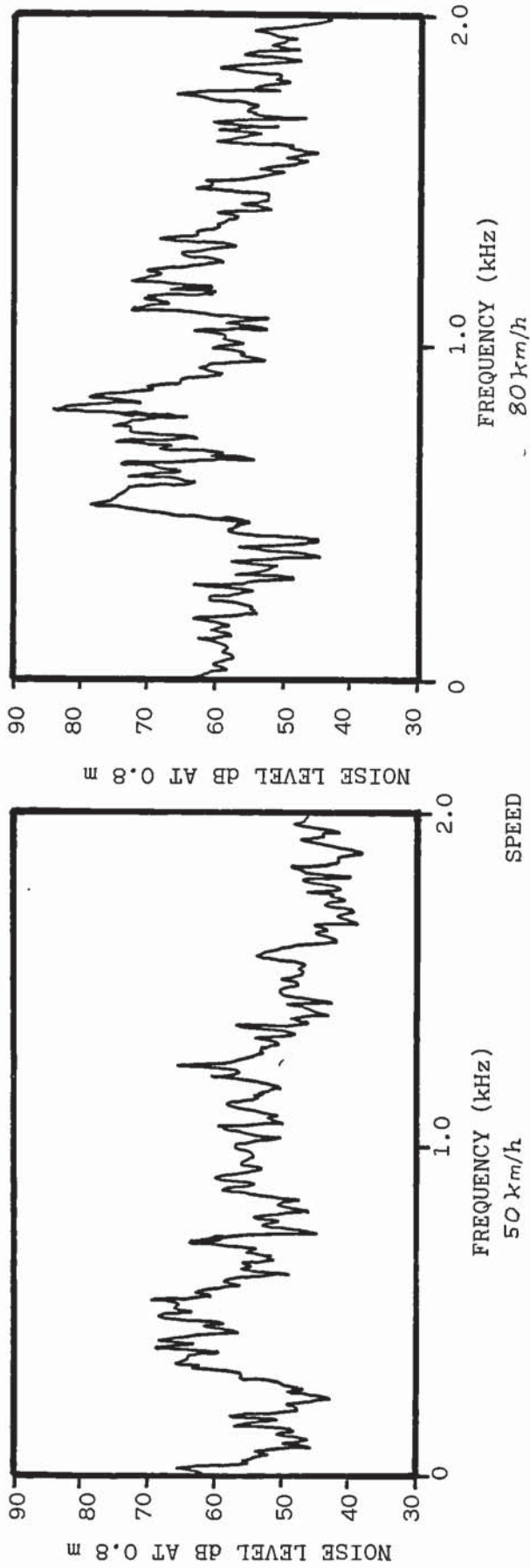
EXPERIMENTAL RESULTS
 TREAD PATTERN - IN PHASE BLOCKS - SIDE MICROPHONE POSITION STACKED SPECTRA
 OVER SPEED RANGE 30 - 125 km/h

Figure 9.12.



TREAD PATTERN
SEQUENCED DIAGONAL BLOCKS
CONTACT PATCH

Figure 9.13.

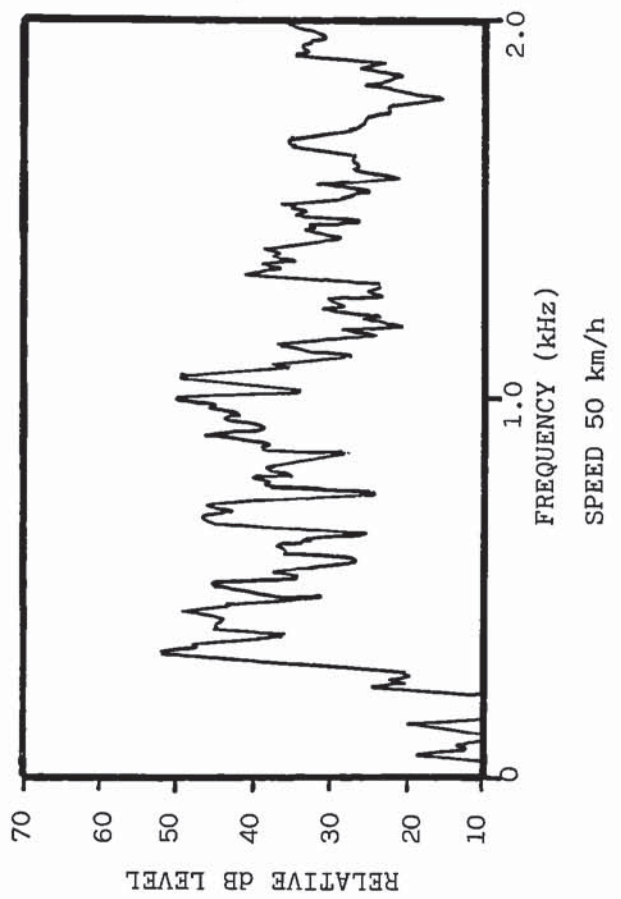
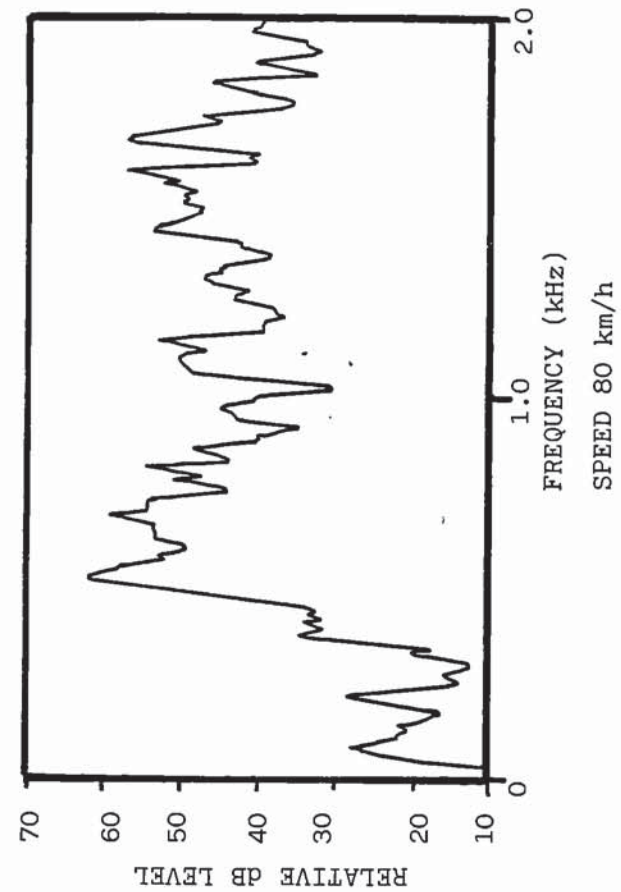


SEQUENCE -----/11/-----/1111/-----/1/--/1/-/111/-----/11/--/11111/-/11/

SEGMENT LONG : MEDIUM : SHORT
 REFERENCE - : / : 1
 LENGTHS (mm) 41.0 : 35.5 : 28.0

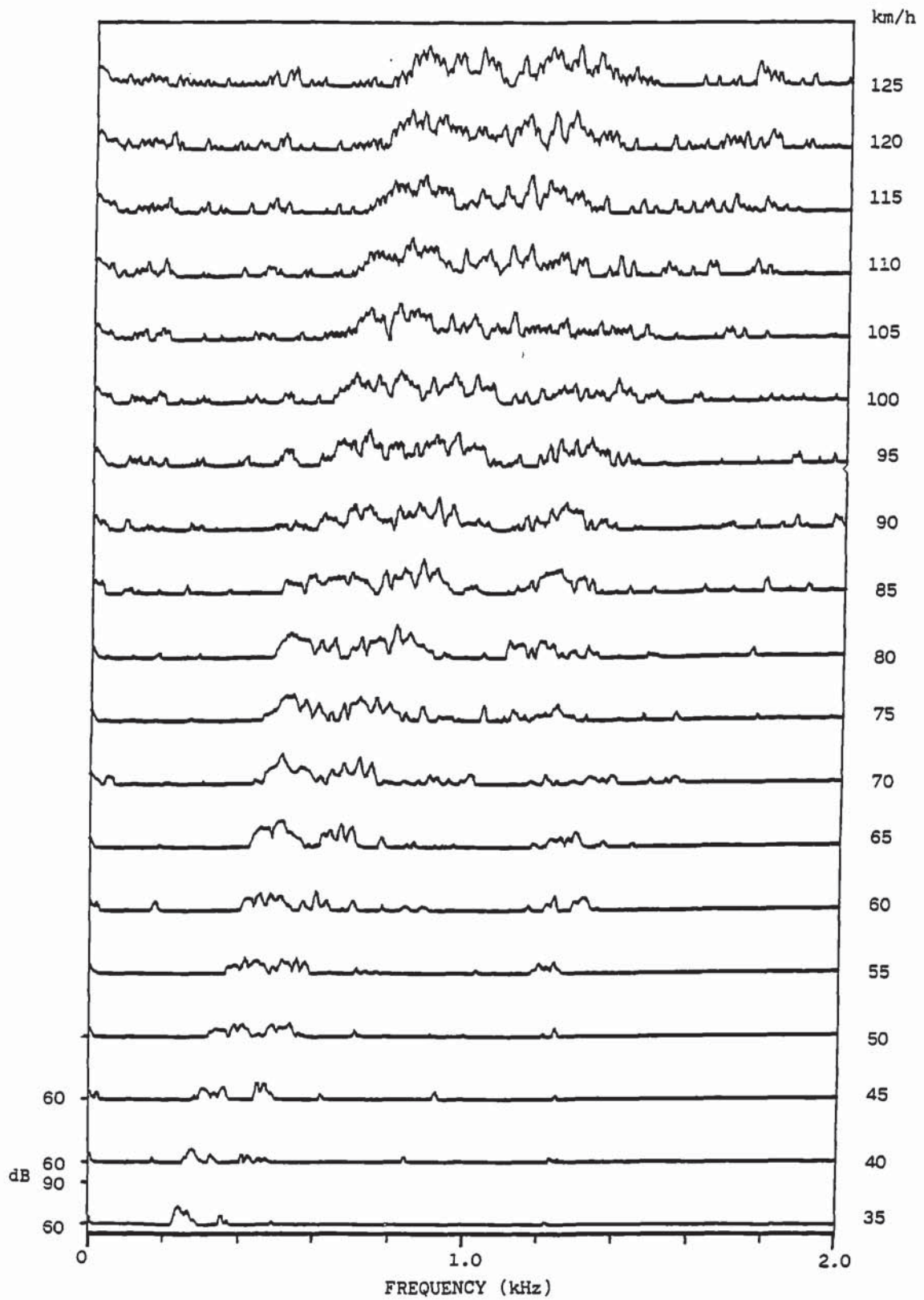
EXPERIMENTAL SPECTRA - WELL SEQUENCED BLOCK PATTERN - SIDE MICROPHONE POSITION

Figure 9.14.



SIMULATED SPECTRA - WELL SEQUENCED BLOCK PATTERN - SIDE MICROPHONE POSITION

Figure 9.15.



EXPERIMENTAL RESULTS - STACKED SPECTRAL PLOTS OVER SPEED RANGE 35 - 125 km/h
 WELL SEQUENCED DIAGONAL BLOCK PATTERN - SIDE MICROPHONE POSITION

Figure 9.16.

9.5. Constant Pitch Tread Pattern Experimental Noise Waveform

In order to investigate whether any variations in the amplitude of the noise wave from a constant pitch in phase block pattern were occurring at once per revolution of the tyre, a photo pick up signal was used. The hub of the tyre assembly was divided into two sectors, one black and the other white. A fibre optic photo pick up head was placed in front of the hub to generate the signal.

The signal from the photo pick up was used to trigger the Nicolet 660A Analyser for a time period of 0.2 seconds. The sound wave from the microphone in the side position 0.8 m from the tyre, is in the upper trace and the photo pick up wave is in the lower trace. One cycle of the wave in the lower trace corresponds to one revolution of the tyre.

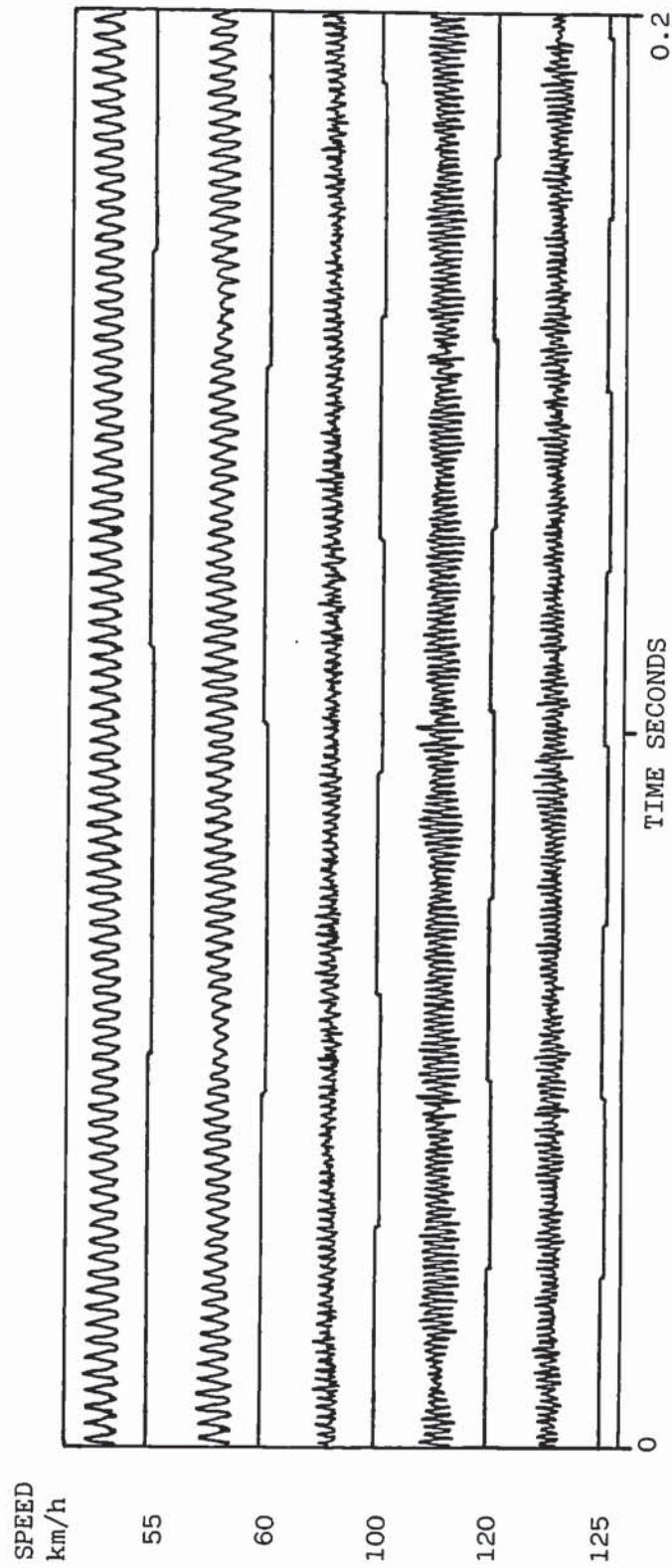
It can be seen in Figure 9.17 that although the in phase block tyre has precise spacing of the blocks, the sound wave shows considerable changes in amplitude repeating once per revolution at several speeds. This variation in amplitude is probably strongly related to the non uniformity of the tyre giving rise to torsional vibration of the assembly. Non uniformity was discussed by J C Walker and Reeves (1974).

The time period used in Figure 9.18 was 0.04 seconds which expands the trace and shows the waveform of the sound waves more clearly.

9.5.1. Phase of Constant Pitch Tread Pattern Experimental Noise Waveforms

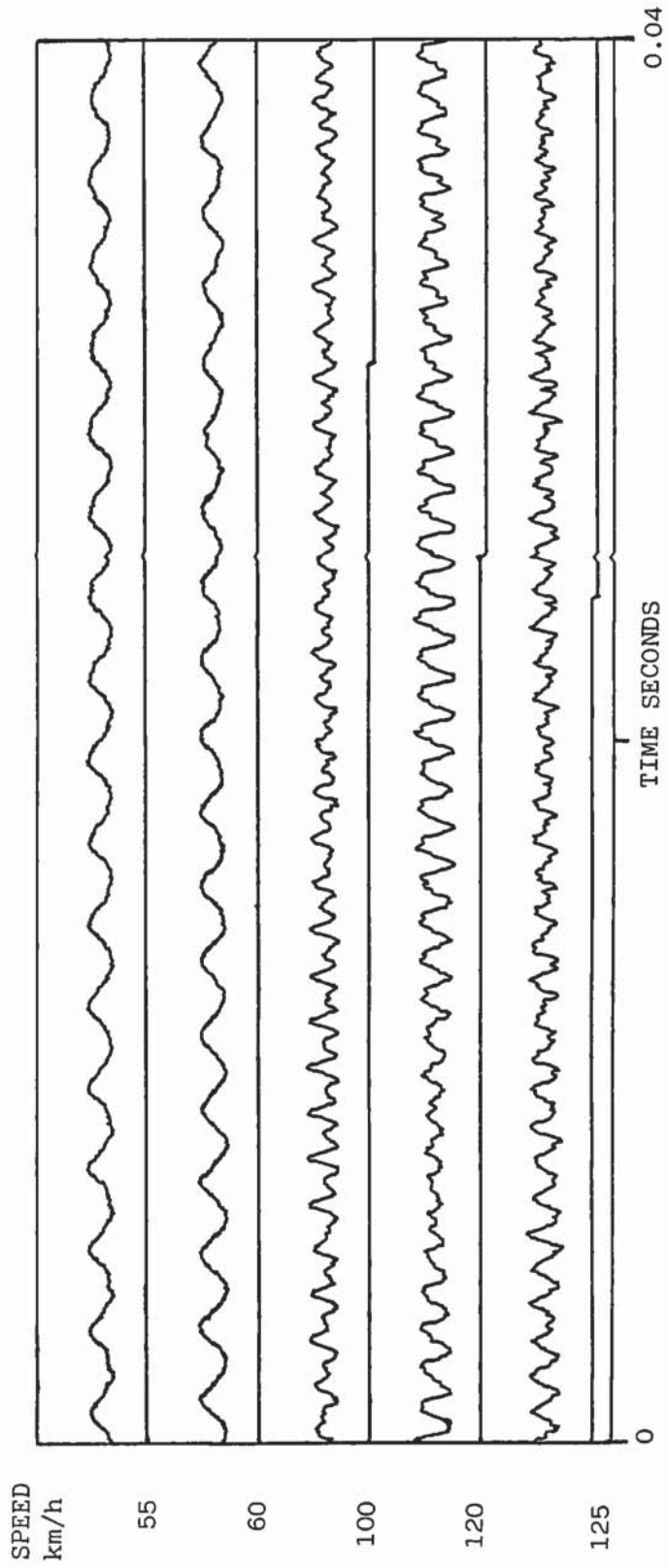
In order to get an indication of the phase of the noise from the in phase block pattern tyre, the side of each block was painted white and the photo pick up was aligned to give a signal as each block touched the drum at nearly zero speed.

Two microphones and a Racal Store 7 frequency modulated tape



TIME HISTORY (0.2 sec) OF SOUND WAVE FROM A CONSTANT PITCH IN PHASE BLOCK TYRE OVER A RANGE OF SPEEDS, TRIGGERED FROM A FIXED POINT ON THE TYRE CIRCUMFERENCE - SIDE MICROPHONE POSITION

Figure 9.17



TIME HISTORY (0.04 sec) OF SOUND WAVE FROM A CONSTANT PITCH IN PHASE BLOCK PATTERN TYRE OVER A RANGE OF SPEEDS, TRIGGERED FROM A FIXED POINT ON THE TYRE CIRCUMFERENCE - SIDE MICROPHONE POSITION

Figure 9.18.

recorder were used to record the waves. The tape speed was 15 inches per second with wide band operation. This gives a frequency response up to 10 kHz and retains the sharpness of the photo pick up pulses.

A check on the phase response of the two microphone and recorder channels was carried out by putting the microphones as close together as possible in the noise and measuring the cross correlation function of the system. The peak at 0.00000 seconds in Figure 9.19 shows that any delays in the two channels are less than 5 microseconds.

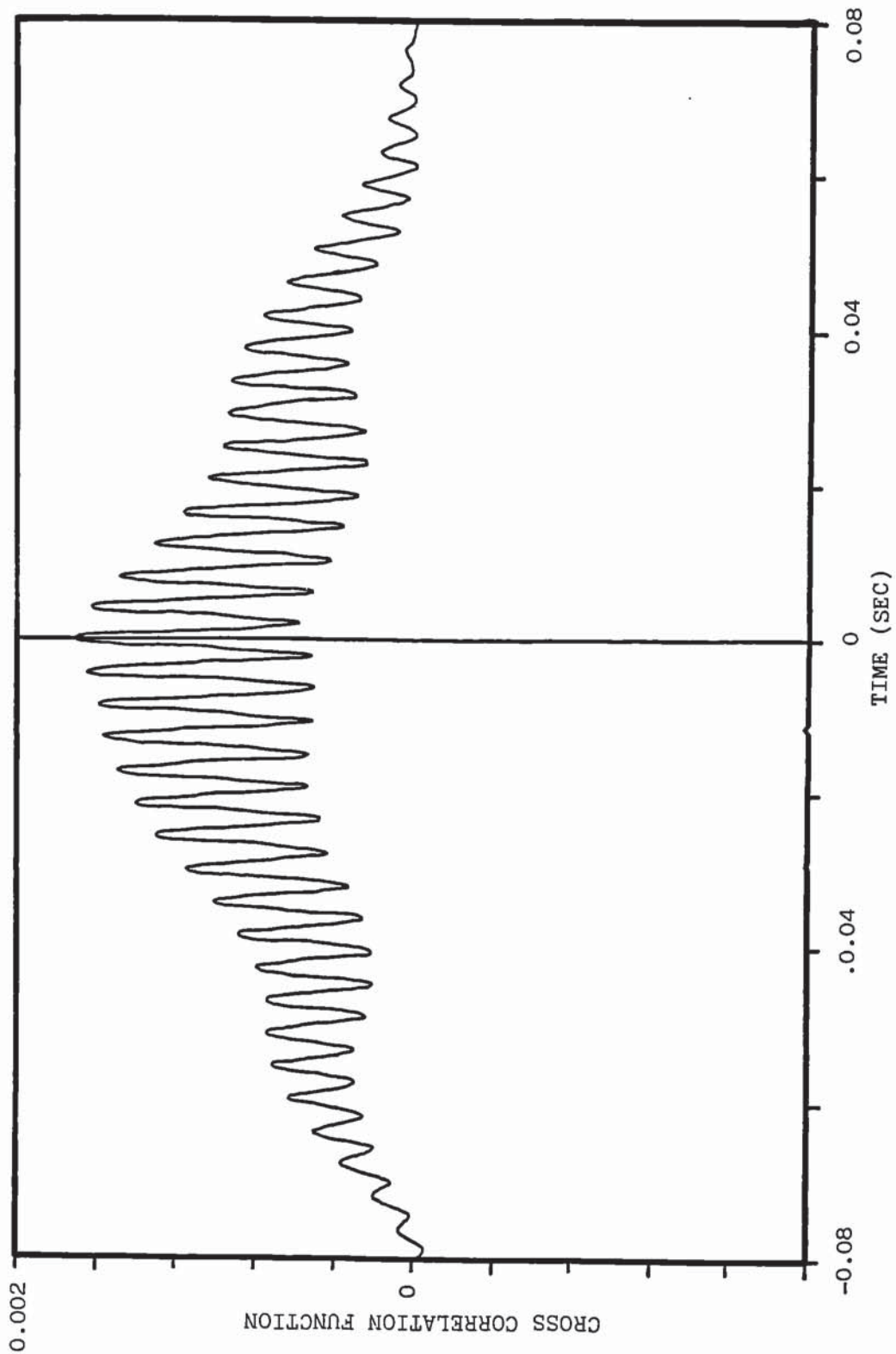
Two microphones were positioned in front of the tyre both of which were pointing at the nip, one at a distance of 125 mm and the other at a distance of 280 mm from the nip.

The delay between the microphones was 0.46 milliseconds. There will be approximately 0.37 milliseconds delay between the nearest microphone and the photo pick up signal.

The changes in waveform of the noise wave from the nearest microphone, and the relation with the photo pick up wave over a wide speed range, is shown in Figure 9.20. A positive wave corresponds to an increase in sound pressure in the noise trace and to the block entering the contact patch (at low speed). The figure shows how the wave is dominated by the spacing of the blocks and resonance effects occur. Since the contact patch may increase in length by up to 2 cms as the speed rises as shown by Clark (1971), the phase of the photo pick up wave cannot be taken to be the instant when the blocks impact the drum. The curvature of the leading edge of the contact patch will also affect the noise wave.

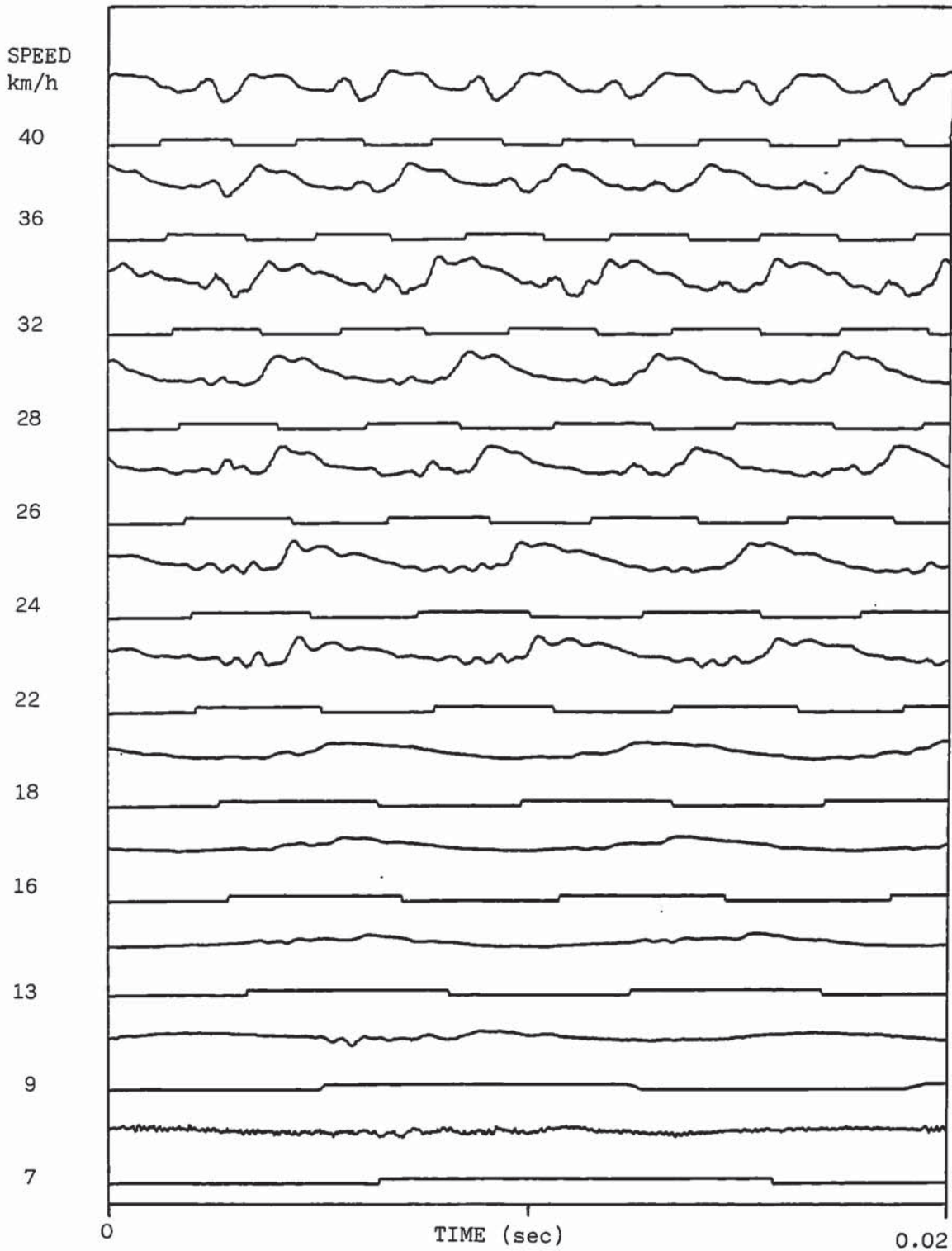
9.6. Transient Wave from "Space Block Space" Tread Segment in a Plain Ribbed Tyre

The single block and the spaces, one before and one after the block, were cut to the same dimensions as on the in phase block tyre. The wave was triggered as the first space entered the contact patch.



CROSS CORRELATION FUNCTION BETWEEN TWO MICROPHONE RECORDER CHANNELS

Figure 9.19.



TIME HISTORY OF SOUND WAVE FROM A CONSTANT PITCH IN PHASE BLOCK PATTERN TYRE OVER A RANGE OF SPEEDS, TRIGGERED FROM A FIXED POINT ON THE CIRCUMFERENCE, TOGETHER WITH A PHOTO PICK UP WAVE FROM EACH TREAD BLOCK - FRONT MICROPHONE POSITION

Figure 9.20.

The microphone was 125 mm in front of the tyre nip. This gives an acoustic delay of 0.37 msec. In Figure 9.21 the average of 16 samples is taken. The waveforms in Figure 9.22 for the lower speeds are single waves triggered with a pre advance from the start of the wave.

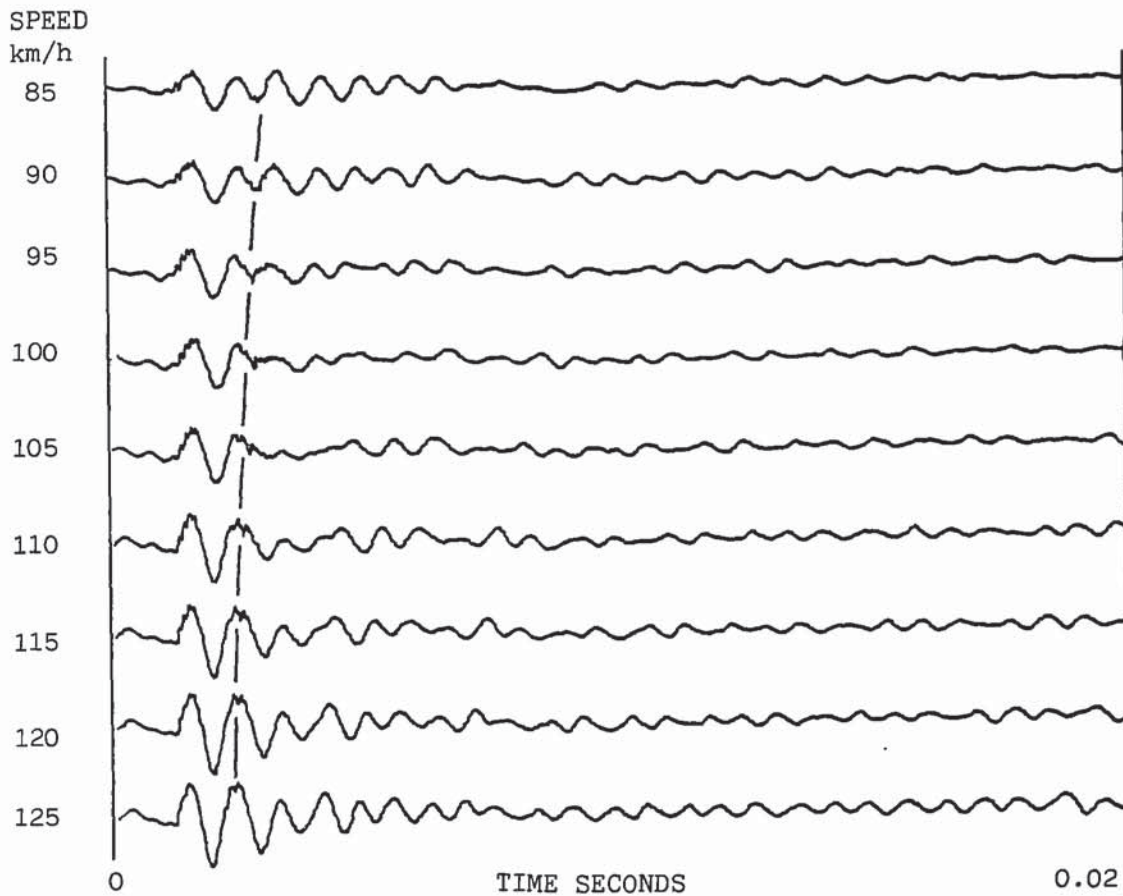
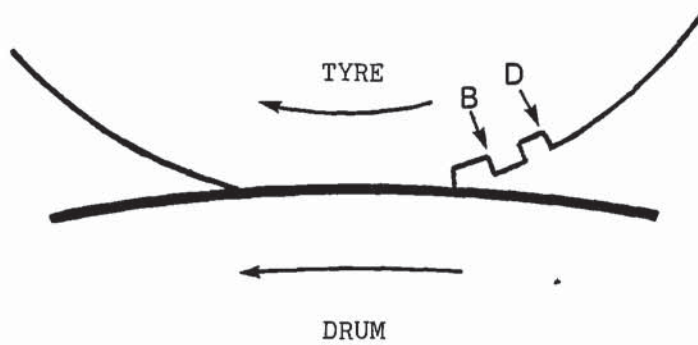
The positive sound pressure wave starts as the block (B) impacts the drum. This generates a resonant frequency independent of speed at approximately 1315 Hz. This resonant frequency showed up in the stacked spectra for the in phase block tyre in Figure 9.12.

In Figure 9.21 it can be seen that the start of the wave from the next hard edge of rubber (D) to impact the drum, which is shown as a dotted line in Figure 9.21 and 9.22, can either add and reinforce the resonant wave as at speeds 85 km/h and 125 km/h or cancel as at 100 km/h. This effect also is shown in the spectra in Figure 9.12.

9.7. Conclusions

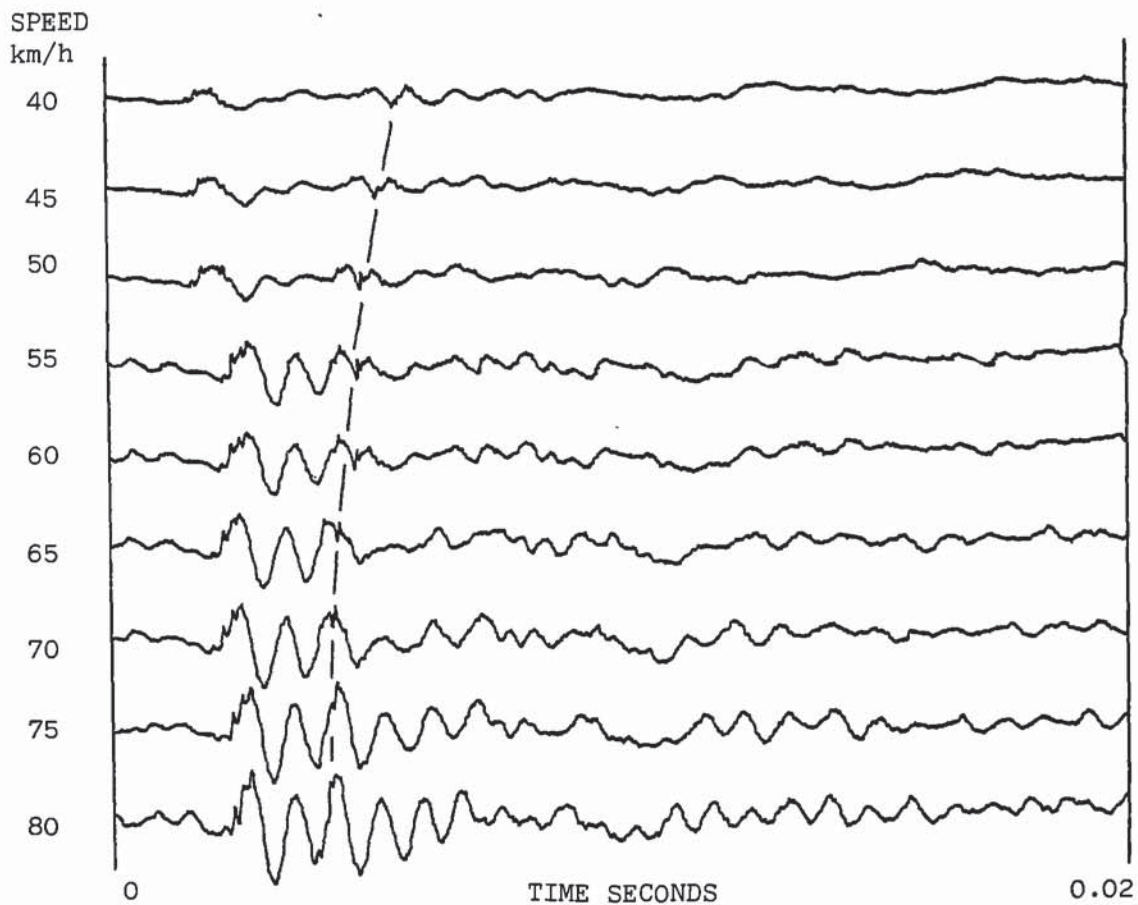
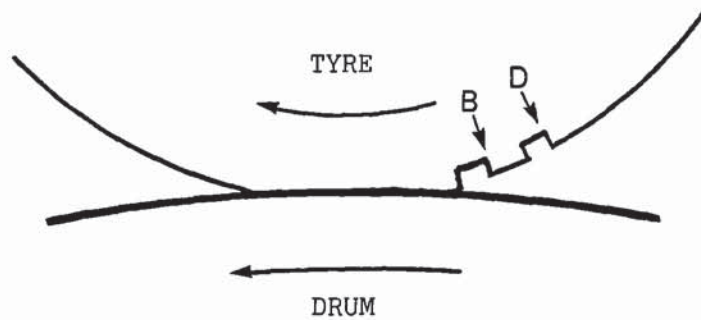
The simulation program gives frequency spectra fairly close to those obtained from experimental tyre noise tests. Although resonances do exist *in experimental results they have a relatively minor effect* on the spectrum.

In experimental results phase changes between the harmonics occur. This detracts very little from the authenticity of the simulated results and the relative phase does not affect audibility.



TRANSIENT WAVE FROM "SPACE BLOCK SPACE" SINGLE TREAD SEGMENT FRONT MICROPHONE POSITION - OVER A SPEED RANGE 80 - 125 km/h

Figure 9.21.



TRANSIENT WAVE FROM "SPACE BLOCK SPACE" SINGLE TREAD SEGMENT FRONT MICROPHONE POSITION - OVER A SPEED RANGE 40 - 80 km/h

Figure 9.22.

CHAPTER TEN: CONCLUSIONS AND SUGGESTIONS FOR FUTURE RESEARCH

10.1. Conclusions

It has been shown that the methods of reducing tyre/road noise fall into two major categories:

- (a) Modification of the road surface
- (b) Modification of the tyre tread pattern

In the review of the literature which has been carried out, the main factors contributing to traffic noise are:-

1. Traffic Speed
2. Traffic Density
3. Truck Engine Noise (technically feasible to quieten)
4. Road Surface Excited Noise
5. Tyre Tread Pattern Noise

The work has consisted of practical experiments involving different types of road surface and different types of tyre tread pattern. It has been appreciated that work on modifying road surfaces is of considerable value.

Delugrip Road Surfacing Material is a major step forward over surfaces currently specified in statutes for use in the U.K. The tyre/road noise is 3 dB(A) quieter than motorway hot rolled asphalt (BS 594), and with commercial tyres it is slightly quieter than a very smooth surface (Figure 3.3). Delugrip R.S.M. is also a major improvement in giving good wet grip and in maintaining the value over the life of the surface due to its polishing resistant nature. Spray is also reduced. It is expected that with respect to noise generation any further progress in road surface topography relative to tyres will be much less of an improvement.

It has also been shown that if noise is to be reduced further, attention must be paid to tyre tread pattern design.

Three types of excitation are involved in tyre/road noise:

- (a) Road surface excitation of blank treaded tyres can raise the noise level 14 dBA above the level on a polished smooth surface. (Figure 3.6).
- (b) Tyre self excitation on a smooth road surface due to a traction pattern can raise the noise level by 15 dBA above the level for a blank treaded tyre. (Figure 3.1).
- (c) Interaction - tyre/road excitation - a medium rough surface can reduce the noise level of a traction tyre to 6 dBA lower than the level obtained on a polished smooth surface. (Figure 3.1).

Indoor drum tests with simulated surfaces which have been carefully manufactured as true replicas of actual road surfaces give a fair correlation with pass-by testing from automobile tyres (Figure 5.14). They have the advantage in that rapid, controlled tests can be made under laboratory conditions and they enable the separation of tread pattern periodic excited noise and road surface excited periodic noise, thus giving greater insight into tyre/road interaction noise.

The other part of the work is the modifying of the spectral distribution of the noise, thus making it more psychologically acceptable.

A computer technique for a comprehensive study of the sequence of different tread block lengths undertaken has shown to be the most economic method for determining the optimum sequence to minimise dominant tones.

The computer work has shown that optimum sequences can be achieved. Firstly frequency modulation theory was considered, and then a computer approach was made to the complex modulation of tread pattern lengths.

The study has shown that with a block type tread pattern, the dominant frequencies of the tyre noise will be strongly influenced by the ratio of the length of the tread segments, and also by the number of identical length adjacent segments. The maximum number is especially important at low ratios. The distribution between maximum and minimum is important to reduce the dominance of modulation frequencies. The optimum sequence is obtained by automatically permuting the order of blocks of segments.

Before these studies were undertaken, a maximum of three identical length adjacent segments were traditionally used and the groups of segments were well modulated but their order was not permuted for optimisation.

As a result of these studies the maximum number of identical length adjacent segments has been increased to five, giving a 3 dB improvement in dominant tones. The groups of segments are now automatically permuted for optimisation and this can give a further 3 dB improvement.

The computer work was extended to simulate tread pattern noise in a similar way to an analogue model which used a drum with a painted tread pattern and photocell pickups. This program gave approximate spectra for many tread patterns, optimised sequencing and was extensively used in tyre development.

The scope of the computer simulation has been extended further to cover a wider range of tread patterns, the effect of microphone position, tyre speed and contact patch shape.

A quiet well sequenced block pattern tyre has been developed with the application of this computer simulation. This tyre has proved

to be only 1 dB noisier than a ribbed and microslotted pattern tyre, and it also has exceptionally good wet grip. The tread pattern is shown in Figure 9.13.

This model has given fairly good agreement with experimental results and is a useful tool to model total tread pattern excited noise with a view to the reduction of total noise with tractive type tread patterns.

10.2. Suggestions for Future Research

The accuracy of the digital model could be somewhat improved with the inclusion of the effects of:

- (a) Ground contact pressure
- (b) Resonances

The scope of the model could be extended to cover tyre pocket noise. Such noise involves a different mechanism of generation and would therefore require a different elemental waveform. However this type of pattern is not used normally.

The model has the flexibility for increased sophistication as further insight is gained into the mechanisms of tyre/road noise generation.

APPENDIX

1.1. The Mechanical Frequency Modulation Program

The original program referred to in Section 7.2.1. has been developed to produce the results previously discussed.

Each segment of a tread pattern is represented by a sawtooth wave e.g. 50 figures in equisteped descending order. 99 to 01. The segments are of a number of different lengths. The segments (up to 12) are grouped into a block of segments, 7 blocks complete the circumference of the tyre.

The resultant wave composed of different length sawtooth waves is then Fourier analysed by the Fast Fourier Transform to give the frequency spectrum.

The order of the blocks may be permuted to minimise the amplitude of the dominant harmonics in the spectrum.

1.2. Program - Schematic Description of Input

Example

512 or 1024 or 2048	The number (N) of equisubdivisions of the tyre circumference to be used in the Fast Fourier Transform (FFT)
7	The number of blocks (NB) of tread segments the order of the blocks can be permuted by the program
01 01 06 10 10 09 01	The number of segments K in each block The list of segments, 12 in each block, NB blocks

100000000000

6 blocks on this line

The segment lengths (SS1, SS2
SS10)

46.42	51.92	58.42	0.0	0.0	0.0
0.0	0.0	0.0	0.0		

50

The number of figures (NIN) in one
segment to constitute the wave

The sawtooth wave

99.97.95
..... 1

40

The number of permutations (NFI)
of the order of the blocks (up to
720 possible).

0

Requests punched tape output of the
synthesised sound wave for use in
the mini computer.

2.1. The Tread Pattern Noise Simulation Program Assuming a Side Listening Position

This program is referred to in Section 9.3.

Program Name: Noise Generated from Tread Pattern and Contact Patch Shape, Assuming a Side Listening Position

Language: FORTRAN IV G1

Computer: IBM 370/158

Description:

The program can optimise a tyre tread pitch sequence taking account of changes from rubber to air along narrow circumferential strips along a segment together with the strip lengths in the contact patch.

Optimisation is on the basis of a spectrum analysis of the resulting tread pitch wavetrain by Fourier Transform methods after permuting the order of blocks of pitches.

Limitations:

The limitation in achieving a better sequence is as follows. It is essential for the user to choose the blocks of segments with adequate modulation and also sufficient modulation of the modulation, in order to put the program on a good starting wicket.

The program will reduce dominant tones by up to 3 dB better than the input sequence chosen, as previously shown in Figure 7.5.

Programs Used:

Main Program: RONNPG1, ROWIND, DBAF, PLOT, JOB

Sub Routines: RORSEG, RORVSE, SPLPLA, SYMBOL, READ
 ROPATT, ROAVER, POINT, NUMBE,
 ROFFT, GRAP, AXISS, SPLBX

Direct Access Files: TE.NOISE.PERM4
 TE.NOISE.PERM5
 TE.NOISE.PERM6
 TE.NOISE.PERM7
 TE.NOISE,PERM8

Introduction

The program has some similarities with the previous program but differs in the following points:

- (1) Input data is taken in free format as changes from air to rubber in a thin strip along the segment for each strip across the segment. The contact lengths of the strips are also entered.
- (2) Five permutation files may be accessed depending on the number of sectors. (These exclude reflected sequences).

For 8 sectors the file contains 2500 perms

For 7 sectors the file contains 360 perms

For 6 sectors the file contains 60 perms

For 5 sectors the file contains 12 perms

For 4 sectors the file contains 3 perms

- (3) The program automatically runs on 512 points during permutation and changes to 1024 points for the plotted spectra.
- (4) The program automatically uses Blackman shifted windowing at all times but uses rectangular windowing for the audio-wave output.

Next Line

FST

Lower frequency limit (Hz) in scanning for maximum PSD (default is harmonic 1)

FFN

Upper frequency limit (Hz) in scanning for maximum PSD (default is harmonic 256)

A TYPICAL INPUT FOR THE PROGRAM

```

0
10.00-20
8 0 0.0 90.0
6 6 6 6 8 6 6 8
3 1
1 52.68 1
2 62.01 1
3 71.27 1
2 2 1 1 3 3
2 2 3 3 1 1
2 2 3 3 1 1
2 2 1 1 3 3
2 2 3 3 3 3 2 2
1 1 3 3 2 2
1 1 3 3 2 2
3 3 2 2 3 3 1 1
34 5.0
66
  4 1    22 45
  6 1    02 03 24 47
  6 1    04 05 26 49
  6 1    04 05 26 49
  6 1    02 03 24 47
  5 1    02 22 45
  4 1    26 36
  3 1    65
  4 1    63 64
  4 1    58 63
  4 1    52 65
  4 0    12 41
  2 0
  4 1    12 52
  4 1    28 38
  4 1    28 33
  4 1    28 30
  4 1    36 38
  4 1    33 38
  4 1    28 38
  4 1    14 54
  2 0
  4 0    25 54
  4 1    02 14
  4 1    03 14
  4 1    03 08
  4 1    02 03
  3 0    02
  4 1    30 40
  5 1    21 44 64
  6 1    19 42 63 64
  6 1    17 40 61 62
  6 1    17 40 61 62
  6 1    19 42 63 64
  4 1    21 44
250 251 252 254 255 257 258 259 261 263 264 265 265
266 267 268 269 269 268 267 266 265 265 264 263 261
259 258 257 255 254 252 251
80. 3180.
1 1 1
50. 2500.

```

3.1. Aspects of the Use of the Fast Fourier Transform

Normally the simulated noise wave along the circumference of the tyre is divided into a number of points which is a power of two. This allows the Fast Fourier Transform to be used. A harmonic line spectrum is obtained from this waveform. Assuming that the waveform used by the program does not give rise to aliasing effects, and also that the number of points is adequate to separate the individual harmonics of the noise; then doubling the number of points will extend the spectrum up to twice the original highest harmonic. However it will not alter the spectrum within the original range of harmonics.

3.2. Aliasing

This is the folding back into the spectrum due to any input frequencies above half the sampling rate, and thus causing errors in the spectrum.

In commercial real time analysers, analogue antialiasing filters prevent this from happening, the filtering must be carried out before digitisation.

When simulating tyre noise with a program, aliasing errors will occur if the simulated noise wave shape introduces frequencies greater than half the digitising rate either due to:

- (a) The sharpness of the wave
- or
- (b) The coarseness of digitisation, especially if double digitisation occurs

There is a version of the program which uses a formula with a set of sine waves as a basic elemental noise wave. This only gets digitised once and thus there is virtually negligible input at any frequencies that could give rise to aliasing. The results

from this version of the program are identical at harmonics of wheel rotation below the 256th, when using the number of points round the circumference ranging from 512 to 4096. This version does not simulate a range of cross groove widths as does the latest version of the program.

3.3. Leakage and Weighting Function

The following discussion is applicable if the waveform used by the program does not give rise to aliasing effects. It is somewhat arbitrary to take exactly one circumference of noise wave as the data block to be digitised. For example if a different data block length were taken, then a tread pattern pitch which was a unit fraction of the original length but not of the new length, would give results 3.9 dB low.

The new program has a tapering function window which reduces this attenuation effect to less than 1.4 dB and both broadens the bandwidth by 65% and decreases the skirt level by 18 dB.

However this does introduce a further problem, that the effect of part of the tyre circumference is being attenuated. This has been overcome by stepping the window round the tyre circumference and averaging the absolute spectral values.

4.1. Swept Sine Wave Testing of Acoustic Measuring Conditions

A pure tone was fed to a loudspeaker standing on the ground plane, the centre of the cone was 141 mm above this plane. Two microphone positions were used, one 20 mm in front of the speaker cone to monitor the output from it, the other was placed 1 m away from the speaker in order to show any fluctuations in noise level due to reflections in the non-anechoic testing conditions. This microphone was 450 mm above the plane as in tyre noise testing. The frequency of the tone was slowly swept from 2 kHz to 100 Hz.

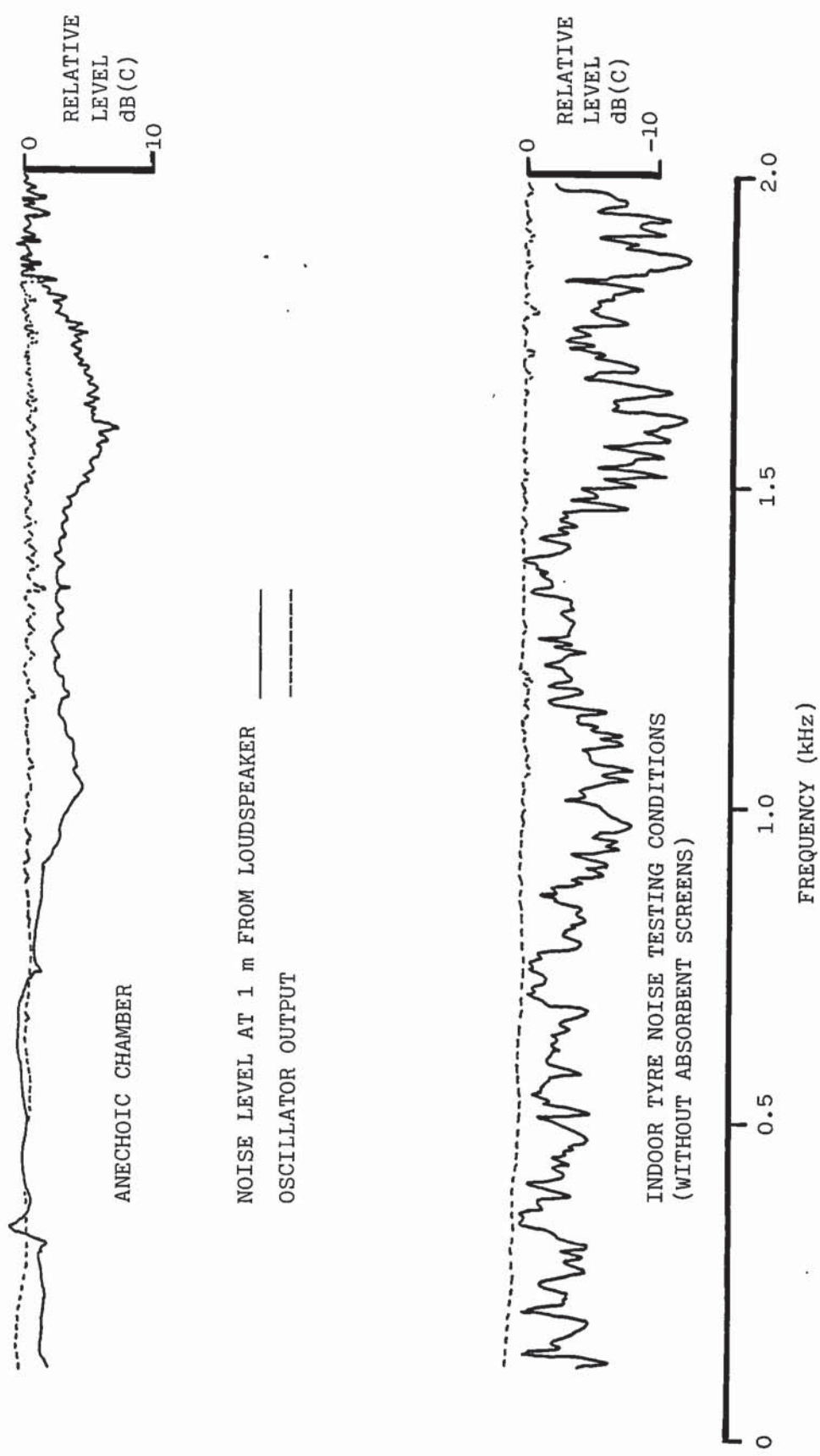


Figure A.4.

4.2. Comments on Results

The level at the 20 mm position stayed fairly constant showing the good response of the speaker. The oscillator output is shown in Figure A4 together with the level at the 1 m position which shows slow undulations with frequency due to standing waves owing to the height of the centre of the cone above the ground plane, this occurs in both rooms. However the main errors due to reflections in the tyre testing conditions are rapid fluctuations with frequency usually within ± 2.5 dB of the mean values.

5. Ambient Noise in Tyre Testing Conditions

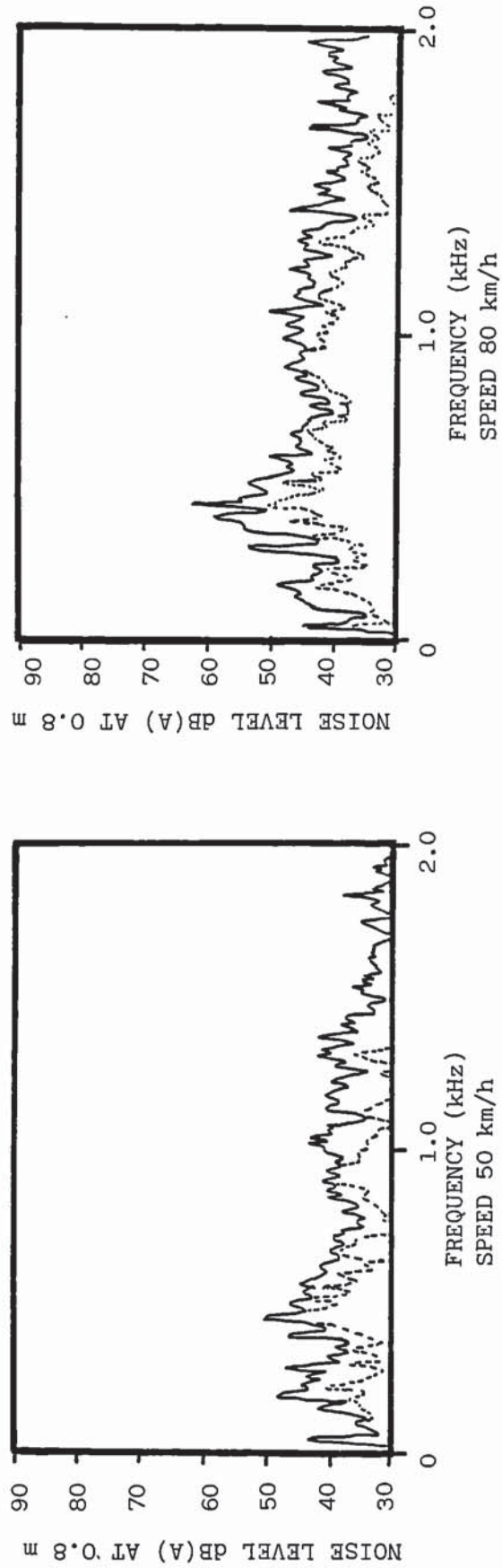
The frequency spectra and levels of ambient noise are compared with those from testing a blank treaded tyre on a smooth steel surfaced drum at speeds of 50 and 80 km/h.

TABLE A5 AMBIENT NOISE VERSUS BLANK TREAD TYRE NOISE ON SMOOTH STEEL DRUM

Drum Speed (km/h)	Tyre Raised Off Drum Level dB(A)	Tyre Loaded Level dB(A)
0	60	-
50	62.5	69
80	64	73

BLANK TREAD TYRE NOISE

AMBIENT NOISE



AMBIENT NOISE VERSUS BLANK TREAD TYRE NOISE ON SMOOTH STEEL DRUM

Figure A.5.

Papers published during the period of research.

1. Noise Generated at the Tyre/Road Interface.
Walker J. C., Major D. J.
Stress, Vibration and Noise Analysis in Vehicles.
Applied Science Publishers Limited, 1975.
2. Noise from the Tyre/Road Interface with Heavy Commercial Vehicles.
Walker J. C.
The Transport Engineer, November 1975.
3. The Reduction of Noise by Applying Basic Design Principles to Roads and Tyres.
Walker J. C.
Proceedings of the SAE Highway Tyre Noise Symposium.
San Francisco, November 1976.
4. The Influence of the Road Surface on Safety and Environmental Aspects of Tyre Performance.
Williams A. R., Major D. J., Walker J. C.
The Transport Engineer, January 1977.
5. The Reduction of Tyre/Road Interaction Noise.
Walker J. C., Oakes R. D.
Aviation, Surface Transportation and Plant Noise Symposium.
Dallas, January 1979.
6. The Improvement of Noise and Traction due to Road/Tyre Interaction.
Walker J. C., Williams A. R.
International Tyre Noise Conference, Stockholm, August 1979.
7. Tyre/Road Interaction Noise.
Walker J. C., Oakes R. D.
FISITA 18th International Congress, Hamburg, May 1980.

List of References

- | | | |
|---|------|--|
| Ackroyd, M H | 1973 | Digital Filters.
Butterworths. |
| Allbert B. J. and
Walker, J. C. | 1965 | Tyre to Wet Road Friction. Proceedings
of Automobile Division Institute of
Mechanical Engineers Proceedings,
1965-66, Volume 180, Part 2A, No. 4. |
| Anderson, D. G.
Benchea, T. and
Matyja, F. E. | 1976 | Round Robin Testing with SAE J57a
P70 SAE 762013. |
| British Standards
Institution | 1973 | Methods for Sampling and Testing of
Mineral Aggregates, Sands and Filters.
BS 812. |
| Bond, R.
Williams, A. R. and
Lees, G. | 1973 | An Approach towards the Understanding
and Design of the Pavements Textural
Characteristics Required for Optimum
Performance of the Tyre. Symposium
on Physics of Tyre Traction General
Motors, October. |
| Bond, R. | 1977 | Internal Report, Dunlop Limited.
TD 906, August |
| Clarke, S. K. | 1971 | Mechanics of Pneumatic Tyres.
National Bureau of Standards Monograph
122, page 452. |
| Close, W. H. | 1974 | Regulatory Implications of Truck Tyre
Noise Studies SAE 740606. |
| Dorsch, L. T. | 1976 | Predicting Tyre Noise and Performance
Interaction. P70 SAE 762032. |
| Eberhardt, A. C. | 1975 | Digital Signal Analysis with Application
to Truck Tyre Sound and Vibration.
North Carolina State University. |
| Eberhardt, A. C. | 1979 | Investigation of the Truck Tyre Vibration
Sound Mechanism. Proceedings of Inter-
national Tyre Noise Conference, Stockholm,
August. |
| Ewald, D.
Pavlovic, A. and
Bollinger, J. G. | 1971 | Noise Reduction by Applying Modulation
Principles. Journal of Acoustical
Society of America. Vol. 49,
No. 5. (Part 1) Pages 1381 - 85. |

Favre, B. and Pachiaudi, G.	1974	Tyre Noise, Theoretical and Experimental Aspects. Internal Report by Research Insitutute of Transport, Arcueil (Private Communication).
Flanagan, W.	1972	Recent Studies give a Unified Picture of Tyre Noise. S.A.E. Journal of Automotive Engineering. April 15-19.
Fuller, W. R.	1976	The Influence of Pavement Roughness upon Tyre/Pavement Interaction Noise Levels. Proceedings of Noise Expo. New York, March.
Gadefelt, G. and Voight, P.	1976	Tyre Noise Screening. P70 SAE 762028.
Harland, D. G.	1974	Rolling Noise and Vehicle Noise. Symposium on Noise in Transportation University of Southampton.
Hayden, R. E.	1971	Road Side Noise from the Interaction of a Rolling Tyre with a Road Surface. Proceedings of the Purdue Noise Control Conference, Purdue University, Lafayette, Indiana.
Henson, D.	1968	The Sound of Tyres. Marketing Division. Dunlop Limited, Birmingham, England.
Hillquist, R. K. and Carpenter, P. C.	1974	A Basic Study of Automobile Tyre Noise. Sound and Vibration, February.
Hillquist, R. K.	1972	An experiment for Relating Objective and Subjective Assessments of Truck Tyre Noise. SP-373 SAE 720928.
H.M.S.O.	1972	Development and Compensation Putting People First. Cmnd 5124.
H.M.S.O.	1973	Land Compensation Act. Chapter 26.
Informatics Inc.	1980	Foreign Research in Tyre Noise Prepared for Office of Noise Abatement and Control. U.S. Environmental Protection Agency. August.
Johansen, J. M.	1979	Effect of Studded Tyres on Vehicle Pass-by Noise. Proceedings of International Tyre Noise Conference, Stockholm, August.

- f
- Katekhda, I.E.D. 1974 The Development of High Friction Dense Asphalt using Natural Rock Aggregates. Ph.D. Thesis, University of Birmingham.
- Krempf, G. 1967 Investigations of Automobile Tyres. Automobiltechnische Zeitschrift, Vol. 69, Nos. 1 and 8, Translation No. 1 by Funer, E. and Clarke, S. K. University of Michigan 08904-1-T, July 1968.
- Kryter, K. D. and 1965 Judged Noisiness of a Band of Random Pearsons, K. S. Noise Containing an Audible Pure Tone. J. Acoustic Soc. America, Vol. 38, pp 106 - 112.
- Landers, S. P. 1976 A vibrational Sound Mechanism of Lug Type Tread Designs. P70, SAE 762025.
- Leasure, W. A. Jnr. Truck Tyre Noise - 1.
Corley, D. M. Peak A - Weighted Levels due to
Flynn, D. R. and Truck Tyres.
Forrer, J. S. 1970 Report No. OST-ONA-71-9
 1972 Report No. OST-TST-72-1
- Leasure, W. A. and 1974 Pecos Truck Tyre Noise Study: A Mathews, D. E. Summary of Results. National Bureau of Standards, Washington.
- Leasure, W. A. Jnr. & 1975 Tyre/Road Interaction Noise. Bender, E. K. J. Acoustics. Soc. America. Vol. 58 pp 39-50, No. 1, July.
- Lees, G. 1970 The Rational Design of Aggregate Grading for Dense Asphalt Compositions. Proceedings Association of Asphalt Paving Technology, 39 pp 30 - 69.
- Lees, G. and 1973 The Design and Field and Laboratory Sharif, R. L. Testing of High Friction and Dense Asphalts. The Highway Engineer, pp 4 - 20, June.
- Lippmann, S. A. 1972 Jury Reactions to Truck Tyre Noise. An SAE Study. SP-373 SAE 720929.

- Major, D. J. 1976 Traffic Noise Reduction on Hammersmith Fly-Over as a Result of Re-surfacing with Delugrip Road Surfacing Material. Internal Report, Dunlop Limited.
- Millard, R. S. 1970 A Review of Road Traffic Noise. Transport and Road Research Laboratory. Report LR 357.
- Miller, R. F. and Thrasher, D. B. 1976 Pass-by Tyre/Pavement Interaction Noise Measurement Problems. P70, SAE 762012.
- Mukai, T. 1974 Tyre Noise (in Japanese).
Sakamoto, N. J.S.A.E. January P61 February P161
Goshima, N. and March P234 (20 p 36 Fig. 22 Ref).
Fukuoka, N.
- Nelson, P. M. and Piner, R. J. 1977 Classifying Road Vehicles for the Prevention of Road Traffic Noise. T.R.R.L. Report 752.
- Oswald, L. J. and Hickling, R. 1976 Possible effect of Vehicle Aerodynamic Noise on SAE J57a Pass-by Measurements. P70 SAE 762019.
- Pope, J. and Reynolds, W. C. 1976 Tyre Noise Generation the Roles of Tyre and Road. P70, SAE 762023.
- Pope, J. and Reynolds, W. C. 1978 Basic Studies of Automobie Tyre Noise. Stanford University Report TNS-1.
- Potts, G. R. 1973 Application of Holography to the Study of Tyre Vibration. Tyre Science and Technology. Vol. 1, No. 3, August pp 255 - 266.
- Potts, G. R. and Csora, T. T. 1975 Tyre Vibration Studies: The State of the Art. Tyre Science and Technology. Vol. 3, No. 3, August. pp 196 - 210.
- Reiter, W. F. Jnr 1973 Investigation of Vibration in Truck Tyre Noise Generation. Ph.D. Thesis. North Carolina State University.
- Reiter, W. F. Jnr. 1974 Resonant Sound and Vibration Characteristics of a Truck Tyre. Tyre Science and Technology. Vol. 2, No. 2, May P130 - 141.

Reiter, W. F. Jnr. Eberhardt, A. C. Harper, L. J. and Atkinson, T. L.	1974	Truck Noise V11 - A. Experimental Investigation of Truck Tyre Sound and Vibration Report No. DOT-TST-75-60.
Richards, M. G.	1974	Automotive Tyre Noise - A Comprehensive Study. Sound and Vibration, May pp 42 - 47.
Robertson, T. A. and Cox, J. N.	1957	Truck Tyre Noise. SAE Detroit Section Meeting, February.
Robertson, T. A. and Cox, J. N.	1958	Truck Tyre Noise. Problems and Solutions. SAE Summer Meeting, June.
Rubber Manufacturers Association	1971	Truck Tyre Noise. Presentation to the Office of Noise Abatement and Control of the Environmental Protection Agency Hearing Washington D.C. November.
Samuels, S. E. and Alfredson, R. A.	1974	The Effect of Tread Pattern on Tyre Noise. Noise Shock and Vibration Conference, Monash University, Melbourne.
Samuels, S. E.	1976	Traffic Noise - A study of Tyre/Road Noise Mechanism. Australian Road Research Board Proceedings, Vol. 8.
Siddon, T. E.	1972	Noise Generation Mechanism for Passenger Car Tyres. Journal of the Acoustical Society of America 53 (2) 305 - 306 (Abstract).
Terman, F. E.	1943	Radio Engineers Handbook. McGraw Hill, London. Pages 578 - 582.
Tetlow, D.	1971	Truck Tyre Noise. Sound and Vibration, August pp 17 - 23.
Thrasher, D. B. Miller, R. F. Bauman, R. G.	1976	Effect of Pavement Texture on Tire/ Pavement Interaction Noise. P70 SAE 762011.
Tompkins. E. S.	1965	Tyres for Modern Roads. Proc. Institute of the Rubber Industry. Vol. 12, No. 9.
Trivisonno, N. M. Beatty, J. R. and Miller, R. F.	1967	The Origin of Tyre Squeal. Kautschuck und Gummi Kunststoffe. No. 5, January.

- Underwood, M. C. P. 1973 A Preliminary Investigation into Lorry Tyre Noise. Transport and Road Research Laboratory. Report LR 601.
- Underwood, M. C. P. 1980 Origins of Tyre Noise. Ph.D. Thesis. University of Southampton.
- Varterasian, J. H. 1969 Quieting Noise Mathematically - Its Application to Snow Tyres. SAE 690520.
- Veres, R. E. 1974 Pavement Macrotecture Characterization by Tyre Noise. Report 562, Pennsylvania State University.
- Veres, R. E. 1976 A Tyre Noise Investigation and Test Method. SAE 760 152.
- Vorih, W. J. 1971 Designing Quiet Tread Spacings for Tyres. 99th Rubber Division Meeting American Chemical Society.
- Walker, J. C. and Reeves, N. H. 1974 Uniformity of Tyres at Vehicle Operating Speeds. Tyre Science and Technology, Vol. 2, No. 3, August, pp 163 - 178.
- Walker, J. C. and Major, D. J. 1975 Noise Generated at the Tyre Road Interface. Stress, Vibration and Noise Analysis in Vehicles. Applied Science Publishers.
- Walker, J. C. 1976 Internal Report Dunlop Limited. TD 846, April.
- Waters, P. E. 1974 Commercial Road Vehicle Noise. Journal of Sound and Vibration 35 (2) pp 155 - 222, Ph.D. Thesis.
- Watkins, L. H. 1974 A Quiet Heavy Lorry. Commercial Motor 139 (3539), pp 28 - 31.
- Wiener, F. M. 1960 Experimental Study of the Airborne Noise Generated by Passenger Automobile Tyres. Noise Control, July/August.
- Wilken, I. D. 1976 Research on Individual Noise Source
Oswald, L. J. and Mechanisms of Truck Tyres: Aeroacoustic
Hickling, R. Sources. P70 SAE 762022.
- Willett, P. R. 1975 Tyre Tread Pattern Sound Generation. Tyre Science and Technology. TSTCA Vol. 3, No. 4, November, pp 252 - 266.

Glossary of Terms

The Tyre/Road Noise field embraces a number of disciplines, and draws on the specialist language of each. This glossary, which is not intended to be comprehensive, attempts to define those specialist terms that have been used in this thesis.

More comprehensive glossaries may be found as follows:

1. Acoustical Terms in the British Standard Glossary of Acoustical Terms BS 661.
2. Vehicle Dynamics Terms in the Society of Automotive Engineers Vehicle Dynamics Terminology S.A.E. 670c.

Most of the abbreviations have been explained as they came in the text.

Aliasing

The folding back into the spectrum due to any frequencies above half the sampling rate.

Breaker

A strip of rubbered cord fabric, of fewer ends per 10 cm than main plies or top plies, placed circumferentially round the cover between top plies and tread.

Coherence

Represents the normalised magnitude of the cross power spectral density.

Continuous Spectra

Over at least part of the spectrum, they contain components at every possible frequency.

dB(A)

The dB(A) scale is taken to have a defined zero at 0 phons = 20×10^{-6} RMS Newton metre⁻².

Discrete Fourier Transform

It produces a good approximation to an actual spectrum

Fast Fourier Transform

A simplified implementation of the Discrete Fourier Transform giving an identical result.

Flow (or Traffic Flow)

The number of vehicles which pass a fixed point in unit time.

Friction Course

An open textured coated macadam of high void content (greater than 20%) when compacted.

Harmonics

They are integral multiples of the fundamental frequency i.e. the tyre rotational frequency.

Leakage

This often has the effect of reduction of the amplitude of the original frequency and an increase in neighbouring sidelobes.

Line Spectra

They consist only of discrete lines at specific frequencies.

Noise

Sound that is not desired by the hearer

Pass-by-Noise

Noise received at a microphone position during the passage of a vehicle.

Picket Fence Effect

This occurs with continuous spectra, since only samples of a spectra are shown, sharp actual peaks between the sample lines could be obscured e.g. There could be up to 3.9 dB error with a rectangular window.

Ply

A piece of rubbered fabric cut to specified width and bias angle.

Slip Angle

The angle between the plane of the tyre and the direction of travel of the centre of tyre contact.

Scheduled Conditions

The combinations of load and inflation pressure recommended in the European Tyre and Rim Technical Organisation ETRTO Data Book which is published annually.

Time Window

This is the time during which the "analyser" is looking at the input signal i.e. the data block.

Tread Contour (Tread Radius)

The unloaded cross sectional shape of the tread, neglecting the tread pattern depressions, usually given as a radius or radii.

Tread Segment Pitch

The length (mm) of a tread pattern segment pitch.

Tyre/Road Noise

This is the noise generated by a tyre rolling on a road surface under given conditions.

Weighting Function

This is a tapering function applied to the data block, e.g. Hanning weighting or Hanning Window.